



# Durham E-Theses

---

## *Novel block Co-polymers as potential photonic materials.*

Riggs, Helen Joanna

### How to cite:

---

Riggs, Helen Joanna (2006) *Novel block Co-polymers as potential photonic materials.*, Durham theses, Durham University. Available at Durham E-Theses Online: <http://etheses.dur.ac.uk/2439/>

### Use policy

---

The full-text may be used and/or reproduced, and given to third parties in any format or medium, without prior permission or charge, for personal research or study, educational, or not-for-profit purposes provided that:

- a full bibliographic reference is made to the original source
- a [link](#) is made to the metadata record in Durham E-Theses
- the full-text is not changed in any way

The full-text must not be sold in any format or medium without the formal permission of the copyright holders.

Please consult the [full Durham E-Theses policy](#) for further details.

# **Novel Block Co-polymers as Potential Photonic Materials.**

A thesis submitted for the degree of  
Master of Science

by

**Helen Joanna Riggs**

The copyright of this thesis rests with the author or the university to which it was submitted. No quotation from it, or information derived from it may be published without the prior written consent of the author or university, and any information derived from it should be acknowledged.

Department of Chemistry  
University of Durham

May 2006



11 JUN 2007

*“Nothing could adde beauty to light.”*

*Sir Christopher Wren, Scientist-Architect, 1632 - 1723*

## **Abstract.**

Photonic crystals, which are a specific type of photonic material, consist of regular, periodic structures composed of alternating high and low refractive index materials. They may exist in 1-D, 2-D or 3-D forms, which are analogous to the morphologies adopted by self-assembling block-copolymers.

Three series of well-defined block co-polymers in which the blocks had high-contrast refractive indices, were synthesised.

The first series consisted of styrene-fluoromethacrylate block co-polymers, which were synthesised by living anionic polymerisation (LAP) of styrene and a fluoromethacrylate. Molecular weights, block molar ratios and fluoromethacrylate monomers were varied.

The second series consisted of *p*-bromostyrene-methacrylate block co-polymers, which were synthesised by the direct bromination of the styrene block of LAP-prepared styrene-methacrylate block co-polymers. Molecular weights and block molar ratios were varied.

The third series consisted of *p*-bromostyrene-fluoromethacrylate block co-polymers, which were synthesised by the direct bromination of the styrene block of LAP-prepared styrene-fluoromethacrylate block co-polymers. Molecular weights and block molar ratios were varied.

All series were analysed by Size Exclusion Chromatography, proton Nuclear Magnetic Resonance spectroscopy (NMR) and, where appropriate, <sup>13</sup>carbon NMR and <sup>19</sup>fluorine NMR. The brominated co-polymers underwent Elemental Analysis.

Refractive indices of the constituent homopolymers of both series, and where possible, the co-polymers, were determined.

Evidence for the self-assembly of one particular styrene-fluoromethacrylate block co-polymer into a 1-D (lamellar) structure was achieved using Small Angle X-Ray Scattering.

## **Acknowledgments.**

Many thanks to:

Professor Jim Feast and Dr. Lian Hutchings for employing me, and particularly Dr. Hutchings for his supervision over the past two years and for SEC chromatograms; Dr. Nigel Clarke for his lecture notes and his official supervision; Stuart Eggleston for the SAXS data on microphase separated co-polymers; Dr. Alan Kenwright, Catherine Heffernan and Ian McKeag for NMR spectra and their invaluable assistance in interpretation thereof; Judith Magee and Jaroslava Dostal for Elemental Analysis; Dr. Richard Thompson for demonstrating refractive index measurement; Peter Coyne and Malcolm Richardson for their preparation and repair of customised glassware; Matthew Gibson for his help whenever my computer skills ran out, his choice of my leaving presents and for organising my leaving “night out;” Jonathan Fay for his design and creation of my leaving card; and the latter two, with David Johnson and everybody else in CG156, for finally making life in the deskroom fun.

Helen Riggs

May 2006

### **Declaration.**

The work reported in this thesis was carried out in the laboratories of the Interdisciplinary Research Centre (IRC) in Polymer Science and Technology, Department of Chemistry, University of Durham, between October 2003 and October 2005. This work has not been submitted for any other degree in Durham or elsewhere and is the original work of the author except where acknowledged by means of appropriate reference.

### **Statement of Copyright.**

The copyright of this thesis rests with the author. No quotation from it should be published without their prior written consent and information derived from it should be acknowledged.

## **Contents.**

Abstract	i
Acknowledgments	ii
Declaration	iii
Statement of Copyright	iii
Contents	iv
 Chapter 1: Introduction.	 1
1.1 Background.	2
1.2 Methods by which White Light can be made to produce Colours.	4
1.3 Young's Theory.	6
1.4 Bragg's Law.	8
1.5 Natural Photonic Materials.	9
1.5.1 Mineral.	9
1.5.2 Animal.	10
1.5.3 Vegetable.	11
1.6 Synthetic Photonic Materials.	13
1.6.1 Total Internal Reflection.	13
1.6.2 The Band Gap Effect.	15
1.7 Polymers used in Optical Applications.	16
1.7.1 Introduction.	16
1.7.2 Low Refractive Index Materials.	16
1.7.3 High Refractive Index Materials.	18
1.8 Methods of Making Synthetic Photonic Materials/Crystals.	18
1.8.1 Inverse Opals.	18
1.8.2 Lithographic Techniques.	19
1.8.3 Block Co-polymer Self-Assembly.	19
1.9 Living Anionic Polymerisation.	20
1.9.1 Introduction.	20
1.9.2 Screened Anionic Polymerisation.	25
1.9.3 Preparation of Semifluorinated diblock Co-polymers.	27
1.9.4 Modified Screened Anionic Polymerisation.	27
1.9.5 Preparation of polyfluoromethacrylates by LAP.	28

1.10	Methods of Polymer Analysis.	30
1.10.1	<i>Size Exclusion Chromatography.</i>	30
1.10.2	<i>NMR Spectroscopy.</i>	31
1.11	Self-Assembly, Self-Organisation and Microphase Separation.	32
1.11.1	<i>Introduction.</i>	32
1.11.2	<i>Variation of Lamellar Spacing (D) with degree of polymerisation (N).</i>	35
1.11.3	<i>Characterisation of Microphase Separated Co-polymers.</i>	37
	<b>Chapter 2: Results and Discussion.</b>	38
2.1	Background	39
2.2	Synthesis and Characterisation of Polystyrene.	39
2.3	Synthesis and Characterisation of Poly(methyl methacrylate).	40
2.4	Syntheses of Fluoromethacrylate Homopolymers.	41
2.5	Syntheses of Poly(styrene- <i>b</i> -fluoromethacrylate) Co-polymers.	46
2.5.1	<i>Method 1, in which tri-isobutylaluminium or its derivative was used as "screening" agent.</i>	46
2.5.2	<i>Method 2, in which solvents were exchanged.</i>	51
2.5.3	<i>Method 3, in which solvents were added sequentially.</i>	56
2.6	Synthesis of Poly(styrene- <i>b</i> -1H,1H,2H,2H-perfluorohexyl methacrylate) Co-polymers, with composition 1:1 by moles.	63
2.7	Calculation of percentage Styrene Homopolymer in a poly(styrene- <i>b</i> -fluoromethacrylate) Co-polymer.	68
2.8	Syntheses of Block Co-polymers containing a Bromostyrene Block.	71
2.8.1	<i>Synthesis of poly(<i>p</i>-bromostyrene).</i>	71
2.8.2	<i>Analysis of poly(<i>p</i>-bromostyrene).</i>	72
2.8.3	<i>Synthesis of poly(styrene-<i>b</i>-methyl methacrylate) co-polymers.</i>	74
2.8.4	<i>Synthesis of poly(<i>p</i>-bromostyrene-<i>b</i>-methyl methacrylate) co-polymers.</i>	76
2.8.5	<i>Synthesis of poly(<i>p</i>-bromostyrene-<i>b</i>-1H,1H,2H,2H-perfluorohexyl methacrylate) co-polymers.</i>	79
2.9	Material Characterisation.	82
2.9.1	<i>Refractive Index Measurement.</i>	82
2.9.2	<i>Solid State Organisation.</i>	84



Chapter 3: Experimental.	87
3.1 Monomers used.	88
3.2 Preparation of Glassware, Solvents, Monomers and other Reagents.	89
3.3 Syntheses of Polystyrene and Poly(methyl methacrylate).	91
3.3.1 <i>Synthesis of Polystyrene.</i>	91
3.3.2 <i>Synthesis of Poly(methyl methacrylate).</i>	91
3.4 Syntheses of Fluoromethacrylate Homopolymers.	92
3.4.1 <i>Synthesis of Poly(2,2,2-trifluoroethyl methacrylate).</i>	92
3.4.2 <i>Synthesis of Poly(1H,1H,2H,2H-perfluorohexyl methacrylate).</i>	93
3.4.3 <i>Synthesis of Poly(1H,1H,2H,2H-perfluorooctyl methacrylate).</i>	93
3.5 Syntheses of Poly(styrene- <i>b</i> -fluoromethacrylate) Co-polymers.	94
3.5.1 <i>Synthesis of poly(styrene-<i>b</i>-1H,1H,2H,2H-perfluorohexyl methacrylate) with composition 1:1 by mass.</i>	94
3.5.2 <i>Synthesis of poly(styrene-<i>b</i>-1H,1H,2H,2H-perfluoro (5-methylhexyl) methacrylate).</i>	95
3.5.3 <i>Synthesis of poly(styrene-<i>b</i>-1H,1H,2H,2H-perfluorohexyl methacrylate) with composition 1:1 by moles.</i>	95
3.6 Synthesis of Poly(styrene- <i>b</i> -methyl methacrylate) Co-polymer.	96
3.7 Bromination of Polystyrene and of Block Co-polymers.	97
3.7.1 <i>Bromination of polystyrene.</i>	97
3.7.2 <i>Bromination of poly(styrene-<i>b</i>-methyl methacrylate).</i>	97
3.7.3 <i>Bromination of poly(styrene-<i>b</i>-1H,1H,2H,2H-perfluorohexyl methacrylate).</i>	98
3.8 Characterisation.	98
3.8.1 <i>Size Exclusion Chromatography.</i>	98
3.8.2 <i>NMR Spectroscopy.</i>	98
3.8.3 <i>Elemental Analysis.</i>	98
3.8.4 <i>Refractive Index Measurement.</i>	98
3.8.5 <i>Solid State Organisation.</i>	99
Chapter 4: Conclusions.	100
4.1 Conclusions.	101
4.2 Future Work.	102
References.	103
Appendices.	108

## **Chapter 1: Introduction.**

1.1 Background.

Photonics involves the propagation and control of photons, in free space or in matter by the use of photonic (dielectric) materials. Photonic crystals are a specific class of photonic materials/media. Materials (generally) and crystals (specifically) can both form “wavelength selective” devices by inhibiting the propagation of light at certain frequencies and in certain directions. This so-called photonic “band gap” effect for synthetic photonic crystals was first described independently by both E Yablonovitch<sup>1</sup> and S John<sup>2</sup> in 1987.

As a general definition, photonic crystals are periodic dielectric structures composed of alternating high and low refractive index materials, with periodicity (spatial period, lattice constant) of the order of the wavelength of visible light from blue (<400nm) to red (~770nm). In principle, the periodicity can be in one dimension (1-D, the “sandwich” model or multi-layer stack, which has important applications as high-reflection mirrors, and anti reflective coatings); two dimensions (2-D, the “Battenberg cake” model); or three dimensions (3-D, the “woodpile” model) (Fig. 1.1):

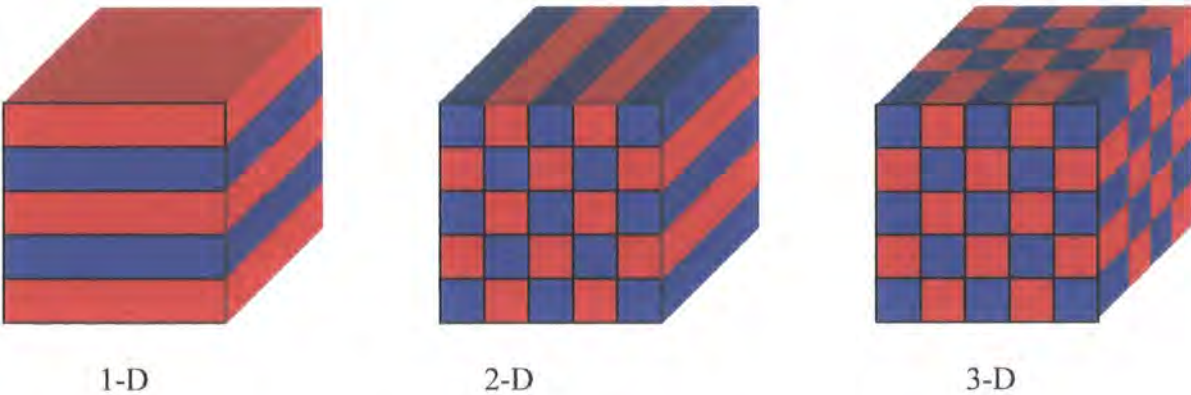


Fig. 1.1      Diagrammatic representations of Photonic Crystals.

They thus resemble large scale versions of the crystalline structures of many solid state materials and this is one reason they are referred to as crystals.<sup>3</sup>

A photonic crystal will reflect and refract visible light from the interfaces of its multiple layers, provided that there is a high contrast in the refractive indices of the alternating layers. The concept of a photonic crystal can therefore be explained in terms of a development of the observation of iridescence (“Colours of Thin Films”)

by Robert Boyle<sup>4</sup> in the seventeenth century; of the theory of interference, developed by Thomas Young<sup>5</sup> in the very early nineteenth century, and of Bragg's Law of X-ray diffraction, developed in the early twentieth century.<sup>6</sup>

There are many naturally-occurring materials and structures<sup>7,8</sup> which have the required periodicity, size of periodicity and refractive index contrast to act as “photonic crystals.” For example, in the mineral world, there is the gemstone opal;<sup>9</sup> in the animal world there are butterfly wings,<sup>10</sup> bird feathers<sup>11</sup> (e.g. peacocks, hummingbirds and kingfishers), insect casings (e.g. beetles), shells (e.g. abalone and mother-of-pearl), fish scales, snake skin and the threads and spines of the sea-mouse;<sup>12,13</sup> and in the vegetable world there are the iridescent blue leaves of the genus *Selaginella*<sup>14</sup> and the iridescent blue ripe fruits of the genus *Elaeocarpus*.<sup>15</sup> In all these examples, their vivid, shimmering colour is produced neither by the presence of transition metal ions nor of conjugated molecules (which are “expensive” in metabolic terms for an animal or plant to produce) but by the refraction, reflection and subsequent interference of visible light, brought about by the presence of a multi-layered, periodic, dielectric structure. The colour thus produced is referred to as “structural colour.”

In addition, man-made “wavelength selective” devices are not new. Plain glass can be considered a photonic material (it will bend light) and when medieval master glaziers stirred certain metallic salts into molten glass, they observed that the resulting glass was coloured – “stained” glass (Fig. 1.2).



Fig. 1.2 Stained glass window in York Minster ([www.york.ac.uk](http://www.york.ac.uk))

The glaziers were unknowingly, by adding the salts, creating nanoparticles of metals within the glass, which refracted specific wavelengths of light, by the phenomenon which later became known as Rayleigh Scattering.<sup>16</sup> Specific metals created specific colours: e.g. gold nanoparticles caused red colouration, manganese caused purple, iron caused yellow and cobalt caused blue.

## 1.2 Methods by which White Light can be made to produce Colours.

Interference<sup>17</sup> is the interaction of two or more wave motions affecting the same part of a medium so that the instantaneous disturbances in the resultant wave are the vector sum of the instantaneous disturbances in the interfering waves. Put more simply, when two (or more) waves interfere, they can do so in two extreme ways, with a continuum of interference between the two extremes. In one extreme, the crests and troughs can interfere constructively (crest meets crest and trough meets trough) in which case the amplitude of the wave is increased to the sum of the crests or the sum of the troughs, e.g. when the amplitudes of the interfering waves are the same then the amplitude of the resultant wave is doubled and the wavelength (colour) is reinforced. In the other extreme case, the waves can interfere destructively (crest meets trough) and if the amplitudes of the interfering waves are the same the “resultant” wave does not exist i.e. it is completely cancelled and there is no colour (light).

Refraction<sup>17</sup> occurs when light passes obliquely from one medium to another, in which its speed of propagation is altered. It is a change in direction of the path of the light ray which is brought about by the interaction of the light with the medium. The wavelength of the light increases or decreases but its frequency (the number of times that a repeated event occurs per unit time) and energy remain constant. The direction is changed in accordance with Snell’s Law, derived in 1621 by Dutch physicist Willebrord Snell (1591-1626),

$$n_1 \sin i = n_2 \sin r \quad \text{Eq. 1}$$

where  $i$  and  $r$  are respectively the angles made by the incident and refracted beam to the normal, and  $n_1$  and  $n_2$  are the refractive indices of the two media.

Thus, if the refractive indices of two materials are known for a given frequency, then it is possible to calculate the angle by which radiation of that frequency will be refracted as it moves from the first into the second material.

The greater the amount of refraction (deviation from the original path) the greater is the value of the so-called refractive index (RI, symbol  $n$ ) of the medium. The refractive index of a substance is a ratio and is therefore dimensionless. It can be defined as:

$$n = \frac{\sin(\text{angle of incidence})}{\sin(\text{angle of refraction})} \quad \text{Eq. 2}$$

or alternatively as:

$$n = \frac{\text{speed of light in material 1}}{\text{speed of light in material 2}} \quad \text{Eq. 3}$$

If the incident light is in a vacuum then the value is called the absolute refractive index. By definition, the refractive index of a vacuum is 1.0000 and the absolute refractive indices of all other materials are, by definition,  $>1$ . In practice, air makes little difference to the refraction of light (having an absolute refractive index of 1.0008). So if the incident light is in air, the absolute value of a refractive index can still be used. Refractive index also varies with the wavelength of light used to determine it - this is known as dispersion. As the wavelength increases, so the refractive index decreases, i.e. the refractive index for violet light ( $<400\text{nm}$ ) is greater than that for red light ( $\sim 700\text{nm}$ ) and therefore the wavelength at which the RI is measured should always be quoted. It is usually given for yellow light (sodium D-lines, wavelength  $589.3\text{nm}$ ).<sup>9</sup> This phenomenon of dispersion is responsible for the familiar splitting of light into its component colours by a glass prism, and for the formation of a rainbow by raindrops.

An accurate physical explanation of why light appears to travel more slowly in a medium is complex. At the microscale, an electromagnetic wave is slowed in a material because the electric field creates a disturbance in the charges of each atom (primarily the electrons) proportional to the permittivity. This oscillation of charges itself causes the radiation of an electromagnetic wave that is slightly out-of-phase with the original.

Refraction, and consequent colour production, also occurs when light is incident upon particles smaller than the wavelength of light, which are suspended diffusely throughout a medium of different refractive index. This is known as Rayleigh Scattering<sup>18</sup> and is the phenomenon by which the sky is seen as blue during the day

and reddish in the morning or evening. However, this system does not produce interference.

Refraction must not be confused with reflection,<sup>17</sup> which is the return of all or part of a beam of particles or waves when it encounters the boundary between two media. In reflection, the angle of incidence always equals the angle of reflection.

Diffraction<sup>17</sup> occurs when light spreads or bends through a narrow aperture (a thin slit) or around the edge of a barrier. The light is diffracted (deflected) from its path in a manner comparable to the refraction of light. The diffracted waves subsequently interfere with each other and depending on the phase difference, colours can be reinforced, weakened or eliminated altogether, resulting in a spectrum of colours. This is the principle of the well-known and widely-used diffraction grating. This phenomenon was first noticed by Francesco Grimaldi in the 17th century.

If the principles of “refraction by particles suspended in a medium of different refractive index” and “refraction by thin films” could be combined into a system where such particles are arranged three-dimensionally on horizontal and vertical planes which are at equal distances from each other, then interference does become possible under certain circumstances. This is the structure of the so-called “space lattice” in which the sub-microscopic particles are distributed precisely in a cubic arrangement on planes that are stacked one on top of the other. When white light is incident, changes in the angle of incidence and variation in the distance between particles causes different colours to appear. The more layers stacked on one another, the purer and more monochromatic the light reflected by the lattice becomes.

### 1.3 Young’s Theory.

According to Young’s theory,<sup>5</sup> iridescent colour, such as that produced by a film of oil on water or by the skin of a soap bubble, works in the following way: some of the incident white light is reflected from the top surface of the film. The unreflected light enters the film from the air and is bent and deflected from its path by the film’s greater density and refractive index. The wave travels on until it meets the lower surface where again some of it is reflected. This reflected light wave from the bottom



surface travels in the same direction as that reflected from the top surface and eventually rejoins it (Fig. 1.3).

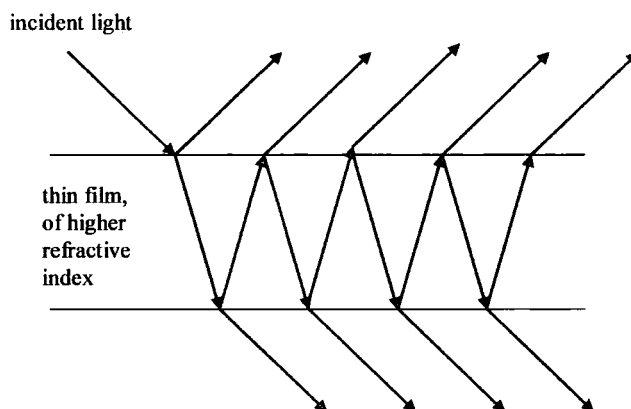


Fig. 1.3 Diagrammatic representation of passage of light through a higher refractive index thin film.

However, due to its slowed journey within the film and its reflection from the bottom surface, it may be out-of-phase with respect to the light wave reflected from the upper surface. The extent to which it is out-of-phase depends on the thickness and refractive index of the film, and on the wavelength and angle of incidence of the light. If the phase difference between the two waves is a multiple of exactly one full wavelength, then the two waves will constructively interfere (i.e. crest meets crest and trough meets trough) with each other and there will be a strong reflection of light at that wavelength. If, however, the phase of the reflected waves differs by half a wavelength or an odd multiple of half wavelengths, then the reflected waves are completely out-of-phase (i.e. crest meets trough) and destructive interference will occur at that wavelength. This is manifested by a weak or absent reflection of light at that wavelength. If it is white light that is incident, then for a given film thickness and refractive index, only one colour is of the correct wavelength to satisfy the conditions for constructive interference. In other words, when white light is directed at the thin film, only one colour will be strongly reflected at a particular angle. Constructive and destructive interference will be strongest and the reflected colour purer, if the waves reflected from each surface have the same amplitude, that is, if their crests and troughs are of equal height. This in turn relies upon the relative refractive indices of the air and the film, and on the angle of incidence of the light onto the surface. If there existed a material with an ordered series of parallel thin films, then even



stronger constructive interference could occur for the correct thickness, refractive index and incident angle conditions. Consequently, the purist, most intense “metallic” colours (wavelengths of light) would be reflected.

#### 1.4 Bragg’s Law.

William Lawrence Bragg (son of William Henry Bragg) observed that X-rays, which are a few nanometres in wavelength, are reflected (rejected) from the atomic planes in crystals for certain limited angles of incidence, and that these “reflected” rays produced a pattern of more bright, less bright and dark points on photographic film.<sup>6</sup> To explain these observations, Bragg reasoned that an X-ray which has been reflected from a single atom in an internal layer of the crystal has travelled further than a ray reflected from the surface of the material ( $x + y$  in Fig. 1.4 below).

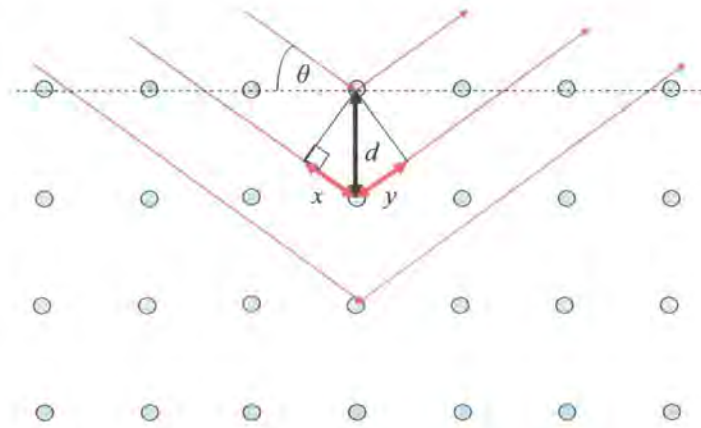


Fig. 1.4 Diagram of Bragg Diffraction.

These observations gave rise to the famous Bragg equation:

$$\begin{aligned} \text{Extra distance travelled} &= x + y = n\lambda \\ &= 2d\sin\theta \end{aligned} \quad \text{Eq. 4}$$

If this extra distance, which depends on the separation of the layers ( $d$ ) and the incident angle ( $\theta$ ) at which the X-ray entered the material, is equal to a whole number of wavelengths ( $n\lambda$ ) of the ray, then both waves are exactly in phase (i.e. crest meets crest and trough meets trough), the signal is reinforced and a bright spot results. If, however, the extra distance travelled is equal to a multiple of  $n\lambda/2$ , then the waves are exactly out of phase (i.e. crest meets trough), the signals cancel each other and a dark

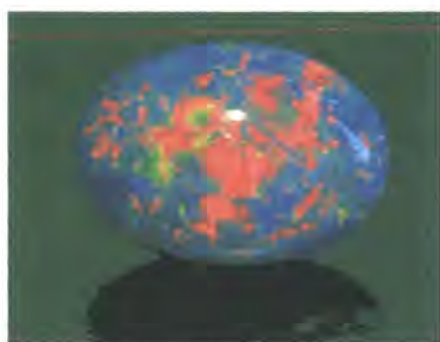
spot results. In their work, the Braggs found that the most important factor for production of interference was the maintenance of equal distances between vertical particle levels, whilst the position of the particles within levels (horizontally) was relatively unimportant.

Bragg's law can apply to any electromagnetic wave in any periodic object, provided the wavelength and the periodicity are of corresponding size.

## 1.5 Natural Photonic Materials.

### 1.5.1 Mineral.<sup>9</sup>

The rock opal occurs naturally in many locations in the world and has long been valued as a semi-precious gemstone (Fig 1.5a). It is formed in either a sedimentary or a volcanic environment and is composed of an hexagonal cubic close packed (*ccp*) array of amorphous silica spheres (Fig.1.5b).



[www.egemstones.com](http://www.egemstones.com)

Fig. 1.5a Polished opal.



[www.ias.ac.in](http://www.ias.ac.in)

Fig. 1.5b ESM of opal structure  
(with larger debris on top.)

The spheres usually range in size between 150nm and 900nm, but have a narrow size distribution (around 5% variation) within any given specimen. The lattice spacing of the spheres is of the correct size to diffract visible light and the bright colours of the gemstone result from Bragg reflection of incident light from these spheres, with spheres at the smaller end of the scale producing blue colouration and those at the larger end producing red. The regularity of the packing affects the stone's brilliance. The impurities present in natural opal are commonly located in the octahedral and tetrahedral interstices in the lattice. Whilst these also colour the opals and enhance their value as gemstones, they limit the stone's potential as a photonic crystal because



they reduce the refractive index contrast which can be obtained between the particles (silica spheres) and voids (surrounding medium, usually air) in the lattice. Hence, it is desirable to form synthetic opal in clean laboratory conditions, to ensure that the interstices are empty and can be used to modify the properties of the photonic crystal. As ever, nature disobligingly fails to fall neatly and unequivocally into any man-made categories and in some texts opal is given as an example of a 2-D photonic crystal and in others as an example of a 3-D photonic crystal.

### 1.5.2 Animal.<sup>8</sup>

The iridescent colours in butterflies' wings, and in particular the bright blue colour of the *Morpho* family (Fig. 1.6a) of tropical butterflies, are derived from constructive interference of light caused by the multiple-slit structure of scales (Fig. 1.6b) on the wing surfaces, giving a "thin film" effect.



Fig. 1.6a *Morpho* butterflies.  
([www.museums.norfolk.gov.uk](http://www.museums.norfolk.gov.uk))

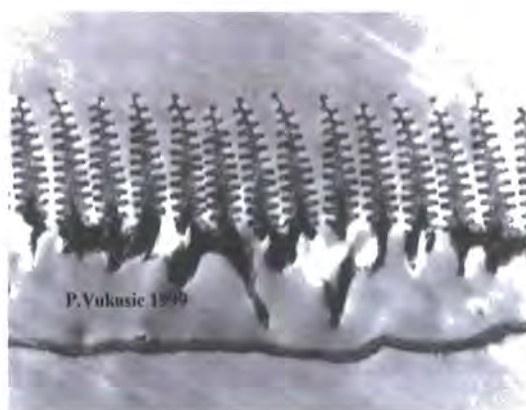


Fig. 1.6b ESM cross-section of butterfly wing scale. ([www.newton.ex.ac.uk](http://www.newton.ex.ac.uk))

The cells on the surface of the wing form an array of slits, which contain a serrated structure. These serrated projections form a multilayer of alternating chitin and air, in which the refractive index alternates between 1.54 and 1.00 respectively. Blue light has a wavelength range of 400 - 480nm, and is the only wavelength that is interfered with constructively by the slits, which are 200nm apart. The slits are attached to a base of melanin, a pigment that absorbs other wavelengths of light, further strengthening the blue appearance. The interference nature of this structural colour on the butterfly wing can be demonstrated by placing a drop of e.g. acetone on the wing, thus displacing the air in the slits and decreasing the contrast in refractive index to

1.54 and 1.36 respectively. This has the effect of changing the colour of the wing from blue to green, but the blue colour returns when the acetone evaporates.<sup>7</sup>

### 1.5.3 Vegetable.<sup>14,15,19</sup>

Although relatively common in animals and marine algae, thin film interference is rare in land plants. However, there is a small group of tropical plants which do exhibit iridescence. Several species of the genus *Selaginella*, (relatives of the ferns and found in the undercanopy of the Malaysian tropical rain forest), the ferns *Danaea nodosa* and *Trichomanes elegans* all have bright blue iridescent leaves. In the first two, the thin film interference is caused by the presence of a two-(or more) layered structure of cellulose located within the cell walls. The layers are about 74 – 94nm thick, which is in close agreement with the film thickness calculated to reflect blue light preferentially.

In *T. elegans* it has been suggested that the “layers” are multiple grana stacks. Leaf iridescence is thought to be an adaptation to low light levels, as is found in an undercanopy, as analysis has shown that compared to green leaves of the same species, the blue leaves of *Selaginella* (Fig. 1.7) are able to absorb more radiation in the longer (redder) wavelengths of the visual range, which are more readily available for photosynthesis in deep shade. In addition, *Selaginella* plants, which have iridescence when grown in the shade, do not develop the structure or display iridescence when grown in full sunlight.



Fig. 1.7 *Selaginella willdenovii* ([www.tfeps.org](http://www.tfeps.org))

The ripe fruits of most of the species of *Elaeocarpus*, a tree genus native to Asia and Australasia, also have blue iridescence, with those of *E. angustifolius* (Fig. 1.8) displaying particular brilliance.



Fig. 1.8 *Elaeocarpus angustifolius* ([www.ctahr.hawaii.edu](http://www.ctahr.hawaii.edu))

The thin film interference here is also due to cellulose layers in the cell wall and this allows longer wavelengths to penetrate into the fruit where they can be used photosynthetically to aid ripening. However, the colour does not fade after ripening suggesting that the colour may be involved in attracting birds and small mammals to eat and disperse the fruits.

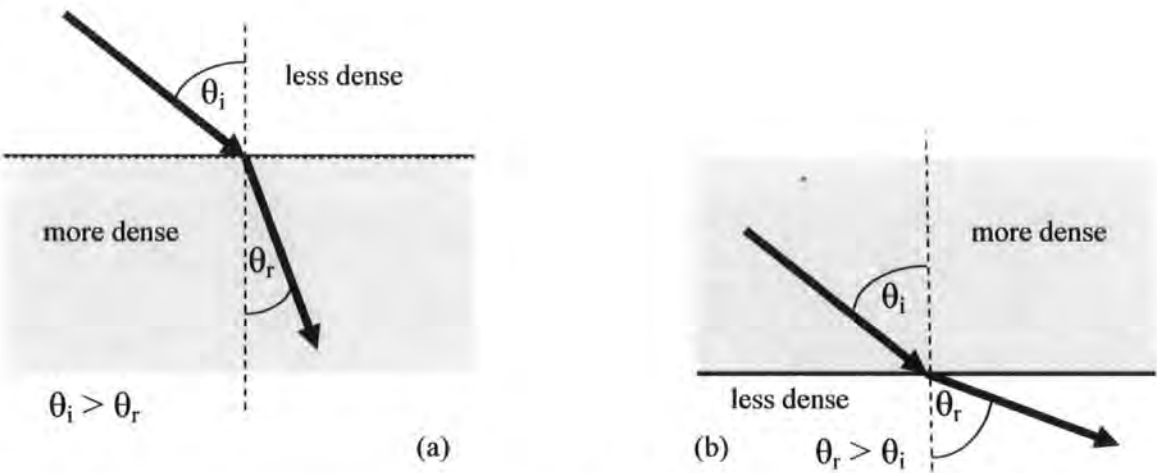


1.6 Synthetic Photonic Materials.

Synthetic photonic materials and devices are used to manipulate and control the flow and direction of light over long distances. These devices are most familiar in applications such as optical fibres. The fibres operate by two main mechanisms: those guiding by total internal reflection (index-guiding or high-index core fibres) and those guiding by photonic band gap (low-index core fibres) effect.<sup>20</sup>

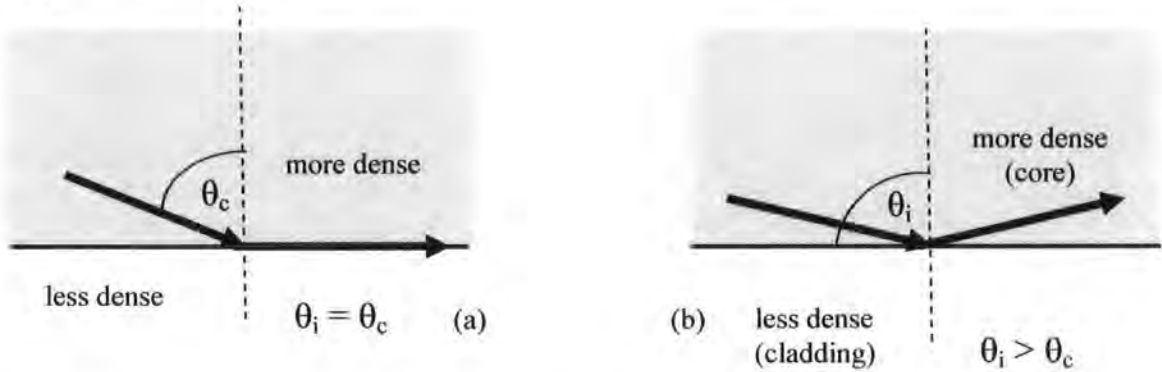
1.6.1 Total Internal Reflection.

When a wave travels from a less dense (lower refractive index) to a more dense (higher refractive index) medium (Fig 1.9a), the angle of incidence is greater than the angle of refraction ( $\theta_i > \theta_r$ ). However, when the situation is reversed and a wave travels from a more dense to a less dense medium (Fig. 1.9b), then the angle of incidence is less than the angle of refraction ( $\theta_i < \theta_r$ ).



Figs. 1.9a,b Refraction between two media of differing Refractive Indices.

As the angle of incidence ( $\theta_i$ ) increases, the angle of refraction ( $\theta_r$ ) will reach  $90^\circ$  before the angle of incidence does. This occurs when the angle of incidence is equal to the so-called “critical angle” ( $\theta_i = \theta_c$ ) and then the wave is neither refracted nor reflected but travels parallel to the interface (Fig 1.10a). If the angle of incidence is then increased even further, so that it is greater than the critical angle ( $\theta_i > \theta_c$ ), the wave is totally reflected, as if the interface of the two media were a perfect mirror (Fig.1.10b).



Figs. 1.10a,b Refraction between two media of differing Refractive Indices, at  $\theta_i \geq \theta_c$ .

In index guiding fibres, the light is “held” within an optical fibre by this physical mechanism of total internal reflection (TIR).<sup>21</sup> The light travels along a transparent fibre (the core) which is surrounded by another material (the cladding) which has a refractive index sufficiently different to, and relatively lower than, the core, causing the light to be reflected back into the core from the interface between the two materials. Thus, light in a fibre propagates by repeated total internal reflection at the core/cladding interface.

The critical angle is determined solely by the refractive indices of the materials at the interface and the greater a material’s index of refraction, the smaller its critical angle.<sup>22</sup>

$$\theta_c = \sin^{-1}(\eta_{\text{cladding}}/\eta_{\text{core}}) \quad \sin\theta_c = \eta_{\text{li}} \quad \text{Eq. 5}$$

Consequently, the more likely a ray of light will strike the inner surface at an angle greater than the critical angle and be internally reflected.

Another measure of light trapping in a fibre is the numerical aperture,  $N_A$ , where<sup>22</sup>:

$$N_A = (\eta_{\text{core}}^2 - \eta_{\text{cladding}}^2)^{0.5} \quad N_A = \eta_{\text{li}} \sin\theta_{\text{max}} \quad \text{Eq. 6}$$

In practice, however, the mechanism of TIR in fibre optics is never perfect and there is always some “leakage” of light from the more-dense core into the less-dense cladding, making the process inefficient. In particular, if the cable makes a tight curve, the angle of incidence at the interface of the two materials is too large for TIR to occur, and light escapes at this point and is lost.

### 1.6.2 The Band Gap Effect.<sup>3</sup>

The reflectivity/transmission of e.g. a 1-D photonic crystal can be calculated as a function of frequency. If the reflectivity (or transmission) is plotted versus frequency (or wavelength) for the special case of the so-called “quarter-wave stack,” in which the optical thickness ( $nd$ , where  $n$  = refractive index and  $d$  = thickness) of each of the high and low index layers is equal to  $\lambda/4$ , then it is possible to see (Fig. 1.11) that over a frequency ( $\nu$ ) range centred on  $\nu = c/\lambda_0$ , there is a spectral range in which light is wholly reflected (and in which zero light is transmitted) and thus cannot propagate through the crystal.

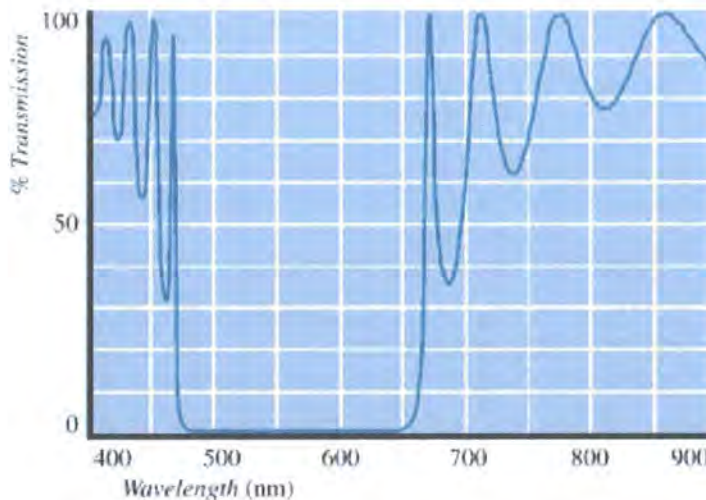


Fig. 1.11 Transmission vs. wavelength for a so-called “quarter-wave stack.”  
([www.omegafilters.com](http://www.omegafilters.com))

This spectral range is called the “photonic band gap.” The gap has an upper ( $\nu_u$ ) and lower ( $\nu_l$ ) frequency limit and the difference between the two depends on the index difference between the layers and on the relative thicknesses of the layers. There is thus a range of wavelengths that will satisfy the periodicity of the crystal lattice. A similar system, in which the optical thickness of the high and low index layers together is equal to  $\lambda/2$ , but with the thicknesses of the layers differing from  $\lambda_0/4n_H$



and  $\lambda_0/4n_L$ , will also have a photonic band gap but its width will be reduced compared to that of the quarter-wave stack.<sup>3</sup>

Photonic crystals can therefore be tailored in which certain frequencies of light are totally inhibited. However, 1-D and 2-D crystals will only inhibit these frequencies at certain angles of incidence. For a crystal to inhibit the propagation of light regardless of its direction, then the periodicity must be in 3-D. The crystal is then said to have a “total” photonic band gap.

Photonic band gap (PBG) crystals therefore offer a much better, more efficient method of guiding light along an optical fibre core: whereas by TIR there is always some leakage of light through the cladding, by using a PBG crystal as a cladding, the light is simply “forbidden to exist” in the cladding and all the light remains within the core, even when the fibre undergoes a sharp change of angle.

## 1.7 Polymers used in Optical Applications.

### 1.7.1 Introduction.<sup>23</sup>

Polymethacrylates commonly employed in optical communications have the drawback of having a small transparency window (560 - 670nm) compared with the broad range of wavelength allowed by glass and silica fibres. This is ascribed to the absorption of the overtone of the C-H stretching vibration. Replacement of the hydrogen atom(s) by heavier atoms such as deuterium, fluorine or chlorine weakens these absorption bands and consequently improves the optical transparency. These heavier atoms can be introduced either in the ester groups or in the vinyl groups of the methacrylate monomers.

### 1.7.2 Low Refractive Index Materials.

The decrease in refractive index (RI) that is observed in fluorine-substituted hydrocarbon chains (Table 1.1) is the result of several effects. Fluorine replacement for hydrogen is known to decrease local electronic polarisation and is thought to increase fractional free volume. Both of these effects can independently decrease RI.<sup>24</sup>

Due to the strong mutual attraction between the electrons and the nucleus of the fluorine atom, its polarisation is small and the electronegativity of covalently-bonded fluorine is the highest (4.0, Pauling scale)<sup>25</sup> among all the elements. In addition, the length of the C-F bond is short (0.132nm)<sup>26</sup> (carbon-fluorine bonds are highly polar) and the bonding energy is higher (540kJ.mol)<sup>26</sup> than that of other bonds. As a result, the polarisability of the C-F bond becomes smaller, lowering the RI and dielectric constant of fluorine compounds. The C-F bond strength increases with the extent of adjacent carbon fluorination; thus the longer the fluoroalkyl chain, the higher its stability.<sup>27</sup>

Many fluorine-containing monomers are commercially available and as these can be polymerised into low RI homopolymers, they have already found applications in the photonic technologies industry.

Table 1.1      Refractive Indices for fluorinated and non-fluorinated analogues.  
(Taken at N<sub>20</sub>D; 589nm)

Fluoro monomer/polymer	RI	RI	Comparative hydrocarbon monomer/polymer
2,2,2-trifluoroethyl methacrylate	1.36 <sup>A</sup>	1.41 <sup>A</sup>	ethyl methacrylate
poly(2,2,2-trifluoroethyl methacrylate)	1.42 <sup>A</sup> 1.40 <sup>B</sup>	1.48 <sup>B</sup> 1.49 <sup>C</sup>	poly(ethyl methacrylate)
1H,1H,2H,2H-perfluorohexyl methacrylate	1.35 <sup>A</sup>	1.43 <sup>A</sup>	<i>n</i> -hexyl methacrylate
poly(hexafluoroisopropyl methacrylate)	1.39 <sup>A</sup>	1.55 <sup>C</sup> 1.47 <sup>D</sup>	poly( <i>isopropyl</i> methacrylate)
pentafluorostyrene monomer	1.45 <sup>D</sup>	1.55 <sup>A</sup>	styrene monomer
poly(tetrafluoroethylene)	1.35 <sup>D</sup>	1.49 <sup>C</sup>	polyethylene

<sup>A</sup> Ref. 28; <sup>B</sup> Ref. 29; <sup>C</sup> Ref. 30; <sup>D</sup> Ref. 31.

### 1.7.3 High Refractive Index Materials.

Aromaticity and bromine-substitution are found to increase RI of monomers relative to the comparable hydrocarbon analogue (Table 1.2). This is known experimentally and by various group contribution theories.<sup>30</sup>

Table 1.2      Refractive Indices for brominated and non-brominated analogues.  
(Taken at N<sub>20</sub>D; 589nm)

<b>Bromo monomer/polymer</b>	<b>RI</b>	<b>RI</b>	<b>Comparative hydrocarbon monomer/polymer</b>
4-bromostyrene monomer	1.59 <sup>A</sup>	1.55 <sup>A</sup>	styrene monomer
poly(4-bromostyrene)	not found	1.59 <sup>A</sup>	polystyrene
poly(pentabromophenyl methacrylate)	1.71 <sup>A</sup>	1.57 <sup>B</sup>	poly(phenyl methacrylate)
poly(pentabromobenzyl methacrylate)	1.71 <sup>A</sup>	1.57 <sup>A</sup>	poly(benzyl methacrylate)
poly(2,4,6-tribromophenyl methacrylate)	1.67 <sup>A</sup>	1.57 <sup>B</sup>	poly(phenyl methacrylate)
poly(4-bromophenyl methacrylate)	1.60 <sup>B</sup>	1.57 <sup>B</sup>	poly(phenyl methacrylate)

<sup>A</sup> Ref. 28; <sup>B</sup> Ref. 31

## 1.8 Methods of Making Synthetic Photonic Crystals.

### 1.8.1 Inverse Opals.<sup>32</sup>

Nanofabrication methods can be divided into roughly two groups: the “top-down” approach, whereby a pattern made on a large scale is reduced in its lateral dimensions to form a nanostructure, and the “bottom up” approach, whereby molecules are built up into nanoscale structures through exploitation of self-assembly or self-organisation propensities. A method which seems to combine elements of both these approaches is the formation of so-called inverse opals.

In natural, silica-based opal, the refractive index contrast (RIC) (from 1.435 to 1.460) is below that required for achievement of a complete band gap in a crystal with conventional symmetry, although it may be sufficient in 2-D systems or in quasicrystalline arrangements. The RIC can be enhanced by using spheres formed from a higher refractive index material or by filling the interstices with a second material that has a higher refractive index. The RIC of the latter can be further enhanced if the spheres can be removed from the structure to leave air-filled spherical

voids. Such a material is termed an “inverse opal” and can be visualised as a close-packed array of air spheres, with the interconnected octahedral and tetrahedral interstices filled with a high refractive index material.

### 1.8.2 Lithographic Techniques.<sup>33-37</sup>

Photonic crystals can be made from a slab of solid dielectric material by the process of lithography, i.e. the removal of material by exposure to light, often through a template, to form the target nanostructure - a so-called “top-down” method. The refractive index contrast is then between the material and air. However, one of the problems of this method is that the required photonic lattice scale becomes more difficult and more expensive to reach, compared to the conventional lithographic processes of the semi-conductor industry. The method is also restricted to planar precursors and does not enable the formation of 3-D photonic crystals.

### 1.8.3 Block Co-polymer Self-Assembly.<sup>38-42</sup>

Synthetic materials which have precise, nano-sized (10 - 100nm) microstructures are most likely to be polymers, which are macromolecules consisting essentially of a repetition of relatively simple monomers. In particular, the 1-, 2- or 3-D periodic morphologies favoured by block co-polymers, and their ability to self-assemble (“bottom-up”) into them, suggest themselves as photonic crystals. The size, location and symmetry of the band gap are determined by the structure and dielectric properties of the components. Essential to the design of block co-polymer photonic crystals is the achievement of high molecular weight and high dielectric contrast between the blocks, whilst maintaining low absorbance in the frequency of interest. Synthetic polymeric materials capable of self-assembling into photonic “crystals” could therefore consist of block co-polymers of high and low refractive index (RI) monomers such as styrene (RI = 1.55)<sup>28</sup> with fluoromethacrylate (RI = 1.33-1.36),<sup>28</sup> monobromostyrene (RI = 1.59)<sup>28</sup> with methyl methacrylate (RI = 1.49)<sup>28</sup> and monobromostyrene with fluoromethacrylate. Each of these systems would have a large refractive index contrast. Block co-polymers also offer the opportunity to tailor the periodicity and topology of the “crystal.” However, their structure has to be precise, and to achieve this level of precision, a stepwise synthesis and a controlled (living) method of polymerisation is required.

## 1.9 Living Anionic Polymerisation.

### 1.9.1 Introduction.<sup>43-46</sup>

Living anionic polymerisation (LAP) is a chain polymerisation (repetitive conjugate addition reaction, Fig. 1.12) carried out in solution, in which the initiator/propagating species is anionic (nucleophilic), all polymer chains are initiated at once and there are no intrinsic termination reactions.

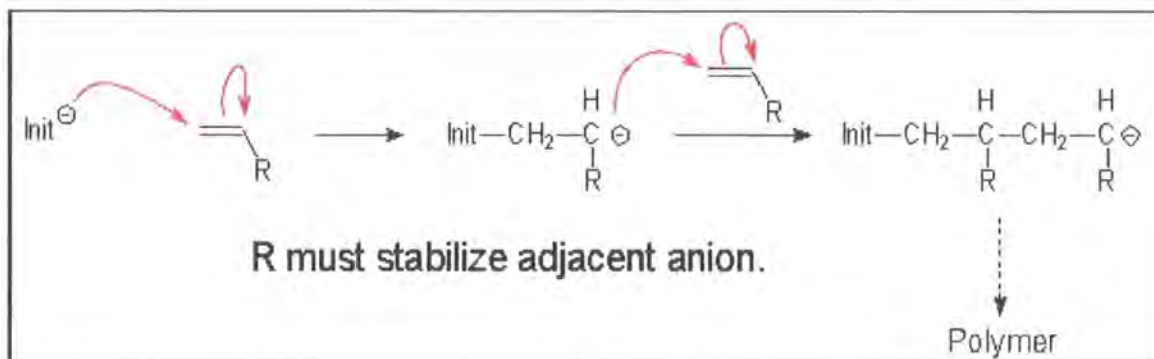


Fig. 1.12 Mechanism for Living Anionic Polymerisation. ([www.chem.rochester.edu](http://www.chem.rochester.edu))

Chain growth by LAP is generally rapid at low temperature but the rate is less sensitive to changes in temperature than chain growth by cationic polymerisation. Their discovery (in the 1950s) has recently been reviewed by one of their discoverers, Szwarc<sup>47</sup> and the experimental techniques involved have been reviewed by Mays.<sup>48</sup>

LAP provides a versatile method for the preparation of macromolecules with well-defined structures and low levels of compositional heterogeneity. Using LAP, it is possible to synthesise polymer molecules whilst exercising control over a wide range of their compositional and structural parameters, such as molecular weight, molecular weight distribution, co-polymer composition, branching and chain-end functionality. The preparation of such well-defined polymers, however, requires stringent conditions: high monomer and solvent purity, and the reduction to negligible levels in the system of impurities and proton donors such as water, alcohols, molecular oxygen and carbon dioxide, all of which would cause the occurrence of unwanted chain termination and chain transfer reactions. In addition, the monomer molecules must not undergo side reactions with each other. All these conditions are required to reach the narrow polydispersities ( $M_w/M_n < 1.05$ ) characteristic of LAP.

In LAP, there can be no termination or chain transfer reactions, as suggested above, and therefore the only elementary reactions which occur within the system are initiation and propagation, the rate of the former being competitive with<sup>46</sup> or comparable to<sup>49</sup> the rate of the latter. That is, the rate constant of initiation is at least as large as the rate constant of propagation ( $k_i \geq k_p$ ).<sup>50</sup> There must be only one propagating species in solution and the propagation steps must be irreversible. The number of initiated chains (growing polymer molecules) is equal to the number of active initiator molecules added, with molecular weight being inversely proportional to that number. Propagation takes place equally with respect to all the chains, with the chains retaining their activity, even after the monomer has been entirely consumed. The target molecular weight for a polymer prepared by LAP using a monofunctional initiator is thus calculated from:<sup>45,46</sup>

$$M_n = \frac{\text{grams of monomer}}{\text{moles of initiator}} \quad \text{Eq. 7}$$

For calculation of molecular weight when using a difunctional initiator, the denominator is reduced by 0.5.<sup>45,46</sup>

For anionic polymerisation to occur, the carbanion formed must be stabilised by the presence of strongly electron-withdrawing groups on the molecule, e.g. acrylonitrile, vinyl chloride, methyl methacrylate or styrene, and for initiation to be successful, the free energy of the initiation step must be favourable. Therefore, it is necessary to match the monomer with the appropriate strength of initiator. The greater the electron-withdrawing power of the groups, then the more strongly the carbanion is stabilised and the less strong (in nucleophilic terms) the initiator needs to be. Conversely, the weaker the electron-withdrawing groups, then the stronger the initiator needs to be.

The anionic propagating species carries a cationic counter-ion (the gegen-ion) and the closeness/separation of the ion pair is strongly affected by the reaction conditions, which in turn affect the rate of propagation. The closer the ion pair, the slower the rate of propagation. Increasing the polarity of the solvent encourages the separation of the ion pair, and therefore the rate of polymerisation increases with increasing polarity of the solvent (Table 1.3).

Table 1.3      Relative Polarity of Solvents.

Solvent	toluene	benzene	dioxane	tetrahydrofuran	1,2-dimethoxyethane
Relative Polarity <sup>A</sup>	0.099	0.111	0.164	0.207	0.231
increasing rate of reaction →					

<sup>A</sup> Ref. 51. The values are normalized from measurements of solvent shifts of absorption spectra.

Similarly, larger counter-cations usually form less close ion pairs, so there is an increase in rate on descent of the Periodic Table (Table 1.4).

Table 1.4      Ionic Radius of Counter (gegen) Ions.

Counter-ion	Li <sup>+</sup>	Na <sup>+</sup>	K <sup>+</sup>	Rb <sup>+</sup>	Cs <sup>+</sup>
Radius (Å) <sup>A</sup>	0.60	0.95	1.33	1.48	1.69
increasing rate of reaction →					

<sup>A</sup> Ref. 52.

An important application of LAP is the synthesis of block co-polymers by sequential monomer addition. This facility is a direct consequence of the stability of the polymeric carbanion. A carbanion chain formed from one monomer can form the chain end of another monomer, provided that the new carbanion species is of equal or greater stability (and thus equal or less reactivity) than the first carbanion species. The first monomer carbanion is able to initiate the polymerisation of the second, i.e. the first monomer carbanion must be a stronger nucleophile than (or as strong a nucleophile as) the second monomer carbanion. Successful block co-polymer synthesis therefore depends on the relative reactivity of the propagating carbanion species, and a consideration for the design and preparation of block co-polymers is the order of monomer addition: the monomers cannot be added to the reaction randomly but must be added in a specific order, determined by their relative reactivity. In general, the ease with which suitable monomers under go anionic polymerisation increases in the order:<sup>53</sup>

butadiene<isoprene<styrene(s)<methyl methacrylate(s)<vinyl chloride<acrylonitrile

After the complete consumption of the first monomer, the second monomer is added and again allowed to run to completion, at which stage a terminating agent is added, e.g. methanol, and the diblock polymer can be isolated, usually by precipitation in a non-solvent, and collected by filtration.

The anionic polymerisation of methacrylates (and acrylates)<sup>46,54</sup> is complicated by chain termination reactions, chain transfer reactions, and side reactions of the monomer at the ester (carbonyl) group instead of the vinyl group, not only with anionic initiators but also with the growing anionic chain ends. However, a controlled polymerisation of methyl methacrylate can be carried out by optimising the effects of counter-ion, solvent, temperature and monomer concentration, and careful choice of initiator.

An initiator for methyl methacrylate may not only react with the vinyl group to give the desired, conjugate “Michael (1,4-) addition” but can also react with the ester (carbonyl) group to give the undesired “Claisen (1,2-) condensation.” The latter can be avoided if the initiator has approximately the same stability as the (desired) propagating-chain-end carbanionic species, and one measure of the stability of a carbanion is the  $pK_a$  of the corresponding conjugate acid. The most useful initiator in this respect has been found to be 1,1-diphenyl-3-methylpentyl lithium, which is formed easily *in situ* by the addition of 1,1-diphenylethylene (DPE) to *sec*-butyllithium in solution (Fig. 1.13).

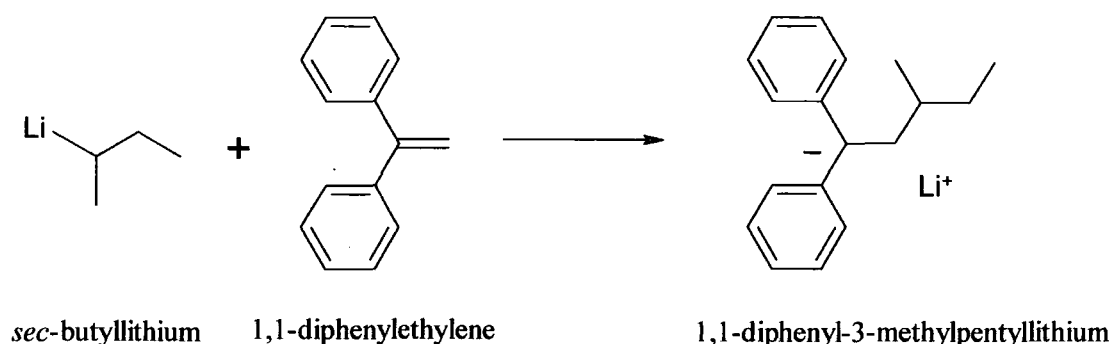


Fig. 1.13 Formation of 1,1-diphenyl-3-methylpentyllithium.

This bulky initiator prevents attack at the carbonyl centre by steric hindrance during initiation and the carbanionic unimer thus formed is an insufficiently strong nucleophile to instigate the unwanted carbonyl attack. That is, the  $pK_a$  of diphenylmethane (the conjugate acid of the 1,1-diphenyl-3-methylpentyl carbanion) is 32,<sup>46</sup> which is approximately the same as that of the conjugate acid of the propagating ester enolate anion of poly(methyl methacrylate) (ethyl acetate,  $pK_a = 31-32$ ).<sup>46</sup> The reaction therefore proceeds in the desired, conjugate “Michael” addition mode.



Diphenylethylene, which is non-polymerisable itself, can also react with growing chains (e.g. polystyrene), reducing their activity and therefore enabling the preparation of block co-polymers of styrene and methyl methacrylate.<sup>55</sup>

The controlled anionic polymerisation of methyl methacrylate is further hampered by the presence of a multiplicity of active species in equilibrium (Fig. 1.14).

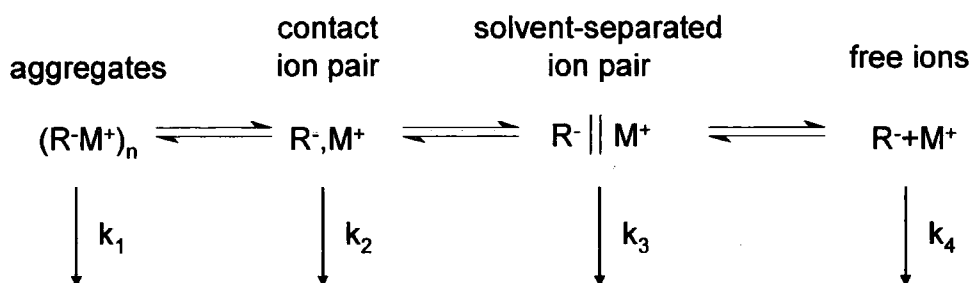


Fig. 1.14 Active species present in LAP of methyl methacrylate.

Each of these can propagate with the monomer under certain conditions, but at different rates, with the aggregated species having much lower reactivity. However, the addition of lithium chloride<sup>46,54,56-61</sup> to the system causes a decrease in aggregation, thus depleting the system of the slowly interconverting aggregates. Instead, the formation of a 1:1 complex between the propagating lithium enolate and lithium chloride (Fig. 1.15) has been suggested.

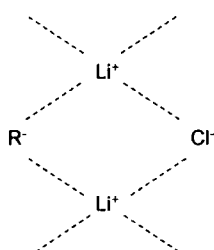


Fig. 1.15 Suggested structure of enolate/lithium chloride complex.

The structure is said to prevent termination and transfer reactions. Best results are achieved when the lithium chloride:initiator ratio is between 3:1 and 10:1, with the optimum at 5:1. The use of a polar solvent such as tetrahydrofuran (THF) (compared to a non-polar solvent such as toluene) also tends to shift the equilibrium of Fig 1.14 towards the right, i.e. towards more dissociated species.

Anionic polymerisation of methyl methacrylate will not occur at ambient temperatures, because the ester groups will preferentially cyclise (see Fig. 1.16) into rings.

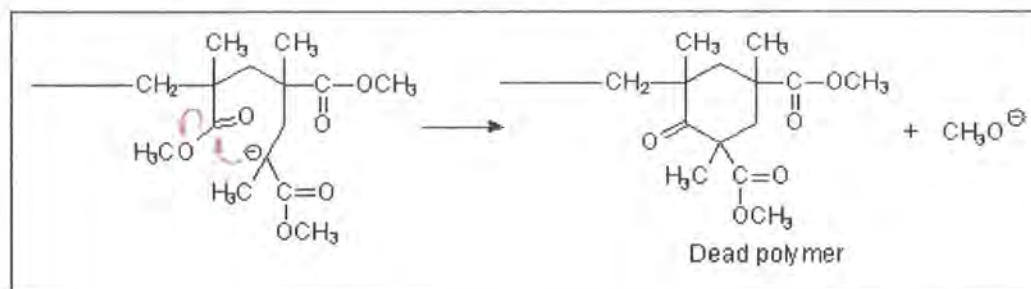


Fig. 1.16 Mechanism for cyclisation in methacrylates. ([www.chem.rochester.edu](http://www.chem.rochester.edu))

However, polymerisation can be accomplished by running the reaction at a low temperature, e.g.  $-78^{\circ}\text{C}$ , using a dry ice/acetone bath as coolant. The activation energy of cyclisation is greater than that of propagation, so the former is affected more by temperature than the latter. That is, the low temperature decreases the rate of both the cyclisation and propagation reactions, but decreases the rate of cyclisation more. The fraction of the chains which become terminated is also affected by monomer concentration: the higher the initial monomer concentration, the higher the fraction of terminated chains and conversely, when monomer is added to the reaction slowly, the formation of terminated chains is suppressed.

### 1.9.2 Screened Anionic Polymerisation.

So-called “screened” anionic polymerisation (SAP) was reported by Ballard *et al.*<sup>62</sup> in 1992. This system was developed in response to the low temperatures required (from  $-40^{\circ}\text{C}$  to  $-100^{\circ}\text{C}$ ) for the living anionic preparation of poly(methyl methacrylate) using lithium alkyls as initiators. At higher temperatures, termination reactions occur, in which the carbanion, in the predominant (non-propagating) resonant form, reacts intramolecularly with adjacent ester groups to form a ring-structure as already mentioned in Section 1.9.1 above. This situation can be avoided if the stability of the propagating resonant carbanion form is increased by increasing the cross-section of the gegen-ion. Ballard formed his anionic initiator and cationic gegen-ion by the reaction between tri-*iso*-butylaluminium and *tert*-butyllithium. In hydrocarbon solvents, such as toluene, the separation of the ions is minimised and the bulky gegen-

ion “screens” the propagating centre of the polymer chain from unwanted side-reactions. Solvents which cause the ion pair to separate, such as tetrahydrofuran, inactivate the system. Polymerisation of methyl methacrylate could be successfully carried out at 0 - 40°C in toluene solution, when this ion pair was used, making a more realistic method for industrial production. Ballard used this system to prepare a range of living methacrylate homo- and co-polymers (though none using fluoromethacrylates) in toluene, under a variety of polymerisation conditions.

In 1995, Haddleton *et al.*<sup>63</sup> elucidated the structure of Ballard’s “screening” anionic initiating complex. It had been observed that  $M_n$  of the poly(methacrylate)s differed consistently from those expected by the normal calculation (of  $M_n = [\text{monomer}]/[\text{initiator}]$ ) and could be better calculated from  $M_n = [\text{monomer}]/0.5[\text{initiator}]$ . This led to the conclusion that the tri-*iso*-butylaluminium and *tert*-butyllithium reacted together to form a new complex, which was responsible for the subsequent initiation and propagation. Investigation of the reaction between the two metal alkyls using proton nuclear magnetic resonance spectroscopy (NMR) and mass spectroscopy (MS) found that NMR showed two *iso*-butyl (<sup>*i*</sup>Bu) groups in the ratio 2:1, and two *tertiary* butyl (<sup>*t*</sup>Bu) groups in the ratio 1:1, whilst the MS showed a peak corresponding to  $\text{Bu}_4\text{AlLi}_2$ . From this evidence, it was postulated that the reaction illustrated below in Fig. 1.17 occurred.

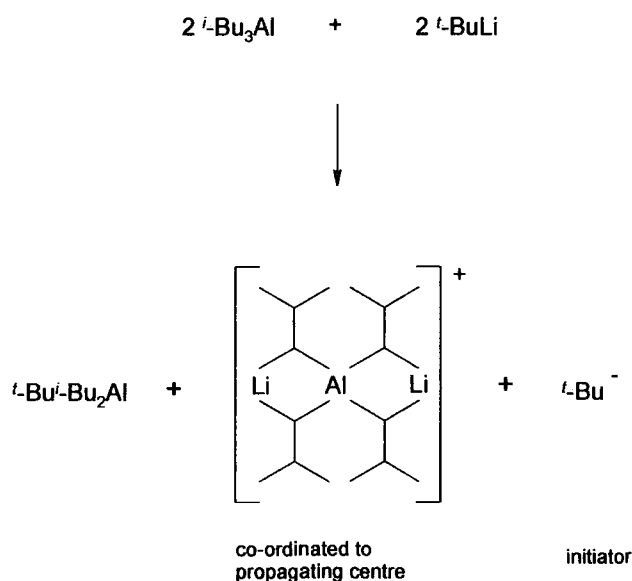


Fig. 1.17 Ballard’s screening agent, as elucidated by Haddleton.

This scheme gives one mole of the *tert*-butyl anion for every two moles of *tert*-butyllithium added, which is consistent with the observed values of  $M_n$ . The bulky aluminiumalkyl and *tert*-butyllithium complex formed was found to be extremely effective at stabilising the propagating centre of a methacrylate polymerisation in hydrocarbon solvents.

### 1.9.3 Preparation of Semifluorinated diblock Co-polymers.

In 1996, Krupers *et al.* reported<sup>64,65</sup> the preparation of block co-polymers of methyl methacrylate (MMA) and perfluoromethacrylates by the living method of nucleophilic catalysed group transfer polymerisation (GTP).<sup>65</sup> Out of six examples, the polydispersities for the MMA block were in the range 1.10 - 1.20. Experimental molecular weights (from size exclusion chromatography, SEC) for the MMA block were slightly higher than the target in four out of the six examples. For the MMA-*b*-fluoromethacrylate co-polymers, polydispersities were generally similar to those for the MMA block alone (1.09 - 1.24). Target, experimental (by SEC) and calculated (from proton NMR) molecular weights showed variation for any one example but followed no obvious pattern for the six. Yields were good (>78% w/w) except for one (55%w/w) when the target molecular weight for the prepolymer and the corresponding co-polymer were highest (19.1k and 39.3k respectively).

### 1.9.4 Modified Screened Anionic Polymerisation.

In 1997, Yong and Holmes *et al.*<sup>66</sup> suggested a modified version of the screened anionic polymerisation method developed by Ballard described above. This was specifically applied to the preparation of block co-polymers of MMA and fluoromethacrylates, for use as stabilisers in the dispersion polymerisation of methyl methacrylate in supercritical carbon dioxide (scCO<sub>2</sub>). The modification was to use *tert*-butyllithium with (2,6-di-*tert*-butyl-4-methylphenoxy)diisobutylaluminium as the initiating system. The use of 1,3-bis (trifluoromethyl) benzene as a co-solvent with toluene was also investigated, and both dihydro- and tetrahydro-fluoromethacrylates were used. Yields of 45 - 86% w/w were achieved, with ratios of MMA to fluoromethacrylate between 3:1 and 1:2.3, with experimental (by SEC) molecular weights of co-polymers between 17k and 217k and polydispersities between 1.1 and 1.5.

In 1999, Hems and Cooper *et al.*<sup>67</sup> used a different modification. The initiating complex was prepared using *tert*-butyllithium and excess triisobutylaluminium in a mixture of toluene and 1,3-bis (trifluoromethyl) benzene as solvents, the latter to overcome the relative insolubility of co-polymers with long fluorinated side chains. Co-polymers were prepared by sequential addition of MMA and 1H,1H,2H,2H-perfluorooctyl methacrylate (PFOMA) with the fluoromonomer in a 1,3-bis (trifluoromethyl) benzene solution. The progress of the reactions could be monitored by the appearance and disappearance of a characteristic yellow colour as each monomer was added and consumed. This was described as a highly controlled synthesis of fluorinated diblock co-polymers, with experimental (by SEC) molecular weights for the MMA blocks ranging from 3k to 14k, the MMA:PFOMA ratios around 1:1 and calculated (by proton NMR) molecular weights of the co-polymers ranging from 17k to 75.5k. Yields were good (>81% w/w).

#### 1.9.5 Preparation of polyfluoromethacrylates by LAP.

In 1999, Ishizone and Hirao *et al.*<sup>68</sup> carried out living anionic polymerisation of three perfluoroalkylmethacrylates, namely: 2,2,2-trifluoroethyl methacrylate (TFEMA), 1H,1H,2H,2H-perfluorohexyl methacrylate (PFHMA) and PFOMA in THF at -78°C using 1,1-diphenyl-3-methylpentyllithium (formed from 1,1-diphenylethylene and *sec*-butyllithium) in the presence of lithium chloride (amongst other conditions). The co-polymers were prepared by the addition of the fluoromethacrylate to an initiator solution. The molecular weights attempted were relatively low (target  $M_n$  not intended to be greater than 19k) and solubility problems were encountered in the preparation of both polyPFHMA and polyPFOMA. As the purpose of their preparation was merely to show that each of the monomers could be anionically polymerised in a controlled manner, Ishizone and Hirao co-polymerised these two monomers, the former with *tert*-butyl methacrylate (*t*-BuMA) as the second sequential polymer and the latter with living polystyrene as the macroinitiator. Both these steps overcame the solubility problems. The *t*-BuMA-PFHMA co-polymer had a low polydispersity (1.06) and a higher calculated (16k, by proton NMR) molecular weight than the target (12k). The yield was described as quantitative. The styrene-PFOMA co-polymer also had a low polydispersity (1.06) with the target and calculated (proton NMR) weights the same (18k) but a lower (13k) experimental (by SEC) weight.

Sugiyama and Hirao later reported<sup>69</sup> the preparation of poly(styrene-*b*-PFOMA) by polymerisation of styrene with *sec*-butyllithium, end capping with DPE, followed by polymerisation of PFOMA in the presence of lithium chloride in THF at -78°C, and the preparation of poly(MMA-*b*-PFOMA) by the same method, to be used as model polymers for elucidating the effect of the number of alkylfluorocarbon groups on the surface structure and properties of polymers. The co-polymers are described as possessing well-controlled structures with respect to chain length and composition.

Yoshida *et al.*<sup>70</sup> reported in the year 2000 the synthesis by LAP of co-polymers of *tert*-butyl methacrylate with 1H,1H-perfluorooctyl methacrylate (*sic*), using 1,1-diphenylhexyllithium and lithium chloride in THF at -78°C. These were particularly made for their potential self-assembly into micelles in scCO<sub>2</sub> and were characterised by light scattering studies. The polydispersities of the block co-polymers as well as their prepolymers were claimed to be narrow. Yields ranged from 12% w/w to 98% w/w, molar ratios from 1:3 to 3:1 and co-polymer molecular weights from 44.7k to 336k (by proton NMR).

### Conclusion.

From this brief review (Section 1.9), it was concluded that little investigation had been made of the preparation of styrene-fluoromethacrylate block co-polymers by LAP, nor of their potential as photonic materials.

## 1.10 Methods of Polymer Analysis.

### 1.10.1 Size Exclusion Chromatography.<sup>71</sup>

Size Exclusion Chromatography (SEC) is a chromatographic method by which the molecular weight distribution of a polymer may be determined. The stationary phase consists of a column of porous gel, the pores of which cover a known range of sizes, and the moving phase consists of a high-quality solvent, pumped at a known, constant flow rate. A solution of the polymer in the running solvent is injected into the system to pass through the column. The largest molecules elute from the column first, because there are fewest pores through which they can pass, i.e. if the hydrodynamic radius ( $R_h$ ) of the molecule is greater than the diameter ( $d$ ) of a pore, then the chain would have to “collapse” in order to fit inside the pore. Such a collapse is entropically unfavourable, as it would reduce the number of configurations available to the chain. The largest chains therefore have the fastest passage through the stationary phase. Conversely, the smallest molecules will elute last, as there are most pores through which they can permeate and their passage through the stationary phase is slowest. Molecules of intermediate size elute at intermediate volumes and times as appropriate. Detection is by refractive index, UV/visible radiation or light scattering, or a combination of these.

Sample polymers are run against a calibration curve of known elution times/volumes for carefully prepared polymer standards of narrow polydispersity and defined peak molecular weight. These standards are commercially available but only in a limited range of common homopolymers e.g. polystyrene, poly(methyl methacrylate), poly(ethylene oxide). Thus, if the sample polymer is none of these, or is a copolymer, it is, strictly speaking, the “hydrodynamic volume” distribution of the sample polymer which is determined, relative to the standards used and in the specified solvent.

The ideal shape of an SEC trace for a polymer prepared by LAP is symmetrical, monomodal, Gaussian and with low ( $<1.05$ ) polydispersity.

### 1.10.2 NMR Spectroscopy.<sup>72-75</sup>

Proton NMR is the most commonly used and practised and the  $^1\text{H}$  isotope occurs with almost 100% natural abundance. The signals can occur over the range +20ppm (e.g. alkylidenes) to -50ppm (e.g. metal hydrides)<sup>76</sup> but the vast majority of signals from organic compounds occur in the relatively narrow range +12ppm to -1ppm, which can lead to overlap between signals of different proton environments. However, this form of NMR gives very sharp signals and the number of each type of proton within the sample can be obtained from the integral ratios of the signals or multiplets, provided that these are well-spaced.

The isotope used to determine carbon NMR is  $^{13}\text{C}$ . Unfortunately, this has a rare natural abundance ( $\sim 1\%$ )<sup>76</sup>, giving rise to a high signal-to-noise ratio in the spectra. When run under standard conditions, the integral ratios are less definitive (compared to proton NMR) and therefore less useful as a diagnostic tool. However, used in combination with proton NMR, carbon NMR can provide valuable data, and the larger chemical shift range (0 to  $\sim 250\text{ppm}$ ) increases the effective resolution and enables analysis through the detection of all individual carbon resonances.

The isotope which is used to measure fluorine NMR is  $^{19}\text{F}$ . It occurs with 100% natural abundance and integration of peak areas can therefore, like  $^1\text{H}$ -NMR, be used confidently to determine molecular structures. The range of shifts for organic fluorides (+50 to -250ppm) is even greater than the range of carbon shifts. The value of the shifts is particularly dependant on the nature of the atoms attached to the adjacent carbon atoms. For example, the range for aromatic fluorine shifts is 80ppm, whereas the equivalent for aromatic protons is 2.5ppm (6.5 – 9ppm). This increase in range means that the position of the shifts for  $^{19}\text{F}$  are more unpredictable than for protons, and the shift ranges of different types of fluorine can overlap, thus complicating spectra interpretation. However, like carbon NMR, an advantage of this large range is the discrimination of subtler environmental influences.

However, in some cases with  $^{13}\text{C}$  and in many cases with  $^{19}\text{F}$ , the chemical shift does not easily correlate with a single structural feature, thus complicating spectra interpretation.



## 1.11 Self-Assembly, Self-Organisation and Microphase Separation.

### 1.11.1 Introduction.<sup>38-42</sup>

A definition of self-assembly, or self-organisation is the formation of reversible, thermodynamically stable, well-defined aggregates in which the bonding is through weak, non-covalent forces.

For diblock co-polymers of flexible but chemically incompatible (immiscible) and dissimilar components, self-assembly/organisation can occur by local or so-called microphase separation in the bulk (melt) or in solution (thin films). To avoid unfavourable contact, the block components align like-with-like and segregate into nanometre-scale domains, whilst complete (macrophase) separation is prevented by the covalent linkage between the two components.

The morphology of the domains is governed by the length (size) and composition of the components. As one component increases/decreases in quantity/size relative to the other, the forms generally recognised are: lamellar (layered, parallel to a substrate, occurs when the co-polymer is approximately symmetrical with respect to the size of its components), cylindrical (hexagonal columnar), bicontinuous (gyroid) and spherical (body-centred cubic) arrangement. The morphologies are illustrated below (Fig. 1.18), with the two colours representing the two components.



Fig. 1.18 Self-assembly structures for a block co-polymer.  
(after Floudas G, *et al.*, *Macromolecules* **2001** 34 2947)

The separation is driven by the need to minimise the total free energy of the system, through the optimisation of the decrease in interfacial enthalpy (favourable), which is brought about by the reduction in interactions between dissimilar components, and the inevitable entropy decrease (unfavourable), which occurs when the molecules are stretched from their “random walk” configuration.

Three dimensionless material parameters are needed for modelling the microphase separation:

- $\chi$  the Flory-Huggins interaction parameter, which is a measure of the thermodynamic interaction (incompatibility) between the two monomers and thus controls the enthalpy of the system. It is inversely proportional to the temperature of the system.
- $N$  the overall degree of polymerisation of the diblock.
- $f_A$  the relative length of the A-monomer chain compared with the length of the whole macromolecule.

These last two terms ( $N$  and  $f_A$ ) control the entropy of the system. A phase diagram for a typical diblock co-polymer, with respect to  $\chi N$  versus composition, is shown in Fig.1.19.

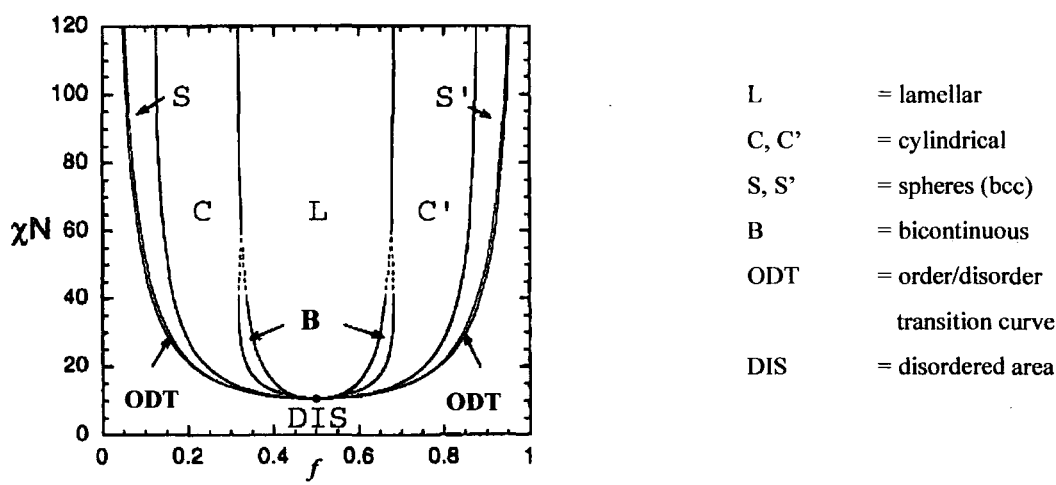


Fig. 1.19 Phase Diagram for self-assembly of a block co-polymer (after Bates & Matsen, *Macromolecules* 1996 29 1091-1098)

The order-disorder transition (ODT) curve minimum gives a critical value for  $\chi$  ( $\chi_c$ ), above which there is ordered immiscibility and below which there is miscible disorder. For a block co-polymer,  $\chi_c$  is approximately equal to  $10.5/N$ .

When the phase diagram is drawn with respect to temperature (versus composition) the shape of the ODT curve is inverted, and the maximum gives a critical value for temperature ( $T_c$ ) above which there is disorder and below which there is order. Within the ordered region, there is a further division into the strong segregation limit (SSL) region and the weak segregation limit (WSL) region.

When  $\chi N \gg 10.5$ , then  $T \ll T_c$  and the SSL applies. The interfaces between the phases are sharp, the polymer chains are stretched (compared to the “random walk” configuration) and changing the temperature does not change the microstructure, which depends only on  $f_A$ . When  $\chi N \sim 10.5$ , then the WSL applies and within this region, there are no distinct interfaces, the chains are in the “random walk” (unstretched) configuration and the microstructure varies with all three parameters ( $\chi$ ,  $N$  and  $f_A$ ).

The different microstructures arise from packing constants and minimisation of interfacial area. Consider a system in which a diblock co-polymer consists of components A and B, of equal “length” ( $D_1$  and  $D_2$  respectively) as represented in Fig. 1.20:

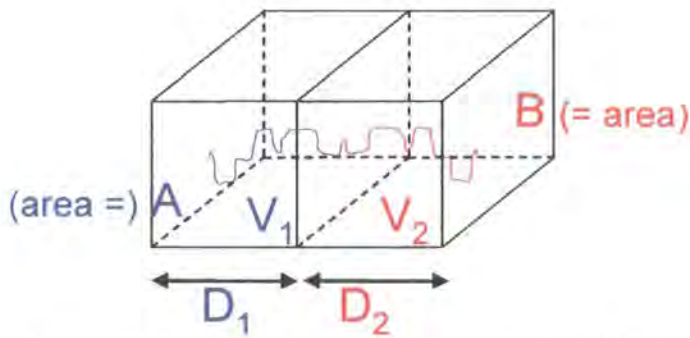


Fig. 1.20 Diagrammatic representation of block co-polymer.

From “random walk” statistics:

$$\text{distance } D_I \approx \sqrt{\langle R_I^2 \rangle} = \sqrt{N_A b^2} = N_A^{1/2} b$$

where  $b$  = “repeat unit” length for either component and  $N$  = the number of repeat units (degree of polymerisation).

Similarly, distance  $D_2 = N_B^{1/2}b$ . The number of chains in volume  $V_2$  is given by:

$$\begin{aligned}
 V_2/\text{volume per chain} &= \frac{AD_2}{N_B b^3} \\
 &= \frac{AN_B^{1/2}b}{N_B b^3} \\
 &= \frac{A}{b^2 N_B^{1/2}}
 \end{aligned} \tag{Eq. 8}$$

and this must be equal to the number of  $A$  chains in volume  $V_1$ . The volume available to each  $A$  chain is given by:

$$V_1/\text{no. of } A \text{ chains} = \frac{V_1}{A/b^2 N_B^{1/2}} \tag{Eq. 9}$$

but since  $V_1 = AD_1 = AN_A^{1/2}b$ , the volume available to each  $A$  chain  $= N_A^{1/2}N_B^{1/2}b^3$ , whereas the actual volume occupied by each  $A$  chain  $= N_A b^3$ . Hence, the volume available does not equal the volume occupied unless  $N_A = N_B$ . In order to allow for this,  $V_1$  must shrink (if  $N_A < N_B$ ) or expand (if  $N_A > N_B$ ), producing curvature of the phases, i.e. the cylindrical, bicontinuous, or spherical forms.

### 1.11.2 Variation of Lamellar Spacing ( $D$ ) with degree of polymerisation ( $N$ ).<sup>77</sup>

The polymer chains in the WSL exist in the “random walk” (unstretched) configuration and therefore (from random walk statistics):

$$\text{lamellar spacing } (= D) \propto N^{1/2}$$

The total interfacial enthalpy of the phase,  $E_{int}$ , is  $A_{tot}\sigma$ , where

$$\begin{aligned}
 A_{tot} &= \text{total interfacial area} \\
 &= L^2 \times \text{no. of lamellae in thickness } L \\
 &= L^2 \times L/D \\
 &= L^3/D
 \end{aligned} \tag{Eq. 10}$$

and,

$$\sigma = \text{interfacial enthalpy per unit area (depends on } \chi \text{ or } T, \text{ but not on } N).$$

Thus,

$$E_{int} = L^3\sigma/D \tag{Eq. 11}$$

and therefore a decrease in  $E_{int}$  requires a corresponding increase in  $D$ , i.e. chain stretching would have to occur, even though this is entropically unfavourable. However in the lamellar phase within the SSL, chain stretching does occur and there are thus two competing contributions to the total free energy of the phase: the total interfacial enthalpy,  $E_{int}$ , and the entropy,  $S$ , due to the chain stretching. For a single chain with  $N$  monomers (repeat units) each of length  $b$ , the entropy decreases as the end-to-end distance ( $D$ ) increases by stretching:

$$S = S_o - \frac{k_B D^2}{Nb^2} \quad \text{Eq. 12}$$

where  $S_o$  is a constant.

The number of chains in volume  $V$  is  $L^3 / Nb^3$  and hence the total entropy is:

$$S = const - \frac{k_B D^2 L^3}{N^2 b^5} \quad \text{Eq. 13}$$

The total free energy of the system is

$$F = E_{int} - TS$$

$$F = \frac{L3\sigma}{D} + \frac{Tk_B D^2 L^3}{N^2 b^5} + const \quad \text{Eq. 14}$$

The interlamellar spacing is determined by minimising free energy ( $F$ ) with respect to distance ( $D$ ). Differentiating equation 14 gives:

$$\frac{dF}{dD} = \frac{-L^3\sigma}{D^2} - \frac{2DTk_B L^3}{N^2 b^5} = 0$$

which rearranges to give:

$$D^3 = \frac{N^2 b^5 \sigma}{2k_B T}$$

and therefore  $D = N^{2/3} (b^5 \sigma / 2k_B T)^{1/3}$

or  $D \propto N^{2/3} \quad \text{Eq. 15}$

The size of the domains within the morphology can, in theory, be altered from tens of nanometres to hundreds of nanometres (i.e. to the order of the wavelength of light) by

increasing the molecular weight (size, degree of polymerisation) of the polymer components from tens of thousands to ~1million or more. However, this can obviously lead to slow equilibrium microphase separation, due to the greater entanglement and slower movement of polymer molecules of this size. Adding homopolymers of the two components to the block co-polymer system can also increase the size of the domains<sup>42</sup> by acting as a “solvent” for, and thus swelling, the appropriate block.

### 1.11.3 Characterisation of Microphase Separated Co-polymers.<sup>78</sup>

Microphase separated co-polymers can be characterised by Small Angle X-ray Scattering (SAXS). The short wavelength of X-rays can provide details of structures on a nanometre scale. Each microstructure has a characteristic SAXS scattering pattern brought about by the Bragg scattering of X-rays from the phase interfaces (Table 1.4).

Table 1.4      Positions of scattering peaks relative to the 1<sup>st</sup> order peak, for the most common polymer microstructures.<sup>44,77</sup>

	Lamellar	Cylindrical*	Spherical (bcc)
1st peak	1	1	1
2nd peak	2	$\sqrt{3} = 1.73$	$\sqrt{2} = 1.41$
3rd peak	3	$\sqrt{7} = 2.65$	$\sqrt{3} = 1.73$
4th peak	4	$\sqrt{9} = 3$	$\sqrt{4} = 2$

\*There should be a reflection at  $\sqrt{4}$ , but this is coincident with a minimum in the form factor of the cylinders and is systematically absent in the SAXS pattern.

## **Chapter 2: Results and Discussion.**

## 2.1 Background.

Anionic polymerisation is a “living” polymerisation technique, that is, it has no intrinsic termination reactions, and it produces polymers of well-defined molecular weight and narrow (typically  $<1.05$ )<sup>38</sup> polydispersity. An important application of its living nature is the synthesis of well-defined block co-polymers by sequential monomer addition: upon complete consumption of a first batch of monomer, a second batch of monomer can be added and propagation continues until this second batch is consumed. This also allows the composition of the block co-polymer to be well-defined, in addition to its molecular weight. However, it is only possible to exercise this level of control over the polymerisation if impurities, which would bring about the undesired termination reactions, are rigorously excluded. Although living anionic polymerisation (LAP) is a well-established technique, it is still a challenging methodology to master. In order to gain understanding and experience in the synthetic procedures and techniques required to prepare polymers successfully by this method, a sample of polystyrene and of poly(methyl methacrylate) were initially prepared.

## 2.2 Synthesis and Characterisation of Polystyrene.

Polystyrene was prepared using standard high-vacuum techniques<sup>48</sup>, with benzene as the solvent, *sec*-butyllithium as the initiator and with the reaction conducted at room temperature. Upon addition of the initiator, the characteristic orange colour of living polystyryllithium was observed. After several hours, the polymerisation was terminated with nitrogen-sparged methanol and the polymer was recovered by precipitation in excess methanol, filtration and drying *in vacuo*. The yield of polymer was quantitative (99+% w/w) and the polydispersity (Pd) was excellent (1.03) but the experimental molecular weight (by SEC,  $M_n = 99,800\text{gmol}^{-1}$ ) was approximately twice that of the target ( $M_n = 50,000\text{gmol}^{-1}$ ). As the molecular weight of a polymer prepared by LAP is inversely proportional to the amount of initiator active in the system, this experimental  $M_n$  suggests that approximately half the amount of initiator added to the reaction mixture was de-activated, probably by impurities present in the system. That the polymer had such a narrow polydispersity, however, indicates that these impurities were fully eliminated at this stage, by the addition of the initiator, and



that no further impurities were introduced in the course of the reaction. The preparation is exemplified in Section 3.3.1.

### 2.3 Synthesis and Characterisation of Poly(methyl methacrylate).

Using a bulky initiator such as 1,1-diphenyl-3-methylpentyl lithium in a polar solvent (e.g. THF) prevents unwanted attack by the initiator at the carbonyl group of the methacrylate through steric hindrance at the active centre (Fig. 2.1).

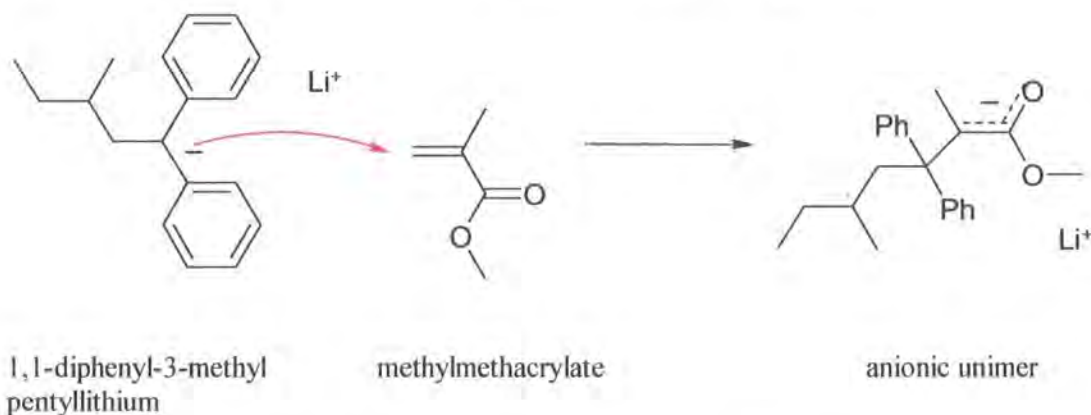


Fig. 2.1 Initiation by 1,1-diphenyl-3-methylpentyl lithium.

The anionic unimer thus formed is an insufficiently strong nucleophile to attack the carbonyl group, and the polymerisation thus proceeds through the desired attack on the vinyl group.

The controlled anionic polymerisation of methyl methacrylate (MMA) is further hampered by aggregation of the growing chain ends, which exist in equilibrium with non-aggregated chains.<sup>54,56-61</sup> The inter-conversion between the two is very slow and they also propagate at very different rates on monomer addition, with the aggregated chains having much lower reactivity, leading to a broad, if not bimodal, molecular weight distribution and thus a high polydispersity. Low polydispersities, typical of a controlled living system, could only be achieved if the rate of monomer addition were slower than the already-slow rate of inter-conversion between aggregated and non-aggregated forms. However, the addition of lithium chloride<sup>46,54,56-61</sup> to the system causes a decrease in aggregation, thus depleting the system of the slowly interconverting aggregates. Instead, the formation of a 1:1 complex (Fig. 1.15, page 24) between the propagating lithium enolate and lithium chloride has been suggested. The structure is said to prevent termination and transfer reactions. Best

results are achieved when the lithium chloride:initiator ratio is between 3:1 and 10:1, with the optimum at 5:1.

The low temperature ( $-78^{\circ}\text{C}$ ) is necessary to prevent the unwanted cyclisation of methacrylate end groups, which occurs in preference to propagation at higher temperatures and which would cause unwanted termination (Fig. 1.16, page 25) of the growing chain.

Poly(methyl methacrylate) was prepared by a ligated anionic polymerisation method using standard high vacuum techniques,<sup>48</sup> with tetrahydrofuran (THF) as the solvent, 1,1-diphenyl-3-methylpentyl lithium as the initiator (formed *in situ* from the reaction between *sec*-butyllithium and 1,1-diphenylethylene (DPE), see Fig. 1.13, page 23), and in the presence of lithium chloride, with the reaction conducted at  $-78^{\circ}\text{C}$ , using a solid  $\text{CO}_2$ /acetone bath as the coolant.

The yield of poly(methyl methacrylate) was high (93% w/w). The experimental molecular weight by SEC ( $M_n = 16,300\text{g mol}^{-1}$ ) and by  $^1\text{H-NMR}$  ( $M_n = 14,400\text{g mol}^{-1}$ ), (calculated by comparing relative integrals for the aromatic protons in the diphenyl residue of the initiator (7.3 - 7.1 ppm) and for the ester methyl group (3.4 ppm)), were in reasonable agreement with the target weight ( $M_n = 10,000\text{g mol}^{-1}$ ). The polydispersity was low (1.08). The preparation is exemplified in Section 3.3.2.

## 2.4 Syntheses of Fluoromethacrylate Homopolymers.

In order to meet the principle objective of this work, which was to prepare well-defined diblock co-polymers with a large refractive index contrast between the two blocks, it was necessary to establish a preferred living anionic method for synthesising well-defined low refractive index blocks. To this end, methacrylates with a perfluoroalkyl ester chain (fluoromethacrylates) were chosen for the low refractive index block, because it was anticipated that these could be anionically polymerised in a controlled manner similar to other alkyl ester chain methacrylates. This was investigated by preparing a series of fluoromethacrylate homopolymers.

Fluoromethacrylate homopolymers were prepared initially using 2,2,2-trifluoroethyl methacrylate (TFEMA) as the monomer. This is the shortest-chain fluoromethacrylate commercially available and thus also has the lowest boiling point.

It has been used in the literature.<sup>22,68</sup> The method used for the preparations was the same as that described above for the preparation of poly(methyl methacrylate) and the results are summarised in Table 2.1.

Table 2.1 2,2,2-trifluoroethyl methacrylate Homopolymers..

Expt.	Yield (% w/w)	M <sub>n</sub>			Pd	<sup>1</sup> H-NMR ratio -O-CH <sub>2</sub> -: backbone
		Target <sup>A</sup>	<sup>1</sup> H-NMR <sup>B</sup>	SEC <sup>C</sup>		
1	92	5k	21.9k	12.9k	1.35	2.0:5.0
2	36	20k	58.1k	26.7k	1.70	1.9:5.0
3	2.2	100k	-	21.7k	2.71	1.8:5.0
4	1.3	50k	-	<i>incompletely soluble in THF</i>		1.6:5.0

<sup>A</sup> Calculated from (mass monomer added)/(moles initiator added).

<sup>B</sup> Calculated from ratio of aromatic (DPE) protons to -O-CH<sub>2</sub>-CF<sub>3</sub> protons. CD<sub>2</sub>Cl<sub>2</sub> is the preferred solvent (compared to CDCl<sub>3</sub>) as this does not have a signal which coincides with the aromatic peak. Where no value is given, the DPE peak was too small to be of use.

<sup>C</sup> In THF against polystyrene standards.

When the target molecular weight was low (expt.1, Table 2.1, M<sub>n</sub> = 5,000gmol<sup>-1</sup>) the yield of recovered polymer was high (92% w/w). The molecular weight calculated from <sup>1</sup>H-NMR analysis (M<sub>n</sub> = 22,000gmol<sup>-1</sup>) by comparing relative intensities of the aromatic protons in the diphenyl residue of the initiator and of the -O-CH<sub>2</sub>- group of the fluorinated ester,<sup>67,79</sup> was much greater than that intended. By SEC, the polydispersity of the polymer was higher (1.35) than desirable (<1.05), probably owing to a low molecular weight tail, which was visible in the SEC chromatogram. The molecular weight by SEC for this polymer (M<sub>n</sub> = 12,900gmol<sup>-1</sup>) was also above that intended, though less than the value calculated by <sup>1</sup>H-NMR. The SEC value is likely to be the less accurate, as there are no fluorinated polymers standards available to allow accurate calibration of a SEC system and the hydrodynamic behaviour of a fluoromethacrylate is likely to be very different from methyl methacrylate or styrene.

As the target molecular weight was increased, the yield became smaller. Expt. 2, with intended molecular weight of M<sub>n</sub> = 20,000gmol<sup>-1</sup> had a yield of only 36% w/w and whilst the molecular weight by SEC (M<sub>n</sub> = 26,700gmol<sup>-1</sup>) gave reasonable agreement, the molecular weight by <sup>1</sup>H-NMR (M<sub>n</sub> = 58,100gmol<sup>-1</sup>) was much greater than that intended. The polydispersity of this polymer was also higher than desired (1.70), again probably owing to the presence of a low molecular weight tail.

Homopolymers with even higher intended molecular weights (expts. 3 and 4) resulted in yields of less than 10% w/w and products that were sparingly soluble in common solvents. Although this might suggest that the polymers were of higher molecular weight, it also meant that representative and reliable  $^1\text{H-NMR}$  or SEC spectra for molecular weight calculation could not be obtained to confirm or deny this. It is suspected that the cause of the limited control over the homopolymerisation of this monomer under these conditions is that TFEMA is a dihydro-fluoromethacrylate and thus the protons of the  $-\text{O}-\text{CH}_2-\text{CF}_3$  group, positioned as they are between the electron-withdrawing ester functionality and the electronegative  $-\text{CF}_3$  group, have a highly acidic character as illustrated below in Fig. 2.2.

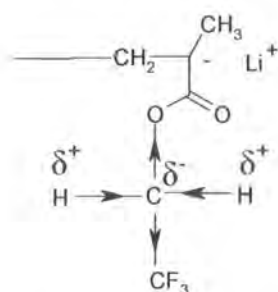


Fig. 2.2 Acidic nature of methylene hydrogens in TFEMA.

This situation can lead to hydrogen abstraction (postulated mechanism Fig. 2.3) by the propagating anion, giving rise to a dead chain and a new anionic species which, if it could reinitiate, would lead to a branched polymer.

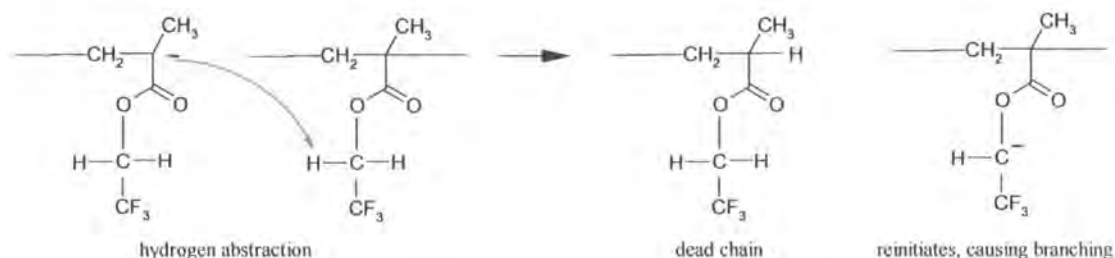


Fig. 2.3 Postulated mechanism of hydrogen abstraction for TFEMA.

Thus, the polymerisation possibly contains a termination mechanism and a second propagating species (which may or may not be capable of reinitiating a chain) and neither of these factors is conducive to a living, controlled system. That some hydrogen abstraction is occurring may have been indicated by the decrease in ratio of

the ester protons to backbone protons from the expected 2.0:5.0 respectively (Table 2.1, expt. 1) to 1.6:5.0 respectively (Table 2.1, expt. 4). The latter ratio equates to ~17.5% of the TFEMA units having undergone proton abstraction. Whilst this is insufficient to account entirely for a yield as low as 1.3% w/w, the presence of terminated chains and a charged species potentially incapable of reinitiating does lead to low yields and an uncontrolled polymerisation.

To overcome this problem, subsequent homopolymerisations (Table 2.2) were carried out using either 1H,1H,2H,2H-perfluorohexyl methacrylate (PFHMA) or 1H,1H,2H,2H-perfluorooctyl methacrylate (PFOMA), both of which are tetrahydro-fluoromethacrylates ( $-O-CH_2-CH_2-C_xF_y$ ) rather than dihydro-fluoromethacrylates ( $-O-CH_2-C_xF_y$ ) and are therefore less likely to suffer proton abstraction. In addition, the ester carbonyl group in tetrahydro-perfluoroalkyl chains is less likely to be activated by the strongly electron-withdrawing perfluoroalkyl chain, than is the ester group in dihydro-perfluoroalkyl chains. Both PFHMA and PFOMA have been used in the literature<sup>67-69</sup> and are the shortest-chain tetrahydro-fluoromethacrylates commercially available.

Table 2.2 1H,1H,2H,2H-perfluorohexyl methacrylate Homopolymers.

Expt.	Yield (% w/w)	M <sub>n</sub>		
		Target <sup>A</sup>	<sup>1</sup> H-NMR <sup>B</sup>	SEC <sup>C</sup>
1	55	10k	11.9k	<i>inverted RI chromatogram</i>
2	26	20k		<i>insoluble</i>
3	1.2	25k		<i>insoluble</i>

<sup>A</sup> Calculated from (mass monomer added)/(moles initiator added).

<sup>B</sup> Calculated from ratio of aromatic (DPE) protons to  $-O-CH_2-$  protons.  $CD_2Cl_2$  is the preferred solvent (compared to  $CDCl_3$ ) as this does not have a signal which coincides with the aromatic peak.

<sup>C</sup> In THF against polyMMA standards.

Polymerisation of PFHMA, by the same method as for polyMMA and polyTFEMA above, met with some success at low molecular weights (target  $M_n = 10,000 \text{ g mol}^{-1}$ , experimental by <sup>1</sup>H-NMR  $M_n = 11,900 \text{ g mol}^{-1}$ , yield 55% w/w) but again as the target molecular weight was increased, the yields and control of the molecular weight diminished. In this case, it was considered that the poor solubility of the propagating chains at the low temperatures ( $-78^\circ\text{C}$ ) required for the method was the main cause of the problem, as the reaction mixtures were observed to become slightly opaque over the course of the reaction, possibly indicating that the polymers were coming out of

solution. For the polymer which was soluble, the SEC chromatogram gave a monomodal but inverted refractive index chromatogram, possibly due to the refractive index of the fluoromethacrylate chain being lower than that of the eluent. Krupers *et al.*<sup>65,80</sup> also obtained negative peaks, when examining poly(MMA-*b*-PFOMA) polymers by SEC and they ascribed this to block co-polymer associates (micelles).

More success in terms of yield (Table 2.3) was achieved for the homopolymerisation of PFHMA and PFOMA by using the so-called “modified screened” anionic polymerisation method, which had been applied in the literature to the preparation of poly(MMA-*b*-fluoromethacrylate) polymers.<sup>67</sup> In this method, the initiator is the *tert*-butyl anion, whilst the stabilising cation co-ordinated to the propagating centre is the tetra-*isodilithium*aluminium complex, both of which are formed in situ from *tert*-butyllithium and tri-*isobutyl*aluminium in an equimolar ratio (Fig. 1.17 page 27). This method allows the reaction to be carried out at 0°C and in a mixture of toluene and 1,3-bis(trifluoromethyl)benzene, the latter of which aids the solubility of the growing fluoromethacrylate chain.

Table 2.3 Fluoromethacrylate Homopolymers prepared by “screened” method.

Monomer	Yield (% w/w)	M <sub>n</sub>	
		Target <sup>A</sup>	SEC <sup>B</sup>
PFHMA	74	20k	<i>inverted RI chromatogram</i>
PFOMA	80	20k	<i>insoluble</i>

<sup>A</sup> Calculated from (mass monomer added)/(moles initiator added).

<sup>B</sup> In THF against polystyrene standards.

Yields were greatly improved (>74% w/w) but the insolubility of the homopolymers in common solvents still hampered their analyses. In addition, as 1,1-diphenyl-3-methylpentyllithium had not been used to initiate these polymers, they did not contain the aromatic internal reference by which their molecular weight could be calculated from <sup>1</sup>H-NMR spectra.

Polyfluoromethacrylates were thus found to become increasingly insoluble in common solvents with both increasing (intended) molecular weight and increasing length of the perfluoro monomer chain. In the literature, Gaynor *et al.*<sup>22</sup> was not able to determine the molecular weights of fluoromethacrylate homopolymers, which they had prepared by free-radical polymerisation for refractive index and optical radiation

studies, due to the limited solubility of the fluoromethacrylate polymers in common organic solvents. Tsibouklis *et al.*<sup>81</sup> also described these homopolymers as insoluble in common solvents.

The most successful preparations of fluoromethacrylate homopolymers were taken to be polyTFEMA in Section 2.4, Table 2.1, expt. 1; polyPFHMA in Section 2.4, Table 2.2, expt. 1 and polyPFOMA in Section 2.4, Table 2.3. Their respective preparations are exemplified in Sections 3.4.1, 3.4.2 and 3.4.3.

## 2.5 Syntheses of Poly(styrene-b-fluoromethacrylate) Co-polymers.

Having established reasonably successful routes to synthesise both styrene and fluoromethacrylate homopolymers at low molecular weights, attempts were then made to prepare well-defined block co-polymers of styrene with a fluoromethacrylate. Several slightly different methods were used. It was anticipated that the inclusion of the styrene block would aid the overall solubility of the co-polymer.<sup>68</sup>

### 2.5.1 Method 1, in which tri-isobutylaluminium or its derivative was used as “screening” agent.

The first method used to prepare poly(styrene-b-fluoromethacrylate) polymers was the “screened” method which had been successfully used to prepare homopolymer fluoromethacrylates (Section 2.4 above), i.e. using mixed solvents (toluene and 1,3-bis(trifluoromethyl)benzene) and the *tert*-butyl anion and tetra-*isodilithium*aluminium complex (the latter formed *in situ* from *tert*-butyllithium and tri-*isobutylaluminium* in an equimolar ratio) as the initiator and “screening” complex respectively and with the temperature of the reaction at 0°C. The results of preparations by this method are summarised below in Table 2.4 and the fluoromethacrylate used is indicated. The scales (i.e. total mass monomers used) of the experiments ranged from 5.80g (expt. 5) to 14.92g (expt. 6).

Table 2.4 Poly(styrene-*b*-fluoromethacrylate) polymers, prepared by Method 1, in which tri-*isobutyl*aluminium or its derivative was used as “screening” agent.

Expt.	Conditions.	Yield <sup>A</sup> % w/w	polystyrene block			Co-polymer (styrene- <i>b</i> -fluoromethacrylate)					
			M <sub>n</sub>		Pd	Molar ratio S:F		M <sub>n</sub>			Pd
			Target <sup>B</sup>	SEC <sup>C</sup>		Target <sup>D</sup>	H-NMR <sup>E</sup>	Target <sup>F</sup>	H-NMR <sup>G</sup>	SEC <sup>C</sup>	
1	toluene & 1,3-bis(trifluoromethyl) benzene, <i>t</i> -BuLi and Al <sup>i</sup> Bu <sub>3</sub> added before styrene. 20 hrs reaction time.	46	25k	PFHMA only							
2	styrene polymerised by <i>s</i> -BuLi in toluene; 1,3-bis(trifluoromethyl) benzene added, Al <sup>i</sup> Bu <sub>3</sub> added, followed by PFHMA. 20 hrs reaction time.	82	10.0k	10.3k	1.12	4.53:1 (8.42:1)	11.0:1	17.9k (14.4k)	13.3k	bimodal	
3	styrene polymerised by <i>s</i> -BuLi in toluene; Al <sup>i</sup> Bu <sub>3</sub> added, followed by PFOMA in toluene solution by injection. 42 hrs reaction time.	99	11.6k	11.8k	1.07	3.57:1 (3.57:1)	6.24:1	25.3k (25.0k)	19.6k	12.5k	1.06
4	styrene polymerised by <i>s</i> -BuLi in toluene; Al <sup>i</sup> Bu <sub>3</sub> added, followed by PFHMA added slowly by injection. 20 hrs reaction time.	94	10.0k	10.7k	1.08	16.0:1 (21.3:1)	32.0:1	13.0k (12.0k)	11.8k	10.9k	1.06
5	styrene polymerised by <i>s</i> -BuLi in toluene; Al <sup>i</sup> Bu <sub>3</sub> added, followed by TFEMA distilled from Al <sup>i</sup> Bu <sub>3</sub> . 20 hrs reaction time.	87	10.0k	10.6k	1.07	7.00:1 (21.0:1)	47.0:1	13.2k (11.3k)	11.0k	10.7k	1.07
6	styrene polymerised by <i>s</i> -BuLi in toluene; Al <sup>i</sup> Bu <sub>3</sub> added, followed by TFEMA distilled from Al <sup>i</sup> Bu <sub>3</sub> . 20 hrs reaction time.	87	10.0k	10.1k	1.05	3.25 (5.69:1)	7.60:1	15.1k (13.0k)	12.2k	10.6k	1.05

<sup>A</sup> Calculated from (mass recovered co-polymer + mass recovered sidearm sample)/(mass monomers added), expressed as a percentage.

<sup>B</sup> Calculated from (mass styrene added)/(moles initiator added).

<sup>C</sup> In THF against polystyrene standards.

<sup>D</sup> Calculated from ratio (moles styrene added - moles sidearm sample):(moles fluoromethacrylate added). The second figure, in brackets, then refers to the same calculation but with the moles of fluoromethacrylate reduced by an amount equivalent to the reduction in yield from 100% w/w.

<sup>E</sup> In chloroform

<sup>F</sup> Calculated from M<sub>n</sub> of PS by SEC and (mass fluoromethacrylate added x M<sub>n</sub> of PS by SEC)/(mass styrene added - mass sidearm sample). The second figure, in brackets, then refers to the same calculation, but with the mass of fluoromethacrylate reduced by an amount equivalent to the reduction in yield from 100% w/w.

<sup>G</sup> Calculated from M<sub>n</sub> of PS by SEC and mol ratio styrene (aromatic):fluoromethacrylate (-O-CH<sub>2</sub>-) by <sup>1</sup>H-NMR.



In the first attempt (expt. 1), no colouration of the reaction was observed on addition of styrene to the solvent/initiator/screening-complex mixture, and when, after 1 hour, a sample was removed for analysis, no polymer was recovered from the sample. Subsequent addition of PFHMA by injection to the reaction mixture produced a yellow colour, which gradually faded but did not disappear completely over the reaction time (~22 hours). The recovered product (an opaque liquid in 42% w/w yield on total monomers added, but 93% w/w on PFHMA added) was found by  $^1\text{H-NMR}$  to be solely polyPFHMA. These results indicated that this system did not initiate the polymerisation of styrene.

In subsequent experiments (expts. 2-6), therefore, all preparations of the styrene block were made by initiating the styrene with *sec*-butyllithium in toluene at room temperature, before any further variations were made. In each case, the target molecular weight of the styrene segment ( $10,000\text{ gmol}^{-1}$  for expts. 2 and 4-5;  $11,600\text{ gmol}^{-1}$  for expt. 3), and the SEC measurements of the polystyrene samples taken were in good agreement ( $10,100\text{ gmol}^{-1}$  -  $10,700\text{ gmol}^{-1}$  for expts. 2 and 4-5;  $11,800\text{ gmol}^{-1}$  for expt. 3). The polydispersities for the samples were also good, ranging from 1.05 - 1.08, with only one value above this (1.12, expt. 2).

In expt. 2, after the formation of the polystyrene block, a second solvent (1,3-bis(trifluoromethyl) benzene, said to aid solubility of fluoromethacrylate chains<sup>67</sup>) was distilled into the reactor, in an approximately equivolume amount with toluene, using liquid nitrogen as the coolant, with no loss of orange styryllithium colour, even on returning the reaction to room temperature. On addition of tri-*isobutyl*aluminium, however, the colour changed to yellow. The reaction was cooled to  $0^\circ\text{C}$  (ice/salt/water) before the addition of PFHMA from a nitrogen-purged syringe and the reaction was allowed to proceed for 20 hours before termination with nitrogen-sparged methanol. The yield was reasonable (82% w/w) but assuming that some of the shortfall was due to incomplete reaction of the fluoromethacrylate, then the addition of the second solvent appeared not to have enabled increased solubility of the growing polymer chain over the reaction time (~20 hours). In addition, the SEC peak for the co-polymer was bimodal and its  $^1\text{H-NMR}$  spectrum showed the styrene:PFHMA ratio (calculated from the ratio of styrene protons to  $-\text{O}-\text{CH}_2-$  protons) to be much greater (11.0:1) than that anticipated (4.53:1). Even allowing for

all the shortfall in yield to be due to unreacted PFHMA, the styrene:PFHMA ratio would only be  $\sim 8:1$  (Table 2.4). Neither were the target  $M_n$  of the co-polymer ( $17,900\text{g mol}^{-1}$ ) or the  $M_n$  calculated from SEC and  $^1\text{H-NMR}$  data ( $13,300\text{g mol}^{-1}$ ) in good agreement. The experimental conditions or technique had clearly not produced the desired level of accuracy.

In expt. 3, the preparation was therefore varied from expt. 2 by omitting the second solvent (its addition had not appeared to solve any problems which might be caused by poor solubility of the fluoromethacrylate chain) and by adding the fluoromethacrylate by injection as a toluene solution. The fluoromethacrylate monomer was also changed from PFHMA to PFOMA, in an attempt to replicate more closely the conditions used by Hems and Cooper.<sup>67</sup> However, it was observed that the addition of tri-*isobutyl*aluminium caused the orange polystyryllithium colour to completely disappear but a yellow colour was restored when the fluoromethacrylate was added. Whilst the co-polymer product of this reaction produced a yield (99% w/w, probably due to 42 hours reaction time) and polydispersity (1.06) of satisfying values, the  $^1\text{H-NMR}$  spectrum of the co-polymer again showed the styrene:fluoromethacrylate ratio to be approximately twice (6.24:1) that intended and anticipated (3.57:1), when calculated from the ratio of styrene protons to  $-\text{O-CH}_2-$  protons. The target  $M_n$  of the co-polymer ( $25,300\text{g mol}^{-1}$ ) and the  $M_n$  calculated from SEC and  $^1\text{H-NMR}$  data ( $19,600\text{g mol}^{-1}$ ) also differed.

In expt. 4, the preparation was varied from expt. 3 by reverting to the slightly shorter fluoromethacrylate (PFHMA), greatly reducing the ratio of this to styrene and adding the quantity (1ml, 1.4g,  $4.21 \times 10^{-3}\text{mol}$ ) slowly over 15 minutes from a nitrogen-purged lockable syringe. Again, the co-polymer product of this reaction produced a yield and polydispersity of satisfying values (94% w/w and 1.06 respectively), but the  $^1\text{H-NMR}$  spectrum of the co-polymer once again showed the styrene:fluoromethacrylate ratio, calculated from the ratio of styrene protons to  $-\text{O-CH}_2-$  protons, to be approximately twice (32.0:1) that intended (16.0:1). Even allowing for all the shortfall in yield to be due to unreacted PFHMA, the experimental styrene:PFHMA ratio would have been  $\sim 21:1$ . However, the target  $M_n$  of the co-polymer ( $13,000\text{g mol}^{-1}$ ) and the  $M_n$  calculated from SEC and  $^1\text{H-NMR}$  data ( $11,800\text{g mol}^{-1}$ ) were in reasonable agreement.

In expts. 5 and 6, the preparations were varied by changing the fluoromethacrylate from PFHMA to TFEMA (thus shortening the fluorine chain still further, though at the same time reverting to a di-hydro fluoromethacrylate) and distilling this in to the reaction from tri-*isobutyl*aluminium. In expt. 5, the quantity was less (1.06g,  $10.05 \times 10^{-3}$  mol) than in expt 6 (4.69g,  $27.9 \times 10^{-3}$  mol) but in both cases it was observed that a thick residue, much greater than the volume of tri-*isobutyl*aluminium added, remained after distillation.

Both the resulting co-polymers produced reasonable identical yields (87% w/w) and very good polydispersities (1.07 and 1.05 respectively) but yet again the  $^1\text{H}$ -NMR spectrum of the co-polymer showed the styrene:fluoromethacrylate ratio to be much greater than that intended or anticipated, even allowing for the shortfall in yield to be due to unreacted TFEMA.

The major problems with this set of preparations have therefore been the low yields and the anomalous nature of the  $^1\text{H}$ -NMR results. Further examination of the  $^1\text{H}$ -NMR spectra, in which the ratio of styrene protons to total aliphatic protons was calculated, gave data consistent with the original (anomalous)  $^1\text{H}$ -NMR calculations. The data gained from expt. 2 was then re-examined, this being chosen as it had the highest yield (99% w/w) and greatest incorporation (by intention and by  $^1\text{H}$ -NMR) of fluoromethacrylate. This reaction was carried out using 5.58g styrene and 5.98g PFOMA. The preparation of the polystyrene block was beyond reproach, as indicated by its low polydispersity (1.07) and the close agreement between the target and experimental  $M_n$  ( $11,600\text{g mol}^{-1}$  and  $11,800\text{g mol}^{-1}$  respectively). Assuming, therefore, that 100% w/w of the styrene was polymerised before the PFOMA was added, the shortfall of 1% w/w from the yield is all PFOMA - which on this scale would amount to  $\sim 0.12\text{g}$ . Clearly, this cannot account for the styrene:PFOMA ratio in the  $^1\text{H}$ -NMR sample being approximately twice that intended, which would require a reduction in PFOMA presence of  $\sim 2.33\text{g}$ . An alternative theory for the absence some PFOMA from the  $^1\text{H}$ -NMR sample would be to assume that tri-*isobutyl*aluminium is capable of initiating the polymerisation of PFOMA and that the polyPFOMA thus formed, whilst constituting  $\sim 20\%$  w/w of the overall yield ( $2.33\text{g}/(5.58\text{g} + 5.98\text{g})$ ) did not redissolve<sup>22,81</sup> in the  $^1\text{H}$ -NMR solvent, and was too slight a quantity ( $20\% \times \text{mass } ^1\text{H}\text{-NMR sample} \approx 0.005\text{g}$ ) to be remarked by the naked eye. Supporting evidence for the

ability of tri-*isobutyl*aluminium to initiate the polymerisation of fluoromethacrylates is the observation that a thick residue remained after the distillation of TFEMA from tri-*isobutyl*aluminium in expts. 5 and 6 above. In addition, it was noted that, after recovery, many of these preparations left a residue in the main reactor which could not be dissolved out using common solvents, but had to be burned out using permanganic acid. This suggests that this residue was polyfluoromethacrylate<sup>22,81</sup> rather than polystyrene or poly(styrene-*b*-fluoromethacrylate)<sup>68</sup> and is further evidence for the ability of tri-*isobutyl*aluminium to initiate the homopolymerisation of fluoromethacrylates. It also suggests the cause of the relatively low yields in expts. 2 and 5-6.

When the inclusion of tri-*isobutyl*aluminium in the reaction process was discontinued, and alternative methods of preparation were used (Sections 2.5.2 and 2.5.3, immediately following), this problem of the anomalous <sup>1</sup>H-NMR results disappeared. In addition, the styrene:fluoromethacrylate polymers prepared and successfully analysed by <sup>1</sup>H-NMR in Sections 2.5.2 and 2.5.3 were comparable in composition to those intended to be prepared in this section, which would indicate that it was not the formation of e.g. micelles, which was causing the problem.

Beyond the interference of tri-*isobutyl*aluminium in the control of the reaction, no further explanation of the anomalous <sup>1</sup>H-NMR results in this section is offered, and within the time constraints of this thesis, no further investigation was made.

#### 2.5.2 Method 2, in which solvents were exchanged.

The inclusion of tri-*isobutyl*aluminium being discontinued, a new method was devised whereby the polystyrene block was initiated by *sec*-butyllithium in benzene (~ 100ml) at room temperature, in the presence of lithium chloride (LiCl, at 5x moles initiator), and when its propagation was complete, most of the benzene was removed by distillation and replaced by THF (~100ml), prior to the addition of DPE (equimolar with initiator) and PFHMA at -78°C. The results of preparations by this method are summarised below in Table 2.5. The scales (i.e. total mass monomers used) of the experiments ranged from 7.35g (expt. 12) to 14.62g (expt. 11).

Table 2.5 Poly(styrene-b-PFHMA) polymers, prepared by Method 2, in which solvents were exchanged.

Expt.	Conditions.	Yield <sup>A</sup> % w/w	polystyrene block			Co-polymer (styrene-b-PFHMA)					
			M <sub>n</sub>		Pd	Molar ratio S:PFHMA		M <sub>n</sub>			Pd
			Target <sup>B</sup>	SEC <sup>C</sup>		Target <sup>D</sup>	<sup>1</sup> H-NMR <sup>E</sup>	Target <sup>F</sup>	<sup>1</sup> H-NMR <sup>G</sup>	SEC <sup>C</sup>	
7	polystyryl/benzene/THF at room temp. PFHMA added by injection.	98	10.0k	10.7k	1.05	3.18:1 (3.18:1)	3.47:1	21.6k (21.2k)	20.5k	bimodal	
8	polystyryl/benzene/THF at room temp. PFHMA distilled from TEA.	93	25.0k	30.2k	1.06	2.93:1 (3.38:1)	3.54:1	65.4k (58.5k)	57.4k	30.1k	1.09
9	polystyryl/benzene/THF at -78°C. PFHMA distilled from TEA.	90	25.0k	106k	1.14	2.78:1 (3.33:1)	3.50:1	231k (207k)	203k	111k	1.11
10	as for expt. 9, but adding PFHMA via the “rinsing” flask.	97	25.0k	34.0k	1.05	2.93k (3.03:1)	3.41:1	71.5k (69.2k)	65.9k	bimodal	
11	polystyryl/benzene/THF at -10°C. PFHMA distilled from TEA.	94	25.0k	63.3k	1.01	4.65 (5.64:1)	6.76:1	106k (99.0k)	93.1k	bimodal	
12	polystyryl/benzene/THF at -30°C. PFHMA distilled from TEA.	95	25.0k	37.7k	1.05	18.3:1 (27.5:1)	30.0:1	44.7k (42.3k)	41.7k	37.1k	1.05

<sup>A</sup> Calculated from (mass recovered co-polymer + mass recovered sidearm sample)/(mass monomers added), expressed as a percentage.

<sup>B</sup> Calculated from (mass styrene added)/(moles initiator added).

<sup>C</sup> In THF against polystyrene standards.

<sup>D</sup> Calculated from ratio (moles styrene added - moles sidearm sample):(moles fluoromethacrylate added). The second figure, in brackets, then refers to the same calculation but with the moles of fluoromethacrylate reduced by an amount equivalent to the reduction in yield from 100% w/w.

<sup>E</sup> In chloroform

<sup>F</sup> Calculated from M<sub>n</sub> of PS by SEC and (mass fluoromethacrylate added x M<sub>n</sub> of PS by SEC)/(mass styrene added - mass sidearm sample). The second figure, in brackets, then refers to the same calculation, but with the mass of fluoromethacrylate reduced by an amount equivalent to the reduction in yield from 100% w/w.

<sup>G</sup> Calculated from M<sub>n</sub> of PS by SEC and mol ratio styrene (aromatic):fluoromethacrylate (-O-CH<sub>2</sub>-) by <sup>1</sup>H-NMR.

The target  $M_n$  of the styrene blocks ( $10,000\text{gmol}^{-1}$  for expt. 7 and  $25,000\text{gmol}^{-1}$  for expts. 8-12) and the  $M_n$  by SEC were found to be in reasonable agreement ( $10,700\text{gmol}^{-1}$  for expt. 1 and  $30,200 - 37,700\text{ gmol}^{-1}$  for expts. 8, 10 and 12) except for expts. 9 and 11, where the  $M_n$  by SEC were  $106,000\text{gmol}^{-1}$  and  $63,300\text{gmol}^{-1}$  respectively. However, the polydispersities of all the styrene blocks were very good, ranging from 1.01 - 1.06, except for expt. 9 which was higher than desirable at 1.14.

In expt. 7, after the polystyrene had been formed in benzene, and the benzene removed by distillation, THF was distilled into the reaction using liquid nitrogen as the coolant. At this stage the reaction was (erroneously) allowed to rise to room temperature in order to redissolve the frozen polystyrene/benzene and LiCl in THF. Once this had occurred, the temperature was reduced to  $-78^\circ\text{C}$  before the PFHMA was added by injection, causing the bright orange styryllithium colour to completely disappear. However, before the error of temperature elevation was realised, a second preparation was made, (expt. 8) in which the target molecular weight of the styrene block was increased (from  $10,000\text{gmol}^{-1}$  to  $25,000\text{gmol}^{-1}$ ) but again the reaction was erroneously allowed to rise to room temperature. This time the PFHMA was added by distillation from triethylamine (TEA). It was noted that distillation was difficult and that the monomer tended to condense in parts of the apparatus other than the main reactor.

In both these preparations (expts. 7 and 8), the yields were very good (98% and 93% w/w respectively), the target and experimental  $^1\text{H-NMR}$  ratios were in reasonable agreement, and the target and experimental  $M_n$  were in good agreement. When the shortfall in yield for each preparation was assumed to be due to incomplete PFHMA polymerisation, then the target and experimental figures matched even more closely. However, the SEC trace for expt. 7 was bimodal, and this loss of control of the reaction may have been due to the rise in temperature.

In expt. 9, the styryllithium formed only a yellow colouration rather than the usual bright orange. This was later thought to indicate that some of the quantity of initiator had been consumed in eliminating impurities remaining in the system, thus reducing the amount of initiator available for initiation and meaning that the molecular weight of the styrene block would be greater than intended. This was duly observed when the SEC measurement gave  $M_n$  of  $106,000\text{gmol}^{-1}$ , against the target of  $25,000\text{gmol}^{-1}$ .

The error of allowing the polystyryl/benzene/THF mixture to rise in temperature was finally realised and in this preparation the mixture was only allowed to rise to  $-78^{\circ}\text{C}$ . After dissolution of the polystyryl/benzene/THF mixture, PFHMA was distilled into the reaction from TEA. Again, the target and experimental  $^1\text{H-NMR}$  and  $M_n$  data were in good agreement, with the agreement being improved further when it was assumed that the shortfall in yield was due to incomplete PFHMA reaction.

In expts. 8 and 9 the PFHMA had been added by distillation from TEA in order to increase the purity of the monomer beyond that afforded by the standard method of freeze-thawing over calcium hydride (Sec. 3.2) and injection of the required quantity from a nitrogen-purged syringe. However, distillation was found to be slow and difficult, with a large fraction of the monomer condensing in parts of the reactor other than the cooled main reactor. This would account for the relatively low yield (90% w/w) in expt. 9.

In expt. 10, yet another way of introducing the PFHMA was tried; this time the monomer was first distilled from TEA into the "rinsing" flask of the reactor and then tipped into the main reactor. However, the SEC chromatogram for the co-polymer prepared this way was bimodal, indicating loss of control of the polymerisation on addition of PFHMA. However, agreement was reasonably good between the target and experimental values for both  $^1\text{H-NMR}$  ratios and molecular weights for the co-polymer.

In expt. 11, the frozen styrene/benzene mix was found not to dissolve in THF at  $-78^{\circ}\text{C}$  and the temperature had to be allowed to rise to  $-10^{\circ}\text{C}$  before dissolution would occur. The PFHMA was distilled into the "rinsing" flask from TEA, as in expt. 10, with the intention of then distilling it again into the main reactor; however, this again proved slow and difficult to do, and so the monomer was again tipped into the main reactor. The SEC chromatogram for this reaction was also bimodal and the  $M_n$  of the styrene block by SEC was approximately twice that intended, indicating that overall the entire preparation had not been controlled.

In expt. 12, the frozen polystyryl/benzene was left to dissolve in THF at  $-78^{\circ}\text{C}$  overnight. This had very little effect and the reaction had to be warmed to  $-30^{\circ}\text{C}$  the following day before dissolution occurred. When the initiator was added, there was at

first no bright orange colouration as expected, therefore a second quantity was added, which produced a strong colouration. It was later found that the syringe used to add the initiator had been partially blocked and therefore had been incompletely purged with nitrogen. The first quantity of initiator was rendered inactive by the air still in the syringe, which is why it did not colour the reaction. The second quantity, added from the same “rinsed” syringe was fully active and therefore able to initiate the reaction, thus colouring the system. However, some of the initiator was probably rendered inactive by a small amount of air added to the main reactor from the incompletely-purged syringe, and thus the  $M_n$  by SEC is rather higher ( $37,700\text{gmol}^{-1}$ ) than the target ( $25,000\text{gmol}^{-1}$ ).

This method of preparation therefore had two disadvantages: the difficulty of re-dissolving the frozen, concentrated polystyryl/benzene in THF at the low temperature of  $-78^\circ\text{C}$ , which is essential for the quality of the reaction, and the more general difficulty of distilling the monomer efficiently into the main reactor. It was also observed that distilling from TEA left a residue in the distillation flask and the more TEA that was used, the greater the residue left in the flask. This suggested that TEA was reacting with the PFHMA, possibly because of the relatively high temperatures which had to be used to distil the monomer successfully. In addition, two of the preparations (expts. 9 and 12) and probably a third (expt. 11) were inaccurate because of manipulative errors with the initiator. The non-dissolution of the frozen polystyryl/benzene at  $-78^\circ\text{C}$  did not appear to follow a pattern of either concentration of polystyryl in THF ( $\sim 5\text{g}$  per  $100\text{ml}$  was soluble at  $-78^\circ\text{C}$  for expt. 9 but insoluble for expt. 12, whereas  $\sim 10\text{g}$  per  $100\text{ml}$  was soluble at  $-78^\circ\text{C}$  for expt. 10 but insoluble for expt. 11) or of eventual molecular mass of polystyrene (expt. 9 at  $106,000\text{gmol}^{-1}$  was soluble at  $-78^\circ\text{C}$  whereas expt. 10 at  $34,000\text{gmol}^{-1}$  was insoluble). Though the high yields ( $\geq 90\%$  w/w) of the co-polymers, and the good agreements between target and experimental styrene:PFHMA ratios and target and experimental molecular weights for the co-polymers were a great improvement on the results obtained by the previous method in Section 2.5.1 (Table 2.4), the SEC chromatograms of the block co-polymers were either shouldered and asymmetric or positively bimodal, with the presence of styrene homopolymer in the final product. This suggested a loss of control of the polymerisation, possibly due to some reaction of the THF with



polystyryllithium at elevated temperatures, or the introduction of some impurities into the system accompanying the addition of THF, DPE or the fluoromethacrylate.

### 2.5.3 Method 3, in which solvents were added sequentially.

In order to alleviate the problem encountered in the previous method (Section 2.5.2) with the non-dissolution of frozen polystyryl/benzene in THF at  $-78^{\circ}\text{C}$ , it was decided to carry out the styrene polymerisation in toluene ( $\sim 100\text{ml}$ ) in the presence of LiCl (at 5 x moles initiator) and after the styrene's complete propagation, simply to add THF ( $\sim 100\text{ml}$ ) to the reaction mixture, without removing the toluene. As toluene has a lower melting point ( $-93^{\circ}\text{C}$ ) than benzene ( $5.5^{\circ}\text{C}$ ), it was anticipated that the polystyryl/toluene solution would remain liquid when cooled to  $-78^{\circ}\text{C}$  and that addition of THF and subsequent mixing could then be carried out at this temperature. Seven polymerisations were carried out using this method, whereby the polystyrene was prepared in toluene and initiated by *sec*-butyllithium at room temperature, followed by the addition of THF at  $-78^{\circ}\text{C}$  (but no removal of toluene), prior to the addition of DPE (equimolar with initiator) and subsequent addition of fluoromethacrylate monomer. The results of preparations by this method are summarised below in Table 2.6. The scales (i.e. total mass monomers used) of the experiments ranged from 8.70g (expt. 18) to 13.01g (expt. 13).

Table 2.6 Poly(styrene-*b*-fluoromethacrylate) polymers, prepared by Method 3, in which solvents were added sequentially.  
(All prepared using PFHMA as the fluoromethacrylate, except where indicated.)

Expt.	Conditions.	Yield <sup>A</sup> % w/w	polystyrene block			Co-polymer (styrene- <i>b</i> -fluoromethacrylate)					
			M <sub>n</sub>		Pd	Molar ratio S:F		M <sub>n</sub>			Pd
			Target <sup>B</sup>	SEC <sup>C</sup>		Target <sup>D</sup>	<sup>1</sup> H-NMR <sup>E</sup>	Target <sup>F</sup>	<sup>1</sup> H-NMR <sup>G</sup>	SEC <sup>C</sup>	
13	DPE reacted for 20 hours	96	25.0k	12.1k	1.21	3.32:1 (3.71:1)	3.70:1	23.8k (22.8k)	22.5k	33.5k	1.07
14	DPE reacted for 3 hours	46*	25.0k	88.5k	1.10	all polystyrene					
15	DPE reacted for 4.5 hours	76	25.0k	28.3k	1.04	2.50:1 (4.44:1)	4.86:1	64.1k (48.0k)	46.9k	bimodal	
16	DPE reacted for 3 hours	51 <sup>#</sup>	25.0k	30.0k	1.05	2.35:1 (23.5:1)	23.0:1	71.3k (34.7k)	34.2k	31.1k	1.06
17	DPE reacted for 20 hours	98	25.0k	31.1k	1.04	3.76:1 (4.00:1)	4.38:1	57.3k (56.1k)	53.7k	bimodal	
18	increased DPE reacted for 20 hours	96	25.0k	30.7k	1.05	2.64:1 (2.85:1)	3.23:1	67.9k (65.1k)	61.0k	32.1k	1.02
19	change of fluoromethacrylate (to PFMHMA, sec 3.1)	98	25.0k	29.2k	1.06	4.54:1 (4.54:1)	5.44:1	52.9k (51.8k)	48.9k	39.8k	1.21

<sup>A</sup> Calculated from (mass recovered co-polymer + mass recovered sidearm sample)/(mass monomers added), expressed as a percentage.

<sup>B</sup> Calculated from (mass styrene added)/(moles initiator added).

<sup>C</sup> In THF against polystyrene standards.

<sup>D</sup> Calculated from ratio (moles styrene added - moles sidearm sample):(moles fluoromethacrylate added). The second figure, in brackets, then refers to the same calculation but with the moles of fluoromethacrylate reduced by an amount equivalent to the reduction in yield from 100% w/w.

<sup>E</sup> In chloroform

<sup>F</sup> Calculated from M<sub>n</sub> of PS by SEC and (mass fluoromethacrylate added x M<sub>n</sub> of PS by SEC)/(mass styrene added - mass sidearm sample). The second figure, in brackets, then refers to the same calculation, but with the mass of fluoromethacrylate reduced by an amount equivalent to the reduction in yield from 100% w/w.

<sup>G</sup> Calculated from M<sub>n</sub> of PS by SEC and mol ratio styrene (aromatic):fluoromethacrylate (-O-CH<sub>2</sub>-) by <sup>1</sup>H-NMR.

\* 100% w/w of styrene.

<sup>#</sup> 114% w/w of styrene

For the polystyrene segments of expts. 15-19, there was reasonable agreement between the target molecular weight ( $25,000\text{g mol}^{-1}$  in each case) and the experimental SEC values ( $28,300\text{g mol}^{-1}$  -  $31,100\text{g mol}^{-1}$ ). The decreased experimental value for expt. 13 ( $12,100\text{g mol}^{-1}$ ) is explained by the addition of a second quantity of initiator to this preparation because the first did not produce any colouration. Thus, initiator levels were increased beyond those needed for  $25,000\text{g mol}^{-1}$ , leading to a decrease in molecular weight. Similarly, the increased experimental value for expt. 14 ( $88,500\text{g mol}^{-1}$ ) is explained by the initiator quantity producing only a yellow colouration in the reaction rather than the usual bright orange. This indicated that some of the initiator had been inactivated by impurities remaining in the system, decreasing the amount available for initiation and thus elevating the molecular weight.

The polydispersities of the polystyrene segments prepared without initiator problems (expts. 15-19) were desirably low (1.04 - 1.06).

For the block co-polymers, early attempts (expts. 13-16) showed a variation in yield, from 96% w/w to as low as 46% w/w. Similarly, the experimental styrene:PFHMA molar ratio (by  $^1\text{H-NMR}$ ) was found to be variable and in some cases much greater than expected. On closer examination of the conditions for these reactions, it was noted that the main difference between them was the time allowed for the reaction of DPE with the living polystyryllithium. In expt. 13, this reaction was carried out overnight ( $\sim 20$  hours), whereas in expts. 14-16 only 3 - 4 hours were allowed for this step. An overnight reaction time for DPE was therefore introduced as standard.

For expt. 17, DPE was reacted with polystyryllithium for  $\sim 24$  hours. This resulted in an excellent yield (98% w/w) and the styrene:PFHMA ratio was close to that intended (4.38 experimentally by  $^1\text{H-NMR}$ , compared with 3.97 theoretical). However, the co-polymer was still contaminated with styrene homopolymer, to the extent that the SE chromatogram of the co-polymer appeared bimodal. This may have been due to inadvertent introduction of impurities on addition either of the THF, the DPE or the fluoromethacrylate, and which terminated some of the polystyryl chains.

Three further refinements in method and technique were therefore introduced. The first was the practice of adding, prior to injecting the calculated reaction quantity, some initiator dropwise into the styrene/toluene solution until a faint but persistent

yellow colouration was achieved. This procedure had the effect of removing any impurities still remaining before initiation and thus increasing the accuracy of the styrene polymerisation. Typically, ~30 - 40 $\mu$ l, added in 10 $\mu$ l aliquots, was needed to produce the colouration, which indicated that all impurities had been eliminated. The second modification was the similar practice of adding *sec*-butyllithium dropwise to the stock DPE, until a reddish colour indicated the elimination of impurities, prior to using the DPE in the reaction. The third modification was to increase the amount of DPE added, to 1.5x moles of initiator (from equimolar with initiator), to ensure there was sufficient present to cap all active polystyryl chains. Two further reactions (expts. 18 and 19) were carried out using these refinements.

Expt. 18 was the first in which it was found that all the data points for both the styrene segment and for the block co-polymer were of good quality, including the yield at 96% w/w. Whilst the experimental molecular weight of the styrene segment (30,700gmol<sup>-1</sup>) was ~20% higher than the target (25,000gmol<sup>-1</sup>), this experimental value was consistent with previously well-prepared styrene segments having a target of 25,000gmol<sup>-1</sup> (Table 2.5, expts. 8 and 10; Table 2.6, expts. 15-17) and its polydispersity was admirably low at 1.05.

The experimental molar ratio of the co-polymer (3.23:1 by  $^1\text{H-NMR}$ , Fig. 2.4) was in reasonable agreement with the target molar ratio (2.64:1, calculated from moles styrene after sidearm sample removal and moles PFHMA theoretically added). When the target molar ratio was re-calculated on the assumption that the shortfall in yield (4% w/w) was due to unreacted PFHMA, then the target was slightly closer (2.85:1) to the experimental.

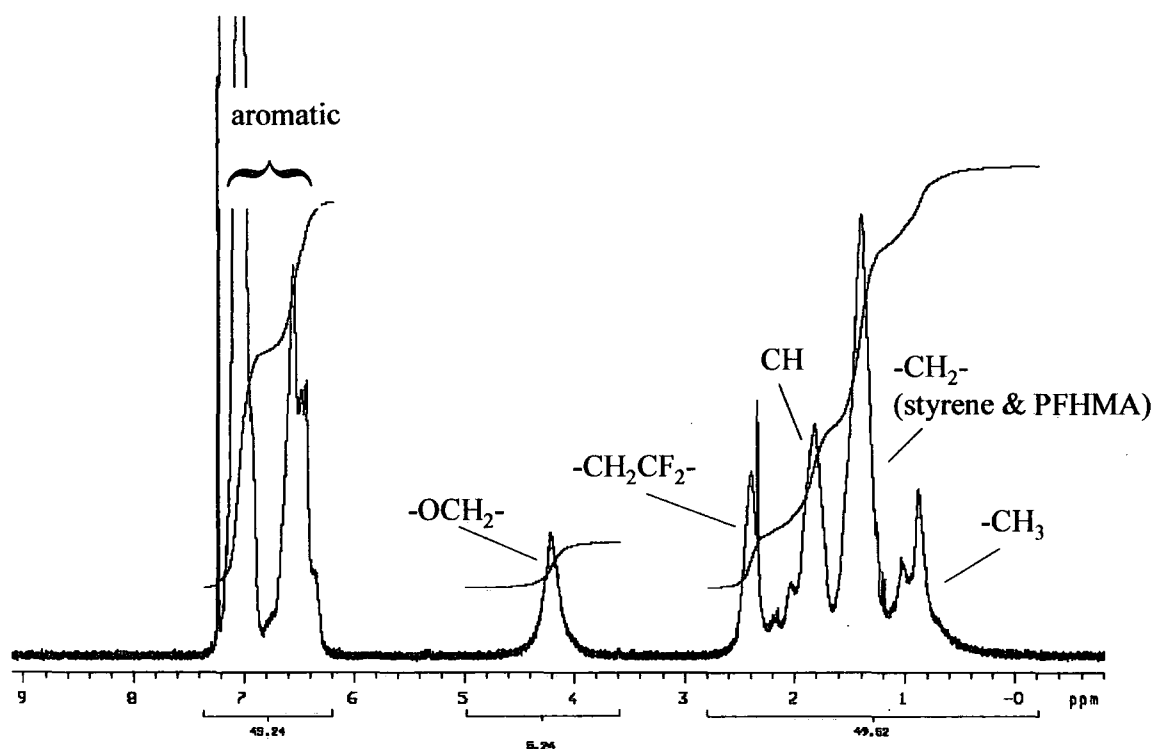


Fig. 2.4  $^1\text{H-NMR}$  of poly(styrene-b-PFHMA), prepared Table 2.6, expt. 18. (~1:1 mass composition, ~3:1 molar composition).

Additionally, the experimental molecular weight of the co-polymer ( $61,000\text{gmol}^{-1}$ , calculated from the  $M_n$  of its polystyrene segment by SEC, and from  $^1\text{H-NMR}$  ratios) was in good agreement with the target ( $67,900\text{gmol}^{-1}$ , calculated from  $M_n$  of its polystyrene segment and the theoretical quantity of PFHMA added). When the target  $M_n$  was re-calculated on the assumption that the shortfall in yield (4% w/w) was due to unreacted PFHMA, then the target was slightly closer ( $65,100\text{gmol}^{-1}$ ) to the experimental. The polydispersity of the block co-polymer was also admirably low at 1.02.

The SEC chromatograms for the polystyrene sidearm sample (blue) and for the block co-polymer (red) are illustrated in overlay in Fig 2.5 below. The main product of each gives a narrow, symmetric peak, with the polydispersities calculated on these peaks being 1.05 for the polystyrene and 1.02 for the co-polymer, i.e. equal to or less than that considered ideal ( $\geq 1.05$ ) for a living anionic polymerisation.

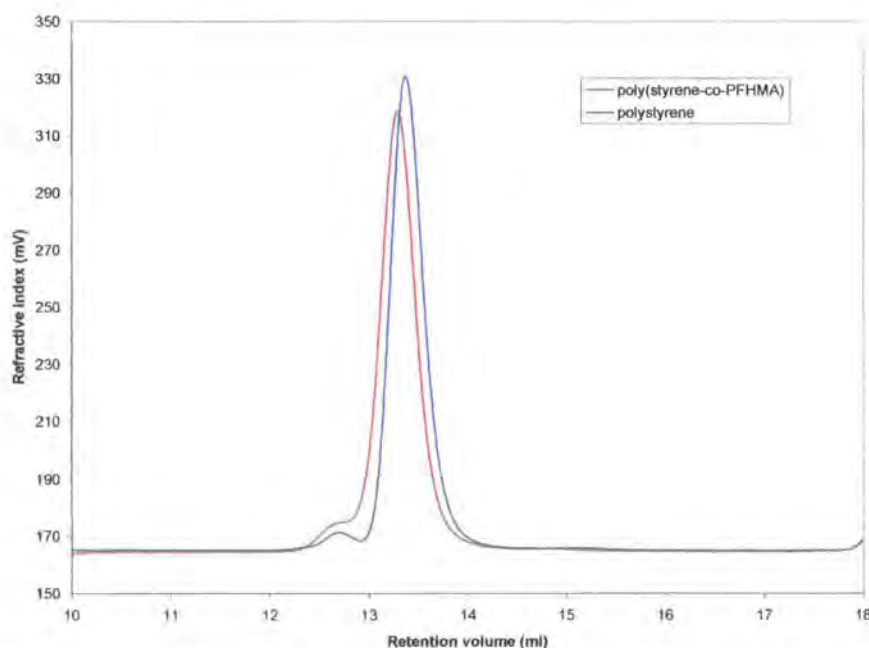


Fig. 2.5 SEC chromatograms by Refractive Index measurement of polystyrene and poly(styrene-b-PFHMA) prepared Table 2.6, expt.18.

The small high molecular weight peak in the polystyrene (blue) chromatogram is probably due to the coupling of living polystyryl chains which can occur when e.g. carbon dioxide ( $\text{CO}_2$ ) is introduced into the system. This probably occurred when the living polystyryl sample was manipulated into the sidearm (into which some  $\text{CO}_2$  may have leaked over the course of the reaction) or when the terminating agent (methanol, from which not all the  $\text{CO}_2$  had been displaced by nitrogen-sparging) was added to the sample.

The small high molecular weight peak in the block co-polymer (red) chromatogram, which occurs at the same retention volume for that in the polystyrene chromatogram, is also probably due to the coupling of living polystyryl chains and the coupling agent (e.g.  $\text{CO}_2$ ) may have been introduced to the main reaction with the addition of the second monomer (PFHMA).

This block co-polymer (Table 2.6, expt. 18) was thus judged to be the best that had been produced, and its preparation is exemplified in Section 3.5.1.

In expt.19, the method and technique of expt. 18 were used to prepare a poly(styrene-*b*-fluoromethacrylate) using 1H,1H,2H,2H-perfluoro(5-methylhexyl) methacrylate (PFMHMA), which has a branched rather than linear fluorocarbon chain. Whilst the experimental molecular weight of the styrene segment ( $29,200\text{gmol}^{-1}$ ) was ~20% higher than the target ( $25,000\text{gmol}^{-1}$ ), this experimental value was consistent with previously well-prepared styrene segments having a target of  $25,000\text{gmol}^{-1}$  (Table 2.5, expts. 8 and 10; Table 2.6, expts. 15-18) and its polydispersity was admirably low at 1.06. The yield was high, at 98% w/w.

The experimental molar ratio of styrene to PFMHMA in the co-polymer (5.44:1, by  $^1\text{H-NMR}$ ) was in reasonable agreement with the target molar ratio (4.54:1, calculated from moles styrene remaining after sidearm sample removal and moles PFMHMA theoretically added). When the target molar ratio was re-calculated on the assumption that the shortfall in yield (2% w/w) was due to unreacted fluoromethacrylate, then the target value was no closer to the experimental value, indicating that the shortfall in yield may have been due to incomplete recovery.

Additionally, the experimental molecular weight of the co-polymer ( $48,900\text{gmol}^{-1}$ , calculated from the  $M_n$  of its polystyrene by SEC and  $^1\text{H-NMR}$  ratios) was in good agreement with the target ( $52,900\text{gmol}^{-1}$ , calculated from  $M_n$  of its polystyrene segment and the theoretical quantity of PFMHMA added). When the target  $M_n$  is re-calculated on the assumption that the shortfall in yield (2% w/w) is due to unreacted PFMHMA, then the target is slightly closer ( $51,800\text{gmol}^{-1}$ ) to the experimental.

The SEC chromatograms for both the styrene segment and the co-polymer were monomodal and symmetric, with only a very small high molecular weight shoulder showing in each, which probably occurred for the same reasons as outlined for expt. 18 above. The polydispersity of the block co-polymer was, however, rather higher than desirable, at 1.21. This was the only co-polymer prepared with a branched-chain fluoromethacrylate, and its preparation is detailed in Section 3.5.2.

It was considered that Method 3, with its three refinements as discussed in this section and exemplified in Section 3.5.1, gave a working method for the preparation of (styrene-*b*-fluoromethacrylate) block co-polymers and would therefore be used for subsequent preparations.

## 2.6 Synthesis of Poly(styrene-*b*-1H,1H,2H,2H-perfluorohexyl methacrylate) Co-polymers, with composition 1:1 by moles..

Thus far, all (styrene-*b*-fluoromethacrylate) co-polymers had been prepared using a greater mass of styrene than fluoromethacrylate (Table 2.4) or approximately equal masses of each (Tables 2.5 and 2.6). The latter meant that the degree of polymerisation (and molar ratio) in the styrene segment was approximately three times that of the fluoromethacrylate segment. Attention was therefore turned to preparing poly(styrene-*b*-PFHMA) co-polymers with equal degrees of polymerisation, i.e. equimolar quantities of styrene and PFHMA. This meant incorporating into the polymer approximately three times the mass of PFHMA previously used. Method 3, discussed in Section 2.5.3 and exemplified in Section 3.5.1 was used. The results of these preparations are summarised below in Table 2.7. The scales (i.e. total mass monomers used) of the experiments ranged from 12.03g (expt. 21) to 29.86g (expt. 25).



Table 2.7 Poly(styrene-b-PFHMA) polymers with composition 1:1 by moles (equal degrees of polymerisation), prepared by Method 3.

Expt.	Conditions.	Yield <sup>A</sup> % w/w	polystyrene block		Co-polymer (styrene-b-PFHMA)				
			M <sub>n</sub>		Pd	Molar ratio S:PFHMA		M <sub>n</sub>	
			Target <sup>B</sup>	SEC <sup>C</sup>		Target <sup>D</sup>	<sup>1</sup> H-NMR <sup>E</sup>	Target <sup>F</sup>	<sup>1</sup> H-NMR <sup>G</sup>
20	PFHMA prepared by standard drying and degassing procedure. (Section 3.2.).	26*	25.0k	28.7k	1.04	all polystyrene <sup>#</sup>			
21		23*	25.0k	23.0k	1.05				
22		25*	25.0k	32.6k	1.12				
23	Inhibitor removed from PFHMA prior to standard drying and degassing procedure.	92	25.0k	28.1k	1.05	0.88:1 (0.98:1)	1.20:1	130k (120k)	103k
24	Inhibitor removed from PFHMA prior to standard drying and degassing procedure; polystyrene sample taken by syringe.	99	25.0k	42.7k	1.03	0.99:1 (1.00:1)	1.11:1	180k (178k)	123k
25	Inhibitor removed from PFHMA prior to standard drying and degassing procedure; polystyrene sample taken by syringe; volume of THF added increased from ~ 100ml to ~ 200-300ml.	96	25.0k	68.5k	1.10	1.01:1 (1.09:1)	1.30:1	278k (267k)	219k

<sup>A</sup> Calculated from (mass recovered co-polymer + mass recovered sidearm sample)/(mass monomers added), expressed as a percentage.

<sup>B</sup> Calculated from (mass styrene added)/(moles initiator added).

<sup>C</sup> In THF against polystyrene standards.

<sup>D</sup> Calculated from ratio (moles styrene added - moles sidearm sample):(moles fluoromethacrylate added). The second figure, in brackets, then refers to the same calculation but with the moles of fluoromethacrylate reduced by an amount equivalent to the reduction in yield from 100% w/w.

<sup>E</sup> In chloroform

<sup>F</sup> Calculated from M<sub>n</sub> of PS by SEC and (mass fluoromethacrylate added x M<sub>n</sub> of PS by SEC)/(mass styrene added - mass sidearm sample). The second figure, in brackets, then refers to the same calculation, but with the mass of fluoromethacrylate reduced by an amount equivalent to the reduction in yield from 100% w/w.

<sup>G</sup> Calculated from M<sub>n</sub> of PS by SEC and mol ratio styrene (aromatic):fluoromethacrylate (-O-CH<sub>2</sub>-) by <sup>1</sup>H-NMR.

\* All 102 - 103% w/w on styrene.

<sup>#</sup> The errors in expts. 20 and 21 were initially ascribed to poor experimental technique.

Early attempts (expts. 20-22) at preparing these co-polymers gave yields of only 23 - 26% w/w (with respect to total monomers added) and with the  $^1\text{H-NMR}$  spectra indicating virtually no fluoromethacrylate incorporation. However, the molecular weights of the polystyrene blocks ( $M_n = 23,000 - 32,600\text{gmol}^{-1}$ ) were found to be in reasonable agreement with those intended ( $M_n = 25,000\text{gmol}^{-1}$ ) and their polydispersities were low (1.04 - 1.12). The problem was therefore assumed to be occurring after the formation of the styrene block and possibly during the addition of the fluoromethacrylate.

Adding approximately three times the mass of fluoromethacrylate compared to previous experiments might result in the introduction of a higher level of impurities, causing termination of the polystyrene chain. It was noted that PFHMA was stabilised with 100ppm (0.01%) *tert*-butylcatechol (molecular weight = 166.22<sup>28</sup>), and that *tert*-butylcatechol has a boiling point (285°C<sup>28</sup> at atmospheric pressure, ~130°C at 5mmHg) close to that of PFHMA (60 - 62°C at 5mmHg,<sup>26</sup> ~200°C at atmospheric pressure), suggesting that it might have co-distilled with the monomer under reduced pressure conditions. As a diphenol, each molecule of *tert*-butylcatechol would be capable of terminating two living chains. Assuming that the stabiliser was added as a weight percentage, then the quantity potentially present in the mass of PFHMA used in these preparations was approximately  $1.32 \times 10^{-3}$  moles (i.e.  $(0.01 \times \sim 22\text{g})/166.22$ ). This was greater than the quantity of initiator added to prepare the styrene block for these preparations, which in each case was approximately  $2.8 \times 10^{-4}$  moles (i.e.  $\sim 7\text{g}/25,000$ ), and would therefore be more than capable of terminating the reaction on the addition of PFHMA.

It was decided to remove the inhibitor by passing the PFHMA monomer down a column of aluminium oxide, prior to the usual purification of drying and degassing by freeze-thawing over calcium hydride. Three further preparations (expts. 23-25, Table 2.7) of poly(styrene-*b*-PFHMA) co-polymers were made, in which this extra purification step for the fluoromethacrylate monomer was incorporated into the method.

Of the three polystyrene blocks prepared with a target  $M_n$  of  $25,000\text{gmol}^{-1}$  (expts. 23-25), only one (expt. 23) had an experimental  $M_n$  in this region ( $28,100\text{gmol}^{-1}$ ). The other two (expts. 24 and 25) had experimental values much

greater than this, at  $42,700\text{gmol}^{-1}$  and  $68,500\text{gmol}^{-1}$  respectively. However, all three had low polydispersities (at 1.03 - 1.11), indicating that the error occurred only at the time of initiator addition. Much later, the problem was found to be due to degradation of the initiator stock

The co-polymer prepared in expt. 23 resulted in a good yield (92% w/w) and there was reasonable agreement between the target styrene:PFHMA ratio (0.88:1, calculated from moles styrene after sidearm sample removal and moles PFHMA theoretically added) with that intended (1.20) when measured by  $^1\text{H}$ -NMR (Fig. 2.6).

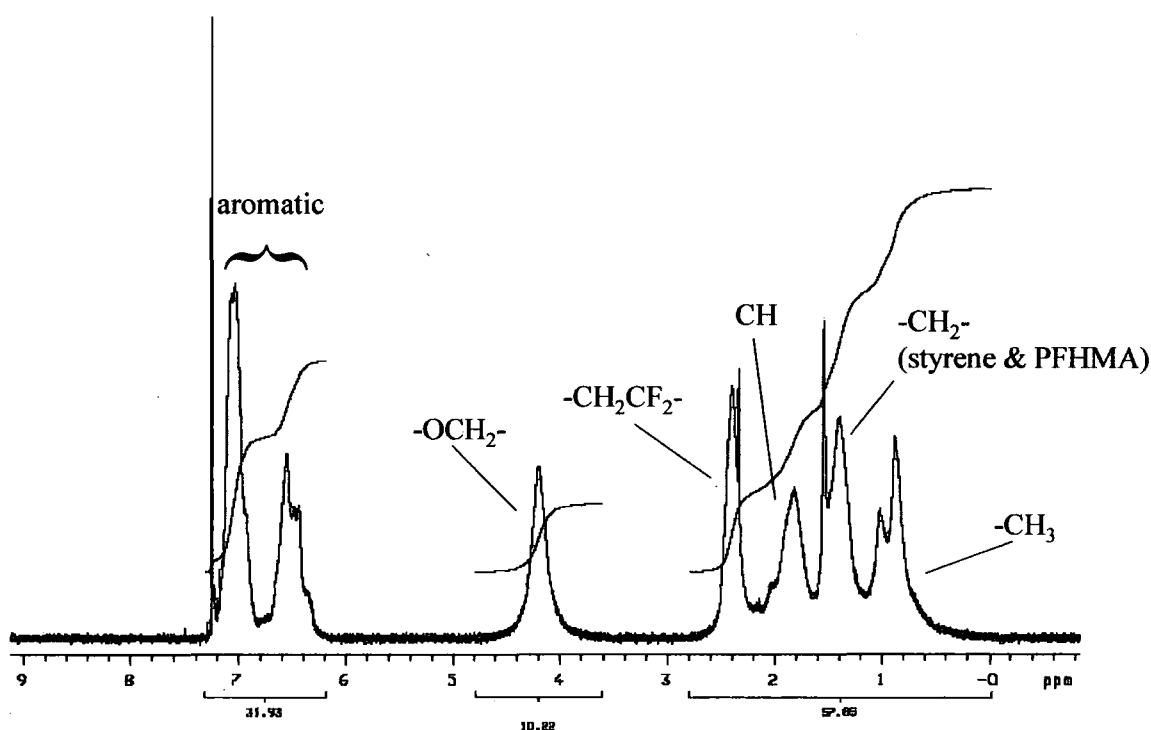


Fig. 2.6  $^1\text{H}$ -NMR of poly(styrene-*b*-PFHMA), prepared Table 2.7, expt. 23. (~1:3 mass composition, ~1:1 molar composition,).

When the target molar ratio was re-calculated on the assumption that the shortfall in yield (8% w/w) was due to unreacted PFHMA, then the target value was slightly closer (0.98:1) to the experimental value. However, the experimental  $M_n$  ( $103,000\text{gmol}^{-1}$ ) was approximately 27% less than the target ( $130,000\text{gmol}^{-1}$ ) and the SEC chromatogram of the co-polymer was bimodal, indicating there was still a loss of control after the formation of the styrene block.

In the next preparation (Table 2.7, expt. 24) an alternative method of taking the polystyrene sidearm sample was used. In all previous preparations, the sample had been taken by manipulating the apparatus off-line, so that the polystyrene flowed into the pre-evacuated sidearm. This had the effect of coating the upper surface of the main reactor with the living polystyryl solution, and this may not have all been re-incorporated into the reaction prior to the addition of the fluoromethacrylate. If this were so, then it might explain the apparent multi-modality of the SEC chromatogram of the co-polymer. In the alternative method therefore, the apparatus was let down to dry nitrogen, after the formation of the polystyrene block. This allowed the polystyrene sample to be taken by syringe and the apparatus could therefore remain static. The polystyryl/toluene solution was then freeze-thawed twice to remove the nitrogen before the addition of the THF by distillation. Whilst this technique appeared to have no detrimental affect on the yield of co-polymer (excellent at 99% w/w), or on the agreement between target (1.00:1, calculated from moles styrene after sidearm sample removal and moles PFHMA theoretically added) and experimental (1.11:1.00, by  $^1\text{H-NMR}$ ) styrene:PFHMA ratios, the target  $M_n$  of the co-polymer ( $180,000\text{gmol}^{-1}$ ) was almost 50% greater than the experimental  $M_n$  ( $123,000\text{gmol}^{-1}$ , calculated from the  $M_n$  of its polystyrene by SEC and  $^1\text{H-NMR}$  ratios). In addition, the SEC chromatogram of the co-polymer was again bimodal.

In a final preparation in this series (expt. 25, Table 2.7), the same conditions as for expt. 24 were used, except that the volume of THF added after the formation of the polystyrene block, but before the addition of PFHMA, was increased from  $\sim 100\text{ml}$  to  $\sim 200 - 300\text{ml}$ . This modification gave a very good yield (96% w/w), but not very good agreement between the target (1.01:1) and experimental (1.30:1) molar ratios. The target  $M_n$  ( $278,000\text{gmol}^{-1}$ ) was bigger than the experimental  $M_n$  ( $219,000\text{gmol}^{-1}$ ) and the SEC chromatogram of the co-polymer was again bimodal.

On the evidence of the bimodal SEC chromatograms, the block co-polymers detailed in Table 2.7, with their equimolar quantities of styrene and PFHMA, became uncontrolled after the formation of the polystyrene segment and during the formation of the PFHMA block. This may have been due, despite the increased purification of the monomer, to introduction of impurities at this stage of the reaction. Within the time constraints of this thesis, no further investigations were made.

## 2.7 Calculation of percentage Styrene Homopolymer in a poly(styrene-b-fluoromethacrylate) Co-polymer.

It is possible to use SEC as a quantitative method to calculate the amount of a homopolymer “impurity” present in a bulk sample of a block co-polymer.

The refractive index detector on the SEC instrument was calibrated by preparing a solution of a homopolymer standard, of comparable molecular weight to the experimental homopolymer, of accurately-known concentration. The solution was then chromatographed, and the area beneath the peak produced (relative to the baseline) was calculated, using integral software. The area of this peak correlated directly with the accurately-known quantity of polystyrene in the solution.

A solution of the experimental co-polymer, also of accurately-known concentration, was then prepared, chromatographed and the area of the peak produced by the homopolymer “impurity” was calculated. This area correlated directly with the quantity of homopolymer present in the sample, and the mass that the area represented was calculated, from the following relationship:

$$\frac{\text{mass homopolymer “impurity” (unknown)}}{\text{mass homopolymer standard (known)}} \equiv \frac{\text{peak area for homopolymer “impurity” (known)}}{\text{peak area for homopolymer standard (known)}}$$

Thus, the calculated mass of the homopolymer “impurity” present in the accurately-weighed experimental sample can be expressed as a mass percentage, which is the same percentage of homopolymer “impurity” present in the bulk sample of the block co-polymer:

$$\frac{\text{calculated mass homopolymer “impurity”}}{\text{weighed mass co-polymer sample}} \times 100 = \% \text{ w/w homopolymer present}$$

The co-polymer chosen for this exercise was that described in Table 2.7, expt. 24, for which the <sup>1</sup>H-NMR spectrum of the bulk product confirmed that the degree of polymerisation of styrene and PFHMA was approximately equal, as intended. The molecular mass of PFHMA is just over three times that of styrene (page 88), therefore most of the mass in this co-polymer (over 75% w/w) is due to PFHMA, thus making the molecular weight of the co-polymer approximately four times that of the concomitant polystyrene. It was therefore anticipated that greater resolution of the co-

polymer and homopolymer peaks in the SEC chromatogram could be achieved. In previous co-polymers, in which the incorporated masses of styrene and PFHMA were approximately equal, thus making the molecular weight of the co-polymer only approximately twice that of the concomitant polystyrene, good resolution between the co-polymer and homopolymer peaks had not been achieved.

The SEC chromatograms for expt. 24, Table 2.7 are illustrated below (Fig. 2.7).

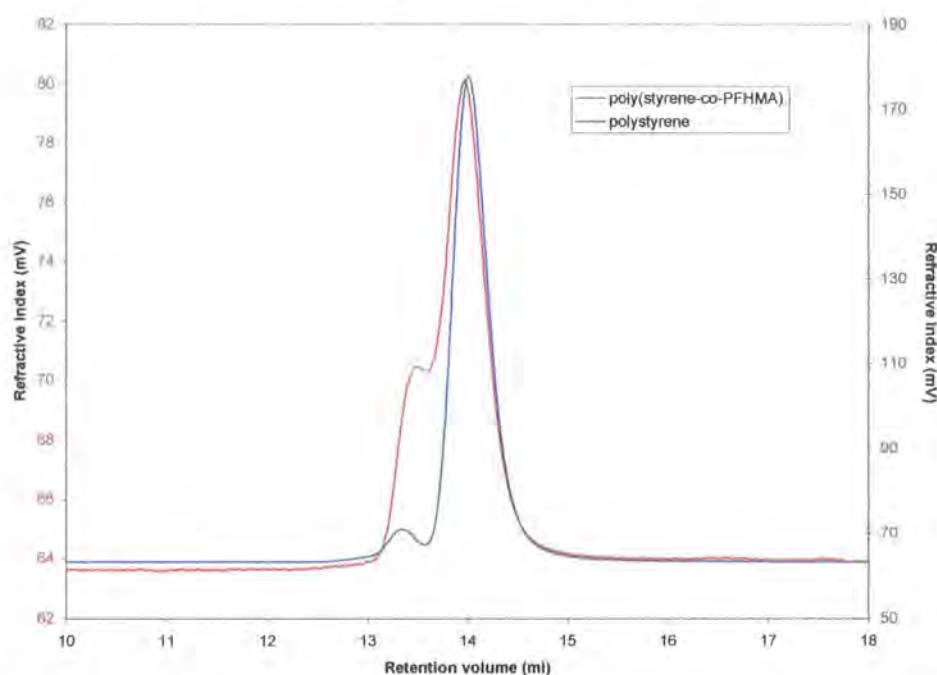


Fig. 2.7 SEC chromatograms of block co-polymer and concomitant homopolymer for expt. 24 (Table 2.7) in which co-polymer composition  $\sim 1:3$  by mass ( $\sim 1:1$  by moles). Note the different y-scale values for the chromatograms.

The chromatogram for polystyrene (blue) has a main peak at a higher retention volume, produced by the bulk of the sample, and a small shoulder at a lower retention volume, produced by a small quantity of a higher molecular weight component. The reason for the presence of this high molecular weight component within the homopolymer is probably due to the coupling of living polystyryl chains, which can occur for reasons already discussed on pages 61-62.

The chromatogram for the co-polymer sample (red) also has two peaks, with that at lower retention volume produced by the co-polymer itself (higher molecular weight), and that at higher retention volume produced by the homopolymer “impurity” (lower

molecular weight). This is confirmed by the close correlation of this lower molecular weight peak with that of the main peak in the polystyrene chromatogram.

At this stage, it must be emphasised that the vertical scales of the chromatograms have been manipulated in order that both chromatograms can be contained within the one illustration. This is necessary because the refractive index response of the co-polymer, with its large mass percentage of low-refractive index PFHMA, is vastly less than that of polystyrene. In other words, the relative size of the red and blue chromatograms as seen in Fig. 2.7 are not indicative of the relative size of the chromatograms from which data was calculated.

Similarly, within the co-polymer (red) chromatogram, the relative visual sizes of the lower retention volume (co-polymer) peak and the higher retention volume (homopolymer) peak do not indicate that the sample contained “less” co-polymer and “more” homopolymer. Rather, this disparity in visual size is due to the high percentage (~75% w/w) of low refractive index PFHMA present in the co-polymer, which has the effect of suppressing the refractive index response for the co-polymer component.

Having calibrated the RI detector as outlined above with a known, accurately-prepared THF solution of polystyrene standard ( $66,000\text{g mol}^{-1}$ ), the area beneath the peak of the homopolymer “impurity” in the experimental co-polymer solution (concentration  $2.168\text{mg ml}^{-1}$  in THF) was calculated (by integral software) to be produced by 0.226mg of polystyrene. Thus, the quantity of homopolystyrene “impurity” in the bulk co-polymer sample was calculated to be:

$$\frac{0.226}{2.168} = 10.4\% \text{ w/w}$$

## 2.8 Syntheses of Block Co-polymers containing a Bromostyrene Block.

An alternative approach to synthesising block co-polymers with a large refractive index contrast between the two blocks is to introduce a block synthesised from a high refractive index monomer such as bromostyrene, rather than a low refractive index monomer, such as a fluoromethacrylate.

### 2.8.1 Synthesis of poly(*p*-bromostyrene).

It is not possible directly to polymerise bromostyrene via an anionic mechanism, as the initiator/propagating species would undergo side reactions with the aryl bromide group, leading to loss of control of the polymerisation. It is, however, possible to brominate the styrene block after polymerisation. To establish a method for this, some previously prepared polystyrene (Section 2.2) was brominated in nitrobenzene solution by a simple, direct method at room temperature, over a period of ~24 hours.<sup>82</sup> Nitrobenzene was used as the solvent as it has a high dielectric constant and as such does not require a catalyst of the usual type (e.g. ferric bromide).<sup>82</sup> The whole reaction flask was encased in foil to exclude light and thus prevent the light-catalysed free radical reactions that would otherwise have produced backbone bromination.<sup>82</sup> The apparatus was vented through aqueous sodium hydroxide solution to scrub out the hydrogen bromide which was slowly generated. The progress of the reaction was monitored by withdrawing samples (~5ml) from the reaction at timed intervals, quenching the unreacted bromine with octene and precipitating any polymer in methanol. The resultant white solids were collected by filtration and analysed by <sup>13</sup>C-NMR and Elemental Analysis (EA). The preparation is exemplified in Section 3.7.1.



### 2.8.2 Analysis of poly(*p*-bromostyrene).

When a styrene ring is *para* brominated, the *para* (*p*) carbon signal shifts from 126 ppm to 120ppm.<sup>83</sup> The shifts of the *ortho* (*o*) and *meta* (*m*) carbon signals are also affected by the *para* substitution (from 128 to 129ppm, and from 128 to 132ppm respectively)<sup>83</sup> but the shift of the quaternary aromatic carbon remains largely unchanged, at 145ppm for styrene and 144ppm for *p*-bromostyrene<sup>83</sup> (Fig. 2.8).

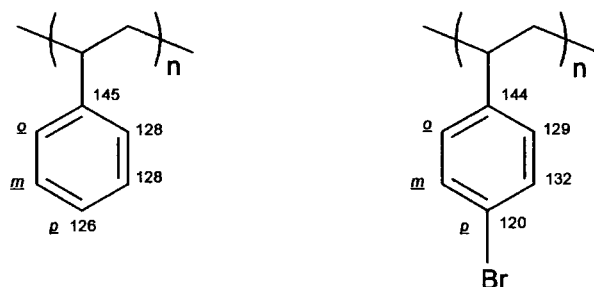


Fig. 2.8 Aromatic  $^{13}\text{C}$  NMR shifts ( $\delta$ , ppm) for polystyrene (*left*) and poly(*p*-bromostyrene) (*right*).

The  $^{13}\text{C}$ -NMR spectra of polystyrene and brominated polystyrene (respectively Fig. 2.9 and Fig. 2.10 overleaf), were obtained under specifically quantitative conditions, i.e. the relaxation time was increased and the de-coupler was switched off during the relaxation delay. The spectra confirmed that bromination had taken place solely on the aromatic ring and in the *para* position. The quantitative conditions enabled an assessment to be made of the percentage of styrene rings brominated by comparing the integral of the *p*-ArBr peak in poly(*p*-bromostyrene) (120ppm) with that of the *p*-ArH peak in polystyrene (126 - 125ppm). This comparison indicated that bromination of 95 - 100% of the styrene rings had been achieved by the reaction conditions described above.

Elemental percentage mass was calculated for the brominated polymer, assuming 100% of styrene rings were brominated:

C: 52.49%; H: 3.85%; Br: 43.65%

and compared with the percentage mass determined by EA:

C: 52.71%; H: 3.86%; Br: 43.53%.

As can be seen, there was excellent agreement between the two sets of figures.

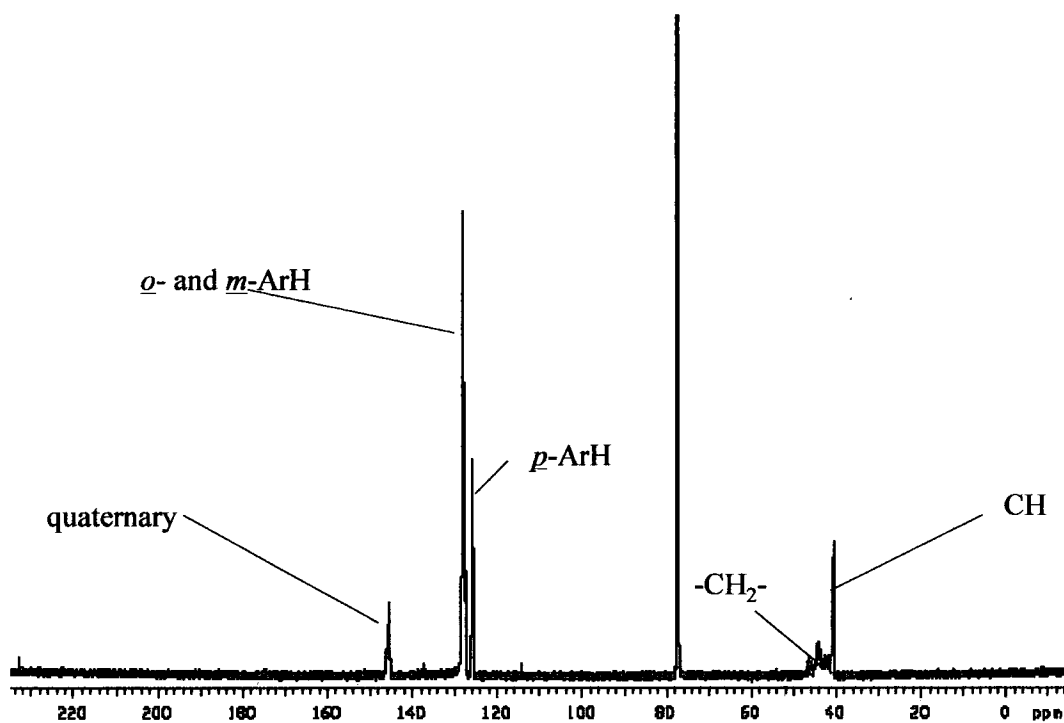


Fig. 2.9  $^{13}\text{C}$ -NMR of polystyrene (prepared in Section 2.2).

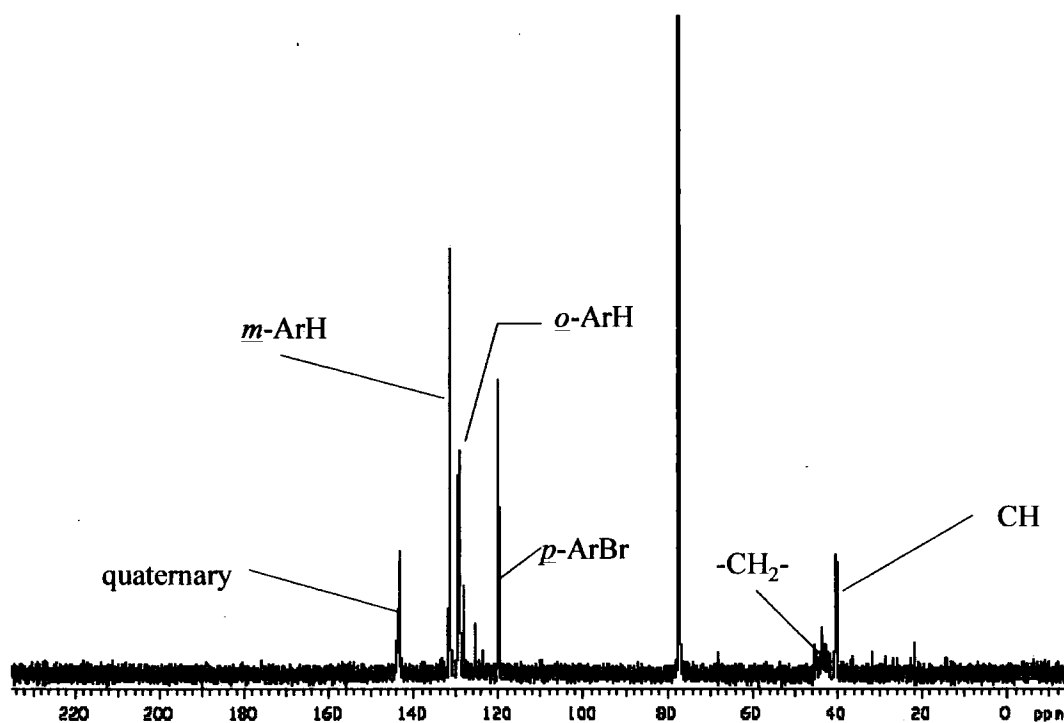


Fig. 2.10  $^{13}\text{C}$ -NMR of poly(*p*-bromostyrene) (prepared in Section 2.8.1).

### 2.8.3 Synthesis of poly(styrene-*b*-methyl methacrylate) co-polymers.

As discussed above, it is not possible directly to polymerise *p*-bromostyrene by an anionic method; therefore poly(styrene-*b*-MMA) co-polymers were prepared as precursors, which could then be brominated on the styrene rings, using the method as described in Section 2.8.1 above.

The poly(styrene-*b*-MMA) co-polymers were made with varying ratios of styrene to methyl methacrylate, using the optimised LAP method developed (Section 2.5.3, expt. 18; exemplified Section 3.5.1) for the preparation of poly(styrene-*b*-PFHMA) co-polymer. The results of the poly(styrene-*b*-MMA) co-polymer preparations are summarised below in Table 2.8, and exemplified in Section 3.6, but no further conditions are detailed here, as the same method and technique was used in each case. The scales (i.e. total mass monomers used) of the experiments ranged from 5.34g (expt. 1) to 22.02g (expt. 3).

For expts. 26 and 27, the polystyrene blocks had experimental molecular weights ( $M_n = 27,000\text{gmol}^{-1}$  and  $40,200\text{gmol}^{-1}$  respectively) very close to those intended ( $M_n = 25,000\text{gmol}^{-1}$  and  $37,500\text{gmol}^{-1}$  respectively) and each had a desirably low polydispersity at 1.04.

For expts. 28 and 29, the experimental molecular weights of the polystyrene blocks ( $M_n = 85,000\text{gmol}^{-1}$  and  $76,400\text{gmol}^{-1}$  respectively) were greatly different to the targets (both  $M_n = 50,000\text{gmol}^{-1}$ ) and in expt. 28 the SEC chromatogram was multi-shouldered. Much later, it was concluded that these erroneous results were not only due to degradation of the initiator stock, but may also have been due to a slow leak in the high vacuum of the system during the formation of the polystyrene.

Table 2.8 Poly(styrene-b-MMA) co-polymers.

Expt.	Conditions.	Yield <sup>A</sup> % w/w	polystyrene block			Co-polymer (styrene-b-MMA)					
			M <sub>n</sub>		Pd	Molar ratio S:MMA		M <sub>n</sub>			Pd
			Target <sup>B</sup>	SEC <sup>C</sup>		Target <sup>D</sup>	<sup>1</sup> H-NMR <sup>E</sup>	Target <sup>F</sup>	<sup>1</sup> H-NMR <sup>G</sup>	SEC <sup>C</sup>	
26	Method according to Section 2.5.3, expt. 18.	99.0	25.0k	27.0k	1.04	0.82:1	0.82:1	58.6k	58.0k	56.4k	1.07
27		100	37.5k	40.2k	1.04	1.85:1	1.84:1	61.1k	61.2k	51.6k	1.23
28		100	50.0k	85.0k	1.13	0.92:1	0.93:1	175k	161k	bimodal	
29		99.0	50.0k	76.4k	1.04	0.92:1	0.96:1	157k	153k	bimodal	

<sup>A</sup> Calculated from (mass recovered co-polymer + mass recovered sidearm sample)/(mass monomers added), expressed as a percentage.

<sup>B</sup> Calculated from (mass styrene added)/(moles initiator added).

<sup>C</sup> In THF against polystyrene standards.

<sup>D</sup> Calculated from ratio (moles styrene added - moles sidearm sample):(moles methyl methacrylate added).

<sup>E</sup> In chloroform

<sup>F</sup> Calculated from M<sub>n</sub> of PS by SEC and (mass methyl methacrylate added x M<sub>n</sub> of PS by SEC)/(mass styrene added - mass sidearm sample). The second figure, in brackets, then refers to the same calculation, but with the mass of fluoromethacrylate reduced by an amount equivalent to the reduction in yield from 100% w/w.

<sup>G</sup> Calculated from M<sub>n</sub> of PS by SEC and mol ratio styrene (aromatic):methyl methacrylate (-O-CH<sub>2</sub>-) by <sup>1</sup>H-NMR.

For each co-polymer prepared, the target and experimental styrene:MMA molar ratios were in excellent agreement, indicating complete polymerisation for each monomer component. This was confirmed by the similarly excellent near-quantitative yields ( $\geq 99\%$  w/w) in each experiment.

The target and experimental molecular weights are also in excellent agreement for each co-polymer, but only one (expt. 26) produced an acceptably low (1.07) polydispersity. Expt. 27 gave a co-polymer with a high molecular weight shoulder, hence the broad polydispersity (1.23) and in expts. 28 and 29 the SEC chromatograms were bimodal.

Expt. 26 was therefore judged to be the best poly(styrene-*b*-MMA) co-polymer produced and its preparation is exemplified in Section 3.6.

#### 2.8.4 Synthesis of poly(*p*-bromostyrene-*b*-methyl methacrylate) co-polymers.

A sample of the poly(styrene-*b*-MMA) co-polymer prepared in expt. 26 was brominated, using the same method as had been successfully used to brominate polystyrene (Section 2.8.1). The bromination is exemplified in Section 3.7.2. The progress of the reaction was monitored by withdrawing samples (~5ml) at timed intervals, quenching the unreacted bromine with octene and precipitating the polymer in methanol. The resultant white solids were collected by filtration and analysed by  $^{13}\text{C}$ -NMR,  $^1\text{H}$ -NMR and EA.

The  $^{13}\text{C}$ -NMR spectra of the unbrominated and brominated polymers (Figs. 2.11 and 2.12 respectively) verified that bromination had taken place quantitatively and solely on the aromatic ring in the *para* position. The presence of the methacrylate methyl ester resonance (at 178ppm) in the  $^{13}\text{C}$ -NMR spectrum of the brominated sample proved that the ester linkage not been cleaved by the bromination reaction conditions.

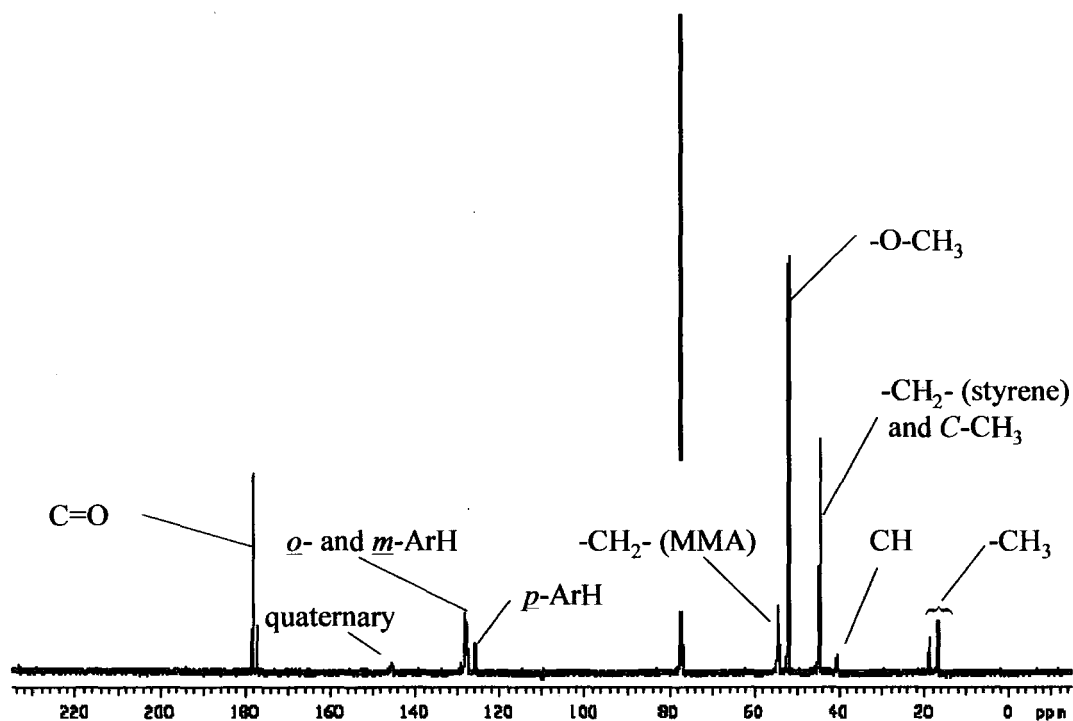


Fig. 2.11  $^{13}\text{C}$ -NMR of poly(styrene-b-MMA) (prepared in Table 2.8, expt. 26).

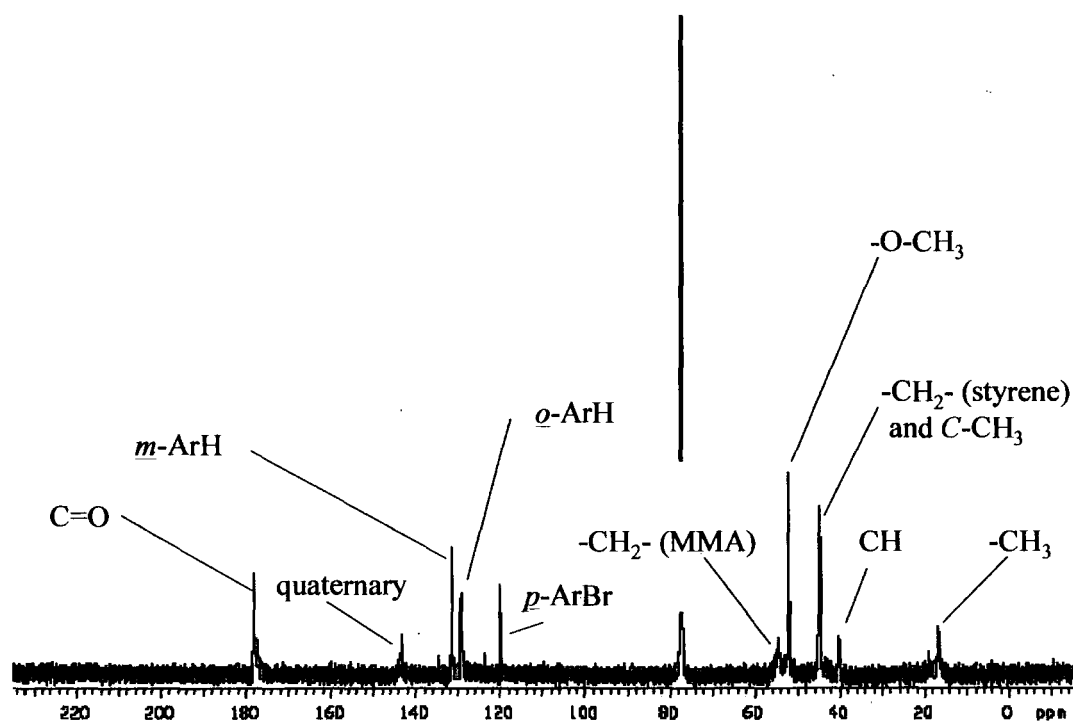


Fig. 2.12  $^{13}\text{C}$ -NMR of poly(*p*-bromostyrene-b-MMA) (prepared by the bromination of expt. 26, Table 2.8).

Elemental percentage mass was calculated the brominated polymer, using the block ratios previously determined by <sup>1</sup>H-NMR and assuming 100% of the styrene rings were brominated:

C 57.26%; H: 6.53%; Br: 15.87%

and compared with the percentage mass determined by EA:

C: 56.96%; H: 6.50%; Br: 15.92%

As can be seen, there is good agreement between the two sets of figures.

Bromination was performed on two more poly(styrene-*b*-MMA) co-polymers. Their elemental analyses are summarised below in Table 2.9 and the calculated (assuming all styrene rings were monobrominated) and experimental figures are in good agreement for each polymer.

Table 2.9      Elemental Analyses of poly(*p*-bromostyrene-*b*-MMA) co-polymers.

Co-polymer		C % w/w	H % w/w	Br % w/w
poly(bromostyrene- <i>b</i> -MMA) <sup>A</sup>	by calculation:	57.26	6.53	15.87
	by EA:	56.96	6.50	15.92
poly(bromostyrene- <i>b</i> -MMA) <sup>B</sup>	by calculation:	54.20	4.81	33.65
	by EA:	53.07	4.64	33.25

<sup>A</sup> poly(S-MMA) not prepared under this thesis.

<sup>B</sup> poly(S-MMA) prepared in Table 2.8, expt. 27.

#### 2.8.5 Synthesis of poly(*p*-bromostyrene-*b*-1H,1H,2H,2H-perfluorohexyl methacrylate) co-polymers.

To achieve maximum refractive index contrast between the components of a co-polymer, a bromostyrene block (high refractive index) would have to be combined with a fluoromethacrylate block (low refractive index). This would require the bromination of the styrene block in a previously prepared (styrene-*b*-fluoromethacrylate) co-polymer.

A sample of the poly(styrene-*b*-PFHMA) polymer prepared in Table 2.6, expt. 18 was brominated by the method already successfully used to brominate polystyrene (Section 2.8.1) and poly(styrene-*b*-MMA) (Section 2.8.4). The progress of the reaction was monitored by withdrawing samples (~5ml) at timed intervals, quenching the unreacted bromine with octene and precipitating the polymer in methanol. The resultant white solids were collected by filtration and analysed by  $^{13}\text{C}$ -NMR and EA. The preparation is exemplified in Section 3.7.3.

The  $^{13}\text{C}$ -NMR spectrum of the unbrominated and brominated polymers (Figs. 2.13 and 2.14 respectively) verified that bromination had taken place quantitatively and solely on the aromatic ring in the *para* position. The presence of the fluorocarbon chain resonance (at 119 - 105ppm) in the  $^{13}\text{C}$ -NMR spectrum of the brominated sample proved that the ester linkage not been cleaved by the bromination reaction conditions.



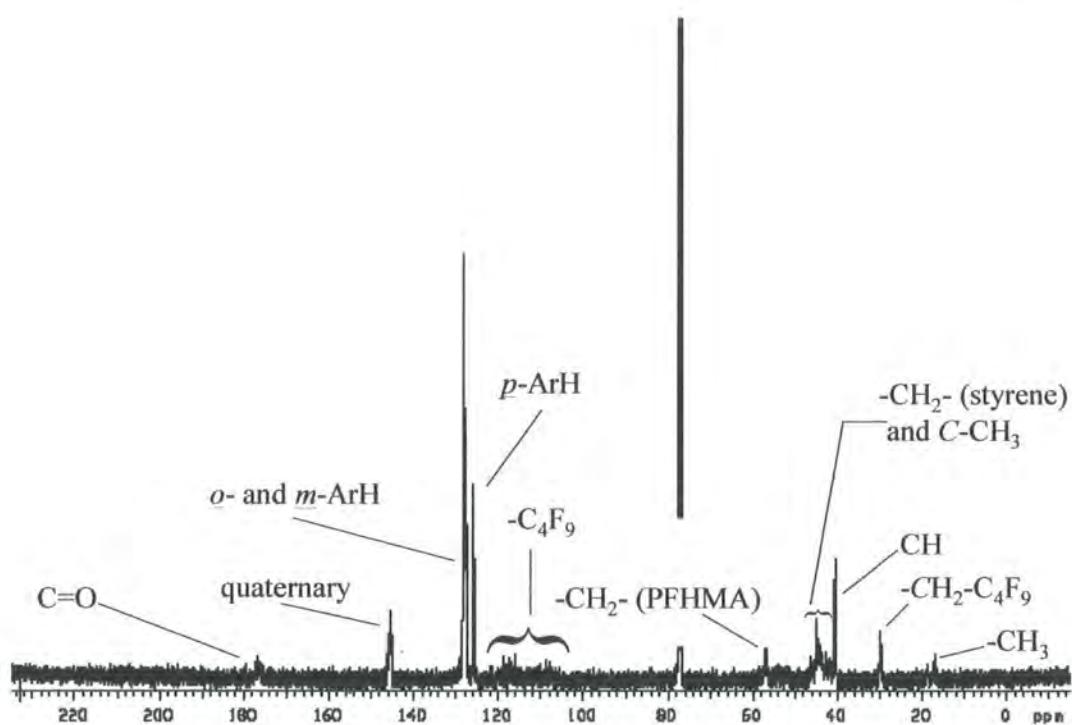


Fig. 2.13  $^{13}\text{C}$ -NMR of poly(styrene-b-PFHMA) (prepared Table 2.6, expt. 18).

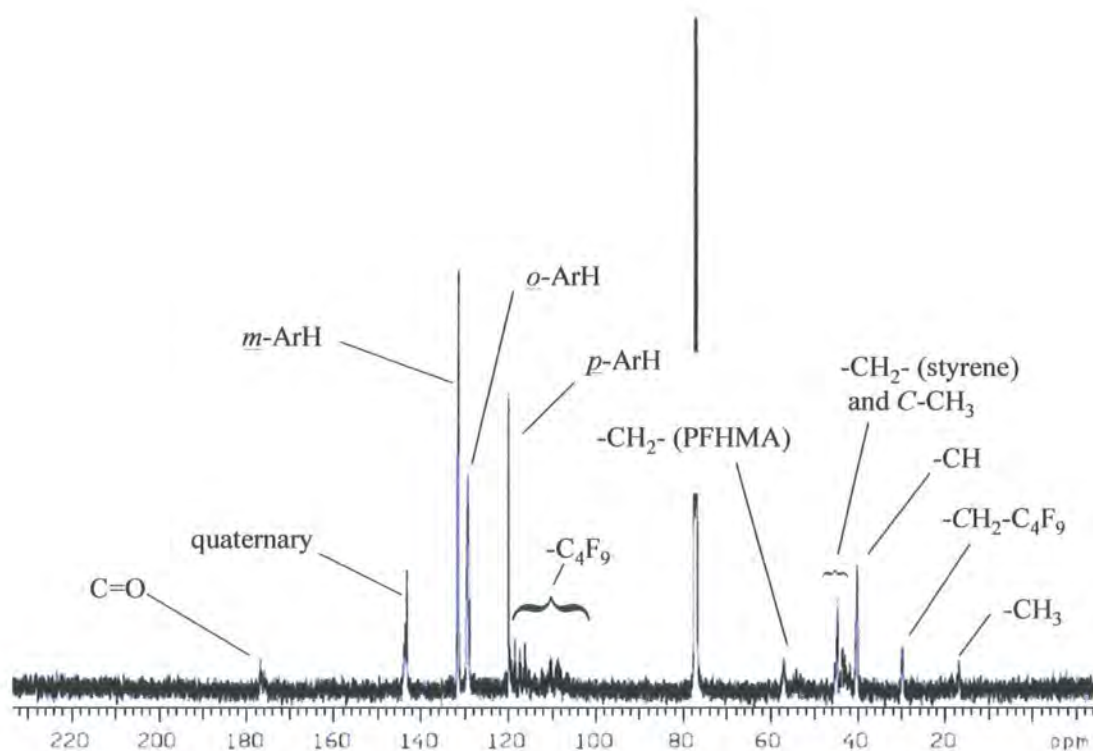


Fig. 2.14  $^{13}\text{C}$ -NMR of poly(*p*-bromostyrene-b-PFHMA) (prepared by the bromination of expt. 18, Table 2.6).

Elemental percentage mass was calculated for the brominated polymer, using the block ratios previously determined by  $^1\text{H-NMR}$  and assuming 100% of the styrene rings were brominated:

C: 46.62%; H: 3.45%; F: 18.52%; Br: 27.95%

and compared with that determined experimentally by EA:

C: 46.13%; H: 3.43%; F: 17.60%; Br: 24.75%

The experimental results are in good agreement for C and H, but not for F and Br. Samples were re-submitted for analysis, with no further improvement in results. Within the time constraints of this thesis, no further investigation was made.

Bromination was performed on two more poly(styrene-*b*-PFHMA) co-polymers. Their elemental analyses are summarised below in Table 2.10.

Table 2.10 Elemental Analyses of poly(*p*-bromostyrene-*b*-PFHMA) co-polymers.

Co-polymer		C % w/w	H % w/w	Br % w/w	F % w/w
poly(bromostyrene- <i>b</i> -PFHMA) <sup>A</sup>	by calculation:	42.66	3.18	17.38	30.99
	by EA:	42.06	3.12	15.17	32.97
poly(bromostyrene- <i>b</i> -PFHMA) <sup>B</sup>	by calculation:	43.41	3.23	19.39	28.61
	by EA:	42.27	3.17	14.15	31.13

<sup>A</sup> poly(S-PFHMA) prepared in Table 2.7, expt. 23.

<sup>B</sup> poly(S-PFHMA) prepared in Table 2.7, expt. 25.

## 2.9 Material Characterisation.

The materials produced in this work therefore consisted of co-polymers of high-contrast refractive index blocks, and their respective homopolymers. These were characterised, where possible, by refractive index measurement and by solid state organisation, where applicable.

### 2.9.1 Refractive Index Measurement.

For refractive index measurement to be possible, the polymer sample needed to be presented in an amorphous form (random arrangement of the chains) and not in a crystalline form (ordered arrangement of chains) or even semi-crystalline form. Any crystalline domains within the sample would cause light-scattering and thus interfere with the measurement of refractive index.

Films were spun-cast onto silicon wafers from toluene solutions (~6% w/w) at ~50rpm for ~20 seconds. Depending on the polymer, this was found to produce films of thickness ~100 – 400nm. Where the polymer was insoluble in toluene, THF solutions were prepared, but these were found not to give amorphous films.<sup>84</sup> No references were found to solvent casting of films of fluoromethacrylate homo- or co-polymers, but this was unsurprising as references had been found to the insolubility of fluoromethacrylate polymers in common solvents. Only one reference<sup>22</sup> to the “moulding” of a film from polyTFEMA was found and this gave no details as to conditions. Several attempts were made to “heat and press” a sample of polyTFEMA but none of them produced an homogenous sample.

Refractive index measurements were obtained using the “C” line (wavelength = 634nm), meaning that all values would be expected to be slightly lower than literature values, which are quoted for the “D” line (wavelength = 589nm) (refractive index decreases as the wavelength increases). The values are averages of five readings, taken from different positions on the sample, and detailed in Tables 2.11 and 2.12. Some samples were analysed more than once, hence more than one value is given.

Table 2.11 Refractive Index measurements by “C” line of homopolymer films cast from toluene solution onto silicon wafers.

Homopolymer	Experimental RI, “C” line	Literature RI, “D” line
polystyrene <sup>A</sup>	1.55, 1.57	1.59 <sup>E</sup>
polyMMA <sup>B</sup>	1.48, 1.49	1.49 <sup>E</sup>
polyTFEMA <sup>C</sup>	<i>insoluble</i>	1.42 <sup>E</sup>
poly( <i>p</i> -bromostyrene) <sup>D</sup>	1.61, 1.61, 1.61, 1.61	<i>not found</i>

<sup>A</sup> prepared Section 2.2, exemplified Section 3.3.1; <sup>B</sup> prepared Section 2.3, exemplified Section 3.3.2;

<sup>C</sup> prepared Section 2.4 (Table 2.1, expt. 1), exemplified Section 3.4.1;

<sup>D</sup> prepared Section 2.8.1, exemplified Section 3.7.1; <sup>E</sup> Ref. 28.

Table 2.12 Refractive Index measurements by “C” line of block co-polymer films cast from toluene solution onto silicon wafers.

Original co-polymer				<i>p</i> -Bromostyrene form	
Name	M <sub>n</sub> <sup>G</sup> (k)	% w/w styrene	RI	Name	RI
poly(S-MMA) <sup>A</sup>	44.1	25	1.46, 1.47	poly( <i>p</i> -BrS-MMA) <sup>H</sup>	<i>insoluble</i>
poly(S-MMA) <sup>B</sup>	58.0	46	1.52, 1.52	poly( <i>p</i> -BrS-MMA) <sup>I</sup>	<i>insoluble</i>
poly(S-MMA) <sup>C</sup>	61.2	66	1.57, 1.57	poly( <i>p</i> -BrS-MMA) <sup>J</sup>	<i>insoluble</i>
poly(S-PFHMA) <sup>D</sup>	103	27	1.45, 1.46	poly( <i>p</i> -BrS-PFHMA) <sup>K</sup>	<i>insoluble</i>
poly(S-PFHMA) <sup>E</sup>	219	29	1.44, 1.44	poly( <i>p</i> -BrS-PFHMA) <sup>L</sup>	1.47, 1.47
poly(S-PFHMA) <sup>F</sup>	61.0	50	1.50	poly( <i>p</i> -BrS-PFHMA) <sup>M</sup>	1.73, 1.73

<sup>A</sup> not prepared under this thesis; <sup>B</sup> prepared Section 2.8.3, expt. 26, exemplified Section 3.6;

<sup>C</sup> prepared Section 2.8.3, expt. 27; <sup>D</sup> prepared Section 2.6, expt. 23, exemplified section 3.5.3;

<sup>E</sup> prepared Section 2.6, expt. 25; <sup>F</sup> prepared Section 2.5.3, expt. 18.

<sup>G</sup> Calculated from M<sub>n</sub> of PS by SEC and mol ratio styrene:methacrylate by <sup>1</sup>H-NMR.

<sup>H</sup> prepared Section 2.8.4; <sup>I</sup> prepared Section 2.8.4, exemplified Section 3.7.2; <sup>J</sup> prepared Section 2.8.4;

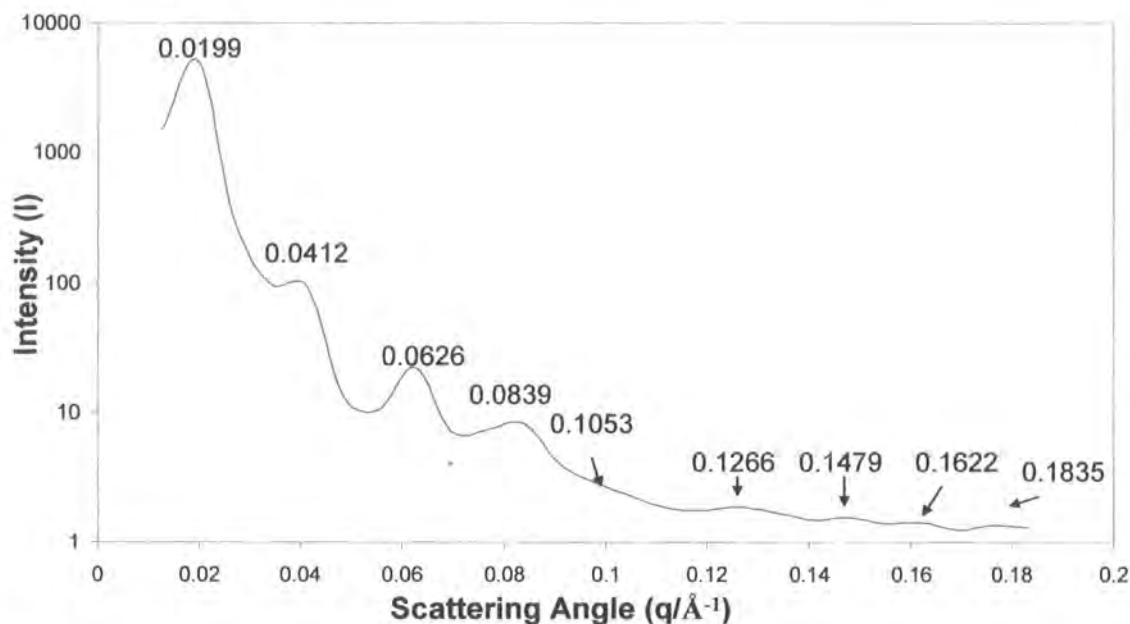
<sup>K</sup> prepared Section 2.8.5; <sup>L</sup> prepared Section 2.8.5; <sup>M</sup> prepared Section 2.8.5, exemplified Section 3.7.3.

Refractive index values for poly(styrene-*b*-MMA) co-polymers appeared to increase slightly with increasing styrene content, as might be expected, and fell within the range for the respective homopolymers (1.49 - 1.59, see Table 2.11 above). Where it could be measured, the refractive index of the brominated form increased, as would be expected. Refractive index values for poly(styrene-*b*-PFHMA) co-polymers also appeared to vary slightly with styrene content. The values are lower than for the equivalent poly(styrene-*b*-MMA) co-polymers, as might be expected. Bromination of the co-polymer raised the experimental refractive index values, as expected, and by considerably more in the sample which contained the greater quantity (by mass) of bromostyrene.

### 2.9.2 Solid State Organisation.

Microphase separation of diblock co-polymers into lamellar structures can be used to generate periodic layers with different refractive indices - which recalls the description of a 1-D photonic crystal, given in Section 1.1. Similarly, the cylindrical (columnar) microphase morphology can be likened to a 2-D photonic structure and the block-centred cubic (bcc) arrangement of spheres to a 3-D structure. The choice of monomers for investigation in this work was based on their contrasting refractive indices and their incompatibility. The co-polymers were thus expected to microphase separate in the solid state.

Attempts were made<sup>78</sup> at solvent casting a thin film to form a simple “wavelength selective” device from a solution of polystyrene (prepared Section 2.2, exemplified Section 3.3.1), polyPFHMA (prepared Section 2.4, Table 2.2, expt. 1; exemplified Section 3.4.2) and poly(styrene-*b*-PFHMA) co-polymer (prepared Section 2.5.3, Table 2.6, expt. 18; exemplified Section 3.5.1), the two homopolymers being included to swell the respective components of the co-polymer. These attempts were unsuccessful, due to a combination of factors: the incomplete solubility of the polyPFHMA homopolymer in toluene (a good solvent for film casting) and the inability of a solution of the polymers in THF to form a non-crystalline film. Melt casting was therefore tried and after some experimentation, a suitable sample was prepared by annealing the three polymer powders (polystyrene, poly(PFHMA) and poly(styrene-*b*-PFHMA)), in a 1:1:1 mass ratio, in a mould at 160°C under vacuum for 72 hours. The sample was returned to ambient temperature by gradual cooling whilst still being held under vacuum. Data from the annealed sample was collected by Small Angle X-ray Scattering (SAXS) over 18 hours and from this data, a graph (Graph 2.1 below) of the scattering intensity ( $I$ ) *versus* scattering angle ( $q$ ) was plotted.<sup>78</sup>



Graph 2.1      Scattering intensity *versus* scattering angle for the annealed mixture of polystyrene, poly(PFHMA) and poly(styrene-b-PFHMA).

The graph thus plotted gave the “Bragg peaks” characteristic of lamellar morphology, i.e. the peaks occur at integer multiples of  $q^*$ , where  $q^*$  is the position of the first order maximum,<sup>85</sup> in this case at  $0.0199 \text{ \AA}^{-1}$  (Table 2.11).

Table 2.11      Positions of scattering peaks relative to 1st order peak for annealed mixture of polystyrene, poly(PFHMA) and poly(styrene-b-PFHMA).

Scattering angle (Å)	peak <i>n</i> /(peak <i>q</i> *) (experimental)	peak <i>n</i> /(peak <i>q</i> *) (theoretical, lamellar)
0.0199	1	1
0.0412	2.07	2
0.0626	3.15	3
0.0839	4.22	4
0.1053	5.29	5
0.1266	6.36	6
0.1479	7.43	7
0.1622	8.15	8
0.1835	9.22	9

The spacing<sup>85</sup> of the lamellae ( $d$ ) is given by  $\frac{2\pi}{q^*}$ , which in this case gives a lamellar spacing of  $\approx 316 \text{ \AA}$ . Separate SAXS data for each homopolymer, the co-polymer and the three component mixture were also collected.<sup>86</sup> Each of these, when converted into scattering intensity *versus* scattering angle graphs proved to be smooth, featureless curves, indicating that the peaks and periodicity obtained in the SAXS

pattern for the annealed three-component system were due to microphase self-assembly.

### Conclusions.

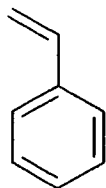
The experimental refractive indices of spun-cast films of the homopolymers were found to be in reasonable agreement with literature values. The refractive indices of the co-polymers fell within the range of the component homopolymers, and showed some direct correlation with component ratios.

The insolubility of certain of the co-polymers, as found previously, made thin-film preparation difficult. However, after melt casting, a three-component mixture of polystyrene, polyPFHMA and poly(styrene-*b*-PFHMA), from the experimental preparations specified above, could be made to self-assemble into a lamellar structure.

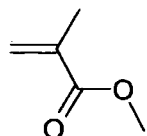
### **Chapter 3: Experimental.**



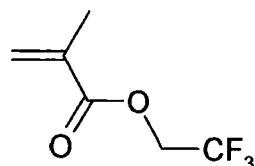
### 3.1 Monomers used.



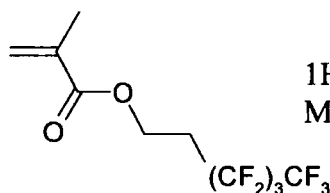
Styrene (S): Mw = 104.15, bp = 145°C, RI = 1.55\*  
(ex-Aldrich, 99+%)



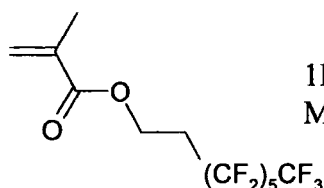
Methyl methacrylate (MMA):  
Mw = 100.11, bp = 101°C, RI = 1.41\*  
(ex-Fisons, 99.5+%)



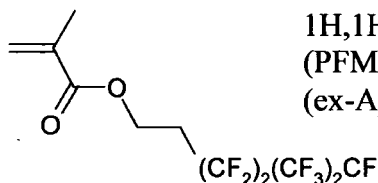
2,2,2-trifluoroethyl methacrylate (TFEMA):  
Mw = 168.11, bp = 107°C, RI = 1.36\* (ex-Fluorochem)



1H, 1H, 2H, 2H-perfluorohexyl methacrylate (PFHMA):  
Mw = 332.16, bp = ~200°C, RI = 1.35\* (ex-Fluorochem)



1H,1H,2H,2H-perfluorooctyl methacrylate (PFOMA):  
Mw = 432.18, bp = ~220°C, RI = 1.35\* (ex-Fluorochem)



1H,1H,2H,2H-perfluoro(5-methylhexyl) methacrylate  
(PFMHMA): Mw = 382.18, bp = 199°C, RI = 1.35\*  
(ex-Apollo Scientific)

\* All data from commercial catalogues.

### 3.2 Preparation of Glassware, Solvents, Monomers and other Reagents.

The reaction vessels (commonly nicknamed “Christmas trees,” see Fig. 3.1) were sealed with either Young’s taps or rubber septa as appropriate.

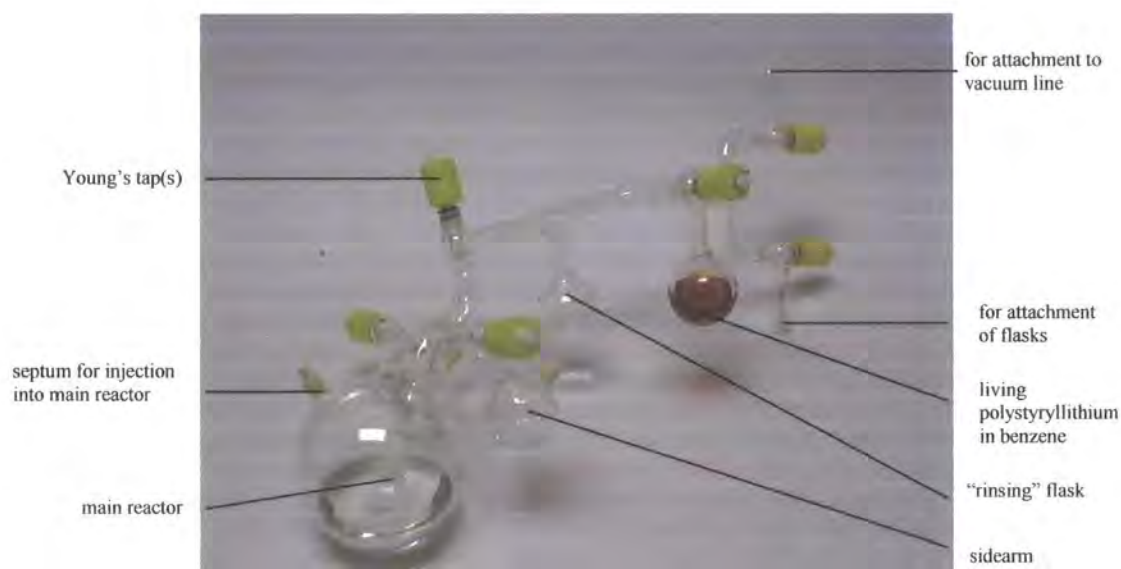


Fig. 3.1 “Christmas tree.”

The vessel was placed under high vacuum for at least two hours and preferably overnight, followed by thorough rinsing with living polystyryllithium in benzene. The remnants of the wash solution were then rinsed back into their receptor by repeated distillation-condensation of benzene from and to the receptor. When the benzene was no longer coloured (i.e. was rinsing water-white) the benzene was condensed back into the receptor by freezing using liquid nitrogen. The vessel was reconnected to the vacuum line and maintained under high vacuum until required.

Flasks, equipped with Young’s taps, if required for pre-measurement of solvents or monomers, were prepared by placing under high vacuum until needed. Gas-tight syringes were dried under vacuum at room temperature and stored in a desiccator prior to use.

Tetrahydrofuran (ex-Fison's, HPLC grade) was purified by placing in an oven-dried but cooled 500ml round-bottomed flask over freshly prepared sodium wire in the presence of a little benzophenone. Subsequent freeze-thaw cycles saw the colour of the solvent change from water-white to yellow to green to blue to indigo and finally to violet (due to the presence of the sodium benzophenone dianion in anhydrous conditions) as the solvent became progressively drier and gases were removed. Toluene (ex-Aldrich, HPLC grade), benzene (ex-Aldrich, HPLC grade) and 1,3-bis(trifluoromethyl) benzene (ex-Aldrich, 99% grade) were purified by placing in an oven-dried but cooled flask over calcium hydride. Freeze-thaw cycles were applied until no further gases could be removed.

Styrene, methyl methacrylate and fluoromethacrylates were dried and degassed over calcium hydride by a series of freeze-thaw cycles. When not frozen, the flasks were enclosed in foil to exclude light.

For each experiment requiring lithium chloride, the calculated quantity was dried in the reactor under high vacuum overnight. 1,1-Diphenylethylene (ex-Aldrich, 97% grade) was distilled, then stored under dry nitrogen. Immediately prior to use, *sec*-butyllithium was added dropwise by injection until a reddish colouration was achieved.

Initiators (*sec*-butyllithium, 1.4M in cyclohexane; *tert*-butyllithium, 1.7M in pentane; and *n*-butyllithium, 1.78M in cyclohexane) were used as supplied by Aldrich. *Triiso*-butylaluminium (1.0M in hexanes), triethylaluminium (1.0M in hexanes) and di-*n*-butylmagnesium (1.0M in heptane) were also used as supplied by Aldrich.

### 3.3. Syntheses of Polystyrene and Poly(methyl methacrylate).

#### 3.3.1 Synthesis of Polystyrene.

Benzene (~100ml) was distilled under vacuum into the main reactor using liquid nitrogen as the coolant and freeze-pumped once. Styrene (11.58g,  $11.1 \times 10^{-2}$  mol) was distilled from purified stock into a pre-weighed flask and then into the main reactor. The mixture was again frozen and freeze-pumped once. The temperature of the mixture was allowed to rise to room temperature with stirring, at which point initiator (*sec*-butyllithium, 0.165ml,  $2.32 \times 10^{-4}$  mol) was injected via a septum into the main flask to give the characteristic orange colour of living polystyryllithium.

The reaction was allowed to proceed for 19 hours (overnight) before being terminated with N<sub>2</sub>-sparged methanol (~0.5ml), which removed the orange colour. The polymer was recovered by precipitation into excess methanol, collected by filtration over a glass sinter and dried under vacuum at room temperature for 24 hours.

Yield: 11.78g (99+%).

Target M<sub>n</sub>: 50,000gmol<sup>-1</sup>; experimental M<sub>n</sub> (GPC): 99,800gmol<sup>-1</sup>; Pd: 1.03.

<sup>1</sup>H-NMR (400MHz, CDCl<sub>3</sub>,  $\delta$ , ppm): 7.40 - 6.15 (ArH); 2.30 - 1.10 (-CH- & -CH<sub>2</sub>-).

#### 3.3.2 Synthesis of Poly(methyl methacrylate).

Tetrahydrofuran (~100ml) was distilled under vacuum into the main reactor using liquid nitrogen as the coolant and freeze-pumped once. After warming to room temperature, the solvent was used to wash the lithium chloride (0.30g,  $7.08 \times 10^{-3}$  mol) from the sidearm into the main reactor, into which solution 1,1-diphenylethylene (DPE, 0.145ml,  $8.16 \times 10^{-4}$  mol) was injected via a septum. After stirring to mix, the mixture was cooled to -78°C (solid CO<sub>2</sub>/acetone bath). Initiator (*sec*-butyllithium, 0.700ml,  $1.00 \times 10^{-3}$  mol) was added by injection, to give the characteristic red colour of the diphenyl anion. After allowing 15 minutes for the formation of 1,1-diphenyl-3-methylpentyllithium, purified methyl methacrylate (MMA, 8.16g,  $8.15 \times 10^{-2}$  moles) was distilled from triethylaluminium (~1ml) into the main reactor. This resulted in a colour change from red to water-white.

The reaction was allowed to proceed overnight at  $-78^{\circ}\text{C}$  before being terminated with  $\text{N}_2$ -sparged methanol (1.0ml). The polymer was precipitated in excess hexane, and recovered as previously described.

Yield: 7.58g (93%).

Target  $M_n$ :  $10,000\text{gmol}^{-1}$ ; experimental  $M_n$  by GPC:  $16,300\text{gmol}^{-1}$ ; and by  $^1\text{H-NMR}$ :  $14,400\text{gmol}^{-1}$ .

$^1\text{H-NMR}$  (400MHz,  $\text{CDCl}_3$ ,  $\delta$ , ppm): 3.40 (O- $\text{CH}_3$ ); 2.00 - 0.60(- $\text{CH}_2$ -&- $\text{CH}_3$ ).

### 3.4 Syntheses of Fluoromethacrylate Homopolymers.

#### 3.4.1 Synthesis of Poly(2,2,2-trifluoroethyl methacrylate).

Tetrahydrofuran (~100ml) was distilled under vacuum into the main reactor using liquid nitrogen as the coolant and freeze-pumped once. After warming to room temperature, the solvent was used to wash the lithium chloride (0.21g,  $5.00 \times 10^{-3}\text{mol}$ ) from the sidearm into the main reactor, into which solution DPE was injected (0.22ml,  $1.28 \times 10^{-4}\text{mol}$ ) via a septum. After stirring to mix, the mixture was cooled to  $-78^{\circ}\text{C}$  using a solid  $\text{CO}_2$ /acetone bath. Initiator was added (*sec*-butyllithium, 1.4M, 0.900ml,  $1.28 \times 10^{-3}\text{mol}$ ) by injection, to give the characteristic red colour of the diphenyl anion. After allowing one hour for the 1,1-diphenyl-3-pentyllithium complex to form, the purified 2,2,2-trifluoroethyl methacrylate (TFEMA, 6.42g,  $3.82 \times 10^{-2}\text{mol}$ ) was distilled into the reaction, causing the colour of the reaction to change from red to orange to yellow. The reaction was allowed to continue for 4 hours at  $-78^{\circ}\text{C}$ , before being terminated with  $\text{N}_2$ -sparged methanol (1.0ml). The polymer precipitated in excess hexane and recovered as previously described.

Yield: 5.75g (90%).

Target  $M_n$ :  $5,000\text{gmol}^{-1}$ ; experimental  $M_n$  by  $^1\text{H-NMR}$ :  $29,800\text{gmol}^{-1}$ ; and by GPC:  $12,900\text{mol}^{-1}$ ; Pd: 1.35.

$^1\text{H-NMR}$  (400MHz,  $\text{CDCl}_3$ ,  $\delta$ , ppm): 4.3, (-O- $\text{CH}_2$ -); 2.20 - 0.50 (- $\text{CH}_2$ - & - $\text{CH}_3$ ).

### 3.4.2 Synthesis of Poly(1H,1H,2H,2H-perfluorohexyl methacrylate).

Poly(1H,1H,2H,2H-perfluorohexyl methacrylate) was prepared in a similar manner to Section 3.4.1, using tetrahydrofuran (~50ml), lithium chloride (0.10g,  $2.36 \times 10^{-3}$  mol), *sec*-butyllithium (1.4M, 0.420ml,  $5.82 \times 10^{-4}$  mol), 1,1-diphenylethylene (0.20ml,  $1.16 \times 10^{-3}$  mol) and 1H,1H,2H,2H-perfluorohexyl methacrylate (PFHMA, 5.82g,  $1.75 \times 10^{-2}$  mol).

Yield: 3.20g (55%).

Target  $M_n$ : 10,000gmol<sup>-1</sup>; experimental  $M_n$  by <sup>1</sup>H-NMR: 11,900gmol<sup>-1</sup>; and by GPC: *inverted RI chromatogram*.

<sup>1</sup>H-NMR (400MHz, CD<sub>2</sub>Cl<sub>2</sub>,  $\delta$ , ppm): 4.20 (s, -O-CH<sub>2</sub>-), 2.60 - 0.60 (m, -CH<sub>2</sub>CF<sub>2</sub>-, -CH<sub>2</sub>- & -CH<sub>3</sub>).

### 3.4.3 Synthesis of Poly(1H,1H,2H,2H-perfluorooctyl methacrylate).

Pre-weighed quantities of toluene and 1,3-bis (trifluoromethyl) benzene were distilled under vacuum into the reactor, using liquid nitrogen as the coolant, to give an approximate volume ratio of 40:60 respectively. The mixture was freeze-pumped once. Triisobutylaluminium (1.50ml,  $1.50 \times 10^{-3}$  mol) was added by injection at room temperature, and after cooling to 0°C using an ice/salt/water bath, *tert*-butyllithium (1.7M, 0.35ml,  $5.98 \times 10^{-4}$  mol) was added. The mixture was stirred for 5 minutes. The purified 1H,1H,2H,2H-perfluorooctyl methacrylate (PFOMA, 4.0ml, 5.98g,  $1.38 \times 10^{-2}$  mol) was then added as slowly as possible, by injection, using a lockable syringe, which caused the expected colour change from water-white to yellow. The reaction was stirred at 0°C for 24 hours, during which time the colouration gradually decreased and was very faint by the time the reaction was terminated with N<sub>2</sub>-sparged methanol (1ml). The polymer was precipitated from excess hexane and recovered as previously described.

Yield: 4.79g (80%).

Target  $M_n$ : 20,000gmol<sup>-1</sup>; experimental  $M_n$  by GPC: *insoluble in common solvents*; and by <sup>1</sup>H-NMR: *not applicable*.

### 3.5 Syntheses of Poly(styrene-*b*-fluoromethacrylate) Co-polymers.

#### 3.5.1 *Synthesis of poly(styrene-*b*-1H,1H,2H,2H-perfluorohexyl methacrylate) with composition 1:1 by mass.*

Toluene (~40ml) was distilled under vacuum into the main reactor using liquid nitrogen as the coolant and freeze-pumped once. After warming to room temperature, the solvent was used to wash the lithium chloride (0.06g,  $1.42 \times 10^{-3}$  mol) from the sidearm into the main reactor. Styrene (4.07g,  $4.00 \times 10^{-2}$  mol) was distilled into a pre-weighed flask and then into the reactor, using liquid nitrogen as the coolant and the frozen mixture was degassed and thawed to room temperature. Initiator (*sec*-butyllithium, 1.4M, ~30 $\mu$ l) was added dropwise into the flask to give a faint persistent yellow-colour, before adding the reaction quantity (0.115ml,  $1.63 \times 10^{-4}$  mol) which gave the characteristic orange colour of polystyryllithium. The reaction was stirred for 3 hours, with the temperature controlled by a cold water bath, after which time a sidearm sample of living polystyrene was withdrawn and quickly terminated with N<sub>2</sub>-sparged methanol (0.5ml). The polystyrene/toluene solution was cooled to -78°C, (solid CO<sub>2</sub>/acetone bath), and THF (~120ml) was added via distillation. Maintaining the reaction at this temperature, DPE (0.043ml, 0.04g,  $2.44 \times 10^{-4}$  mol) was added by injection via a septum, giving the characteristic red colour of the diphenyl anion, and the reaction mixture was stirred at -78°C for 21 hours. Meanwhile, PFHMA (4.63g,  $1.39 \times 10^{-2}$  mol) was dried over calcium hydride and degassed before it was distilled into the main reactor. This resulted in a colour change from red to water-white. The reaction was maintained at -78°C for a further 24 hours before being terminated with N<sub>2</sub>-sparged methanol (1.0ml). The polymer was precipitated in excess methanol and recovered as previously described.

Yield: 7.97g (96%).

Target  $M_n$  of pS: 25,000gmol<sup>-1</sup>;  $M_n$  of pS by GPC: 30,700gmol<sup>-1</sup>; Pd of pS: 1.05.

Target mol ratio S:PFHMA: 2.82:1; mol ratio by <sup>1</sup>H-NMR: 3.23:1;

$M_n$  of p(S-PFHMA) by <sup>1</sup>H-NMR: 61,000gmol<sup>-1</sup>; Pd of p(S-PFHMA): 1.02.

<sup>1</sup>H-NMR (400MHz, CDCl<sub>3</sub>,  $\delta$ , ppm): 7.30 - 6.20 (m, ArH), 4.20 (s, -O-CH<sub>2</sub>-), 2.60 - 0.50 (m, -CH<sub>2</sub>CF<sub>2</sub>-, -CH<sub>2</sub>- & -CH<sub>3</sub>).

<sup>19</sup>F-NMR (400MHz, CDCl<sub>3</sub>,  $\delta$ , ppm): -82 (3F, s, -CF<sub>3</sub>), -115 (2F, s, (-CH<sub>2</sub>CF<sub>2</sub>-), -125.5 (2F, s, -CF<sub>2</sub>CF<sub>2</sub>CF<sub>2</sub>-), -127 (2F, s, (-CF<sub>2</sub>CF<sub>3</sub>).

### 3.5.2 Synthesis of poly(styrene-*b*-1H,1H,2H,2H,-perfluoro(5-methylhexyl) methacrylate).

The method described above (Section 3.5.1) was repeated, using lithium chloride (0.05g,  $1.18 \times 10^{-3}$  mol), styrene (6.55g,  $6.29 \times 10^{-2}$  mol), *sec*-butyllithium (1.4M, 0.185ml,  $2.62 \times 10^{-4}$  mol), DPE (0.070ml, 0.071g,  $3.94 \times 10^{-4}$  mol) and 1H,1H,2H,2H-perfluoro(5-methylhexyl) methacrylate (PFMHMA, 5.02g,  $1.31 \times 10^{-2}$  mol).

Yield: 10.88g (98%).

Target  $M_n$  of pS:  $25,000 \text{ g mol}^{-1}$ ;  $M_n$  of pS by GPC:  $29,200 \text{ g mol}^{-1}$ ; Pd of pS: 1.06;

Target mol ratio S:BCFMA: 4.79:1; mol ratio by  $^1\text{H-NMR}$ : 5.44:1;

$M_n$  of p(S-BCFMA) by  $^1\text{H-NMR}$ :  $48,900 \text{ g mol}^{-1}$ ; Pd of p(S-BCFMA): 1.21.

$^1\text{H-NMR}$  (400MHz,  $\text{CDCl}_3$ ,  $\delta$ , ppm): 6.2 - 7.35 (m, ArH), 4.25 (s, -O-CH<sub>2</sub>-), 2.70 - 0.50 (m, -CH<sub>2</sub>CF<sub>2</sub>-, -CH<sub>2</sub>- & -CH<sub>3</sub>).

$^{19}\text{F-NMR}$  (400MHz,  $\text{CDCl}_3$ ,  $\delta$ , ppm): -74 (6F, d, -C(CF<sub>3</sub>)<sub>2</sub>), -114 (2F, s, -CH<sub>2</sub>CF<sub>2</sub>), -117 (2F, s, -CF<sub>2</sub>CF<sub>2</sub>R), -187 (1F, s, -CF).

### 3.5.3 Synthesis of poly(styrene-*b*-1H,1H,2H,2H-perfluorohexyl methacrylate) with composition 1:1 by moles.

Toluene (~40ml) was distilled under vacuum into the main reactor using liquid nitrogen as the coolant and freeze-pumped once. After warming to room temperature, the solvent was used to wash the lithium chloride (0.04g,  $9.44 \times 10^{-4}$  mol) from the sidearm into the main reactor. Styrene (6.34g,  $6.00 \times 10^{-2}$  mol) was distilled into the reactor using liquid nitrogen as the coolant and the frozen mixture was degassed and thawed to room temperature. Initiator (*sec*-butyllithium, 1.4M, ~40 $\mu$ l) was added dropwise into the flask to give a faint persistent yellow-colour, before adding the reaction quantity (0.180ml,  $2.54 \times 10^{-4}$  mol), which gave the characteristic orange colour of polystyryllithium. The reaction was stirred for ~2.5 hours surrounded by a cold water bath, after which time a sidearm sample was withdrawn and quickly terminated with N<sub>2</sub>-sparged methanol (0.5ml). Tetrahydrofuran (~120ml) was distilled into the polystyrene/toluene solution in the main reactor using solid CO<sub>2</sub>/acetone as the coolant. DPE (0.07g, 0.065ml,  $3.83 \times 10^{-4}$  mol) was added by injection, giving the characteristic red colour of the diphenyl anion, and the reaction was stirred at -78°C for 21 hours. Meanwhile, PFHMA was prepared by passing it



down a column of aluminium oxide prior to drying over calcium hydride and degassing. It was then distilled into the main reactor (21.91g,  $6.60 \times 10^{-2}$  mol).

This resulted in a colour change from red to water-white. The reaction was maintained at  $-78^{\circ}\text{C}$  for a further 24 hours before being terminated with  $\text{N}_2$ -sparged methanol (1.0ml). The polymer was precipitated in excess methanol and recovered as previously described.

Yield: 25.76g (92%).

Target  $M_n$  of pS:  $25,000\text{gmol}^{-1}$ ;  $M_n$  of pS by GPC:  $28,100\text{gmol}^{-1}$ ; Pd of pS: 1.05;

Target mol ratio S:PFHMA: 0.93:1; mol ratio by  $^1\text{H-NMR}$ : 1.20:1;

$M_n$  of p(S-PFHMA) by  $^1\text{H-NMR}$ :  $103,000\text{gmol}^{-1}$ ; Pd of p(S-PFHMA): *multimodal*.

$^1\text{H-NMR}$  (400MHz,  $\text{CDCl}_3$ ,  $\delta$ , ppm): 7.40 - 6.20 (m, ArH), 4.20 (s,  $-\text{O}-\text{CH}_2-$ ), 2.80 - 0.50 (m,  $-\text{CH}_2\text{CF}_2-$ ,  $-\text{CH}_2-$  &  $-\text{CH}_3$ ).

$^{19}\text{F-NMR}$  (400MHz,  $\text{CDCl}_3$ ,  $\delta$ , ppm): -82 (3F, s,  $-\text{CF}_3$ ), -115 (2F, s,  $-\text{CH}_2\text{CF}_2-$ ), -125.5 (2F, s,  $-\text{CF}_2\text{CF}_2\text{CF}_2-$ ), -127 (2F, s,  $-\text{CF}_2\text{CF}_3$ ).

### 3.6 Synthesis of Poly(styrene-b-methyl methacrylate) Co-polymer.

Toluene (~40ml) was distilled under vacuum into the main reactor using liquid nitrogen as the coolant and freeze-pumped once. After warming to room temperature, the solvent was used to wash the lithium chloride (0.07g,  $1.65 \times 10^{-2}$  mol) from the sidearm into the main reactor. Styrene (2.54g,  $2.44 \times 10^{-2}$  mol) was distilled into the reactor using liquid nitrogen as the coolant and the frozen mixture was degassed and thawed to room temperature. Initiator (*sec*-butyllithium, 1.4M, ~40 $\mu\text{l}$ ) was added dropwise into the flask to give a faint persistent yellow-colour, before adding the reaction quantity (0.070ml,  $1.02 \times 10^{-4}$  mol) to give the characteristic orange colour of polystyryllithium. The reaction was stirred for ~3 hours, with the temperature controlled by a cold water bath, after which time a sidearm sample of living polystyrene was withdrawn and quickly terminated with  $\text{N}_2$ -sparged methanol (0.5ml). The polystyrene/toluene solution was cooled to  $-78^{\circ}\text{C}$  using a solid  $\text{CO}_2$ /acetone bath, and tetrahydrofuran (~150ml) was added via distillation. The required quantity of DPE (0.027g, 0.027ml,  $1.50 \times 10^{-4}$  mol) was then added by injection, giving the characteristic red colour of the diphenyl anion, and the reaction was stirred at  $-78^{\circ}\text{C}$  for ~24 hours. MMA (2.80g,  $2.80 \times 10^{-2}$  mol) was distilled into the main reactor. This resulted in a colour change from red to water-white. The

reaction was maintained at  $-78^{\circ}\text{C}$  for a further  $\sim 5$  hours before being terminated with  $\text{N}_2$ -sparged methanol (1ml). The polymer was precipitated in excess methanol and recovered as previously described.

Yield: 5.14g (99%).

Target  $M_n$  of pS:  $25,000\text{gmol}^{-1}$ ;  $M_n$  of pS by GPC:  $27,000\text{gmol}^{-1}$ ; Pd of pS: 1.04.

Target mol ratio S:MMA: 0.85:1; mol ratio by  $^1\text{H-NMR}$ : 0.83:1.

$M_n$  of p(S-MMA) by  $^1\text{H-NMR}$ :  $58,000\text{gmol}^{-1}$ ; Pd of p(S-MMA): 1.07.

$^1\text{H-NMR}$  (400MHz,  $\text{CDCl}_3$ ,  $\delta$ , ppm): 7.35 - 6.00 (m, ArH), 3.50 (s, -O-CH<sub>3</sub>),

2.80 - 0.40 (m, -CH<sub>2</sub>- & -CH<sub>3</sub>).

$^{13}\text{C-NMR}$  (100MHz,  $\text{CDCl}_3$ ,  $\delta$ , ppm): 145.22 (1C, quaternary Ar), 128.00 (4C, *o*- and *m*-ArH), 125.61 (1C, *p*-ArH).

### 3.7 Bromination of Polystyrene and of Block Co-polymers.

#### 3.7.1 Bromination of polystyrene.

Polystyrene (2.0g,  $1.92 \times 10^{-2}\text{mol}$ ) was dissolved in nitrobenzene ( $\sim 20\text{ml}$ ) at room temperature to form a clear solution. Bromine (1.00ml, 3.00g,  $1.94 \times 10^{-2}\text{mol}$ ) was added by syringe. The reaction vessel was vented to an aqueous sodium hydroxide bubbler, to remove the hydrogen bromide generated, and enveloped in foil to prevent ingress of light. Samples were taken at timed intervals, quenched in octene, and the polymer was precipitated in methanol and recovered as previously described.

By Elemental Analysis: C: 52.71%; H: 3.86%; Br: 43.53%.

Theoretical: (100% monobromination): C: 52.49%; H: 3.85%; Br: 43.65%.

$^{13}\text{C-NMR}$  (100MHz,  $\text{CDCl}_3$ ,  $\delta$ , ppm): 144 (1C, quaternary Ar), 129 (2C, *o*-ArH),

131.5 (2C, *m*-ArH), 120 (1C, *p*-ArBr), 46-42 (m, 1C, -CH<sub>2</sub>-), 40.5 (1C, ArCH).

#### 3.7.2 Bromination of poly(styrene-*b*-methyl methacrylate).

The bromination was repeated using poly(styrene-*b*-MMA) co-polymer to give:

By Elemental Analysis: C: 56.96%; H: 6.50%; Br: 15.92%.

Theoretical (100% monobromination): C: 57.26%; H: 6.53%; Br: 15.87%.

$^{13}\text{C-NMR}$  (100MHz,  $\text{CDCl}_3$ ,  $\delta$ , ppm): 178 (>C=O), 143 (1C, quaternary Ar), 131.5

(2C, *m*-ArH), 129.5 (2C, *o*-ArH), 120 (1C, *p*-ArBr), 55 (-CH<sub>2</sub>- MMA), 52 (-O-CH<sub>3</sub>),

46-42 (m, -CH<sub>2</sub>- styrene), 45 (C-CH<sub>3</sub>), 40.5 (ArCH), 17 (-CH<sub>3</sub>).

### 3.7.3 Bromination of poly(styrene-*b*-1H,1H,2H,2H-perfluorohexyl methacrylate).

The bromination was repeated using poly(styrene-*b*-PFHMA) co-polymer to give:

By Elemental Analysis: C: 46.13%; H: 3.43%; F: 17.60%; Br: 24.75%.

Theoretical (100% monobromination): C: 46.62%; H: 3.45%; F: 18.52%; Br: 27.95%.

<sup>13</sup>C-NMR (100MHz, CDCl<sub>3</sub>,  $\delta$ , ppm): 177 (>C=O); 143 (1C, quaternary *Ar*), 129.5 (2C, *o*-*Ar*H), 131.5 (2C, *m*-*Ar*H), 120 (1C, *p*-*Ar*Br), 119-105 (m, -C<sub>4</sub>F<sub>9</sub>), 57 (-O-CH<sub>2</sub>-), 54 (-CH<sub>2</sub>- PFHMA), 45 (C-CH<sub>3</sub>), 45-41 (m, -CH<sub>2</sub>- styrene), 40.5 (*Ar*CH), 30 (-CH<sub>2</sub>-C<sub>4</sub>F<sub>9</sub>), 19-17 (-CH<sub>3</sub>).

## 3.8 Characterisation.

### 3.8.1 Size Exclusion Chromatography (SEC).

SEC measurements were carried out on Viscotek 200 with refractive index, viscosity and light scattering detectors and 2 x 300mm PLgel 5 $\mu$ m mixed C columns. Tetrahydrofuran was used as the eluent, with a flow rate of 1.0ml/min and at a constant temperature of 30°C. Molecular weights were obtained using triple detection and the detectors were calibrated with a single narrow molecular weight distribution polystyrene standard. For poly(methyl methacrylate) a specific refractive index increment ( $dn/dc$ ) value of 0.085 was used, and for styrene co-polymers a value of 0.185 was used.

### 3.8.2 NMR Spectroscopy.

Proton NMR spectra were run on a Bruker-Avance 400MHz. Other NMRs (carbon-13 and fluorine-19) were run on a Varian-Mercury 400MHz.

### 3.8.3 Elemental Analysis.

Elemental analyses for carbon and hydrogen were performed on an Exeter Analytical CE-400 Elemental Analyser. Analyses for bromine and fluorine were performed on a Dionex DX-120 Ion Chromatograph.

### 3.8.4 Refractive Index Measurement.

Refractive indices were measured on a Sentech SE 500 Ellipsometer using "C" lines. Films were spun-cast onto silicon wafers from toluene solution.

### 3.8.5 Solid State Organisation.

The solid state organisation of the selected block co-polymer was investigated by Small Angle X-ray Scattering (SAXS). Samples were made by melt casting a film onto silicon wafer substrate and placing inside a Bruker Nanostar SAXS instrument with a 0.3mm diameter X-ray beam, set up with a path length of 1067mm which covers the range  $2\theta = 0 - 2.6$ , ( $q = 0 - 0.18 \text{ \AA}^{-1}$ ) with a detector resolution of 512 pixels over this range. The centre of the melt cast and the homogeneity of the sample were determined using the built-in radiography software by plotting a 2-D X-ray transmission map of the sample within the cast. The X-ray was then aligned onto the centre and a SAXS pattern was collected over 18 hours.

## **Chapter 4: Conclusions.**

## 4.1 Conclusions.

A working experimental method for the preparation of defined poly(styrene-*b*-fluoromethacrylate) polymers by living anionic polymerisation (LAP) was developed (Section 2.5.3 and Section 3.5.1). This was most successfully applied when the fluoromethacrylate was 1H,1H,2H,2H-perfluorohexylmethacrylate (PFHMA) and the mass ratio of the styrene:PFHMA blocks was approximately 1:1, i.e. a block co-polymer of experimental molecular weight  $61,000 \text{ g mol}^{-1}$  (target  $67,900 \text{ g mol}^{-1}$ ) with a composition of 50% by mass of PFHMA (target 55%) in 96% yield with polydispersity 1.02 (target  $\leq 1.05$ ) was achieved.

The same method was used to prepare one example of a co-polymer of styrene with 1H,1H,2H,2H-perfluoro(5-methylhexyl) methacrylate (PFMHMA, a branched-chain fluoromethacrylate) in approximate mass ratio 1:1, to give a block co-polymer of experimental molecular weight of  $48,900 \text{ g mol}^{-1}$  (target  $52,900 \text{ g mol}^{-1}$ ) with a composition of 40% by mass of PFMHMA (target 45%) in 98% yield but with a polydispersity (1.21) higher than the target ( $\leq 1.05$ ).

The same method was used to co-polymerise styrene with PFHMA in an approximate 1:1 molar ratio. After extra purification of the fluoromethacrylate monomer, the most successful preparation gave a block co-polymer of experimental molecular weight  $123,000 \text{ g mol}^{-1}$  (target  $178,000 \text{ g mol}^{-1}$ ) with a composition of 74% by mass of PFHMA (target 76%) in 99% yield. The polydispersity could not be assessed as the SEC trace was multimodal.

The method developed was also used to prepare poly(styrene-*b*-MMA) polymers in approximately 1:1 and 2:1 mass ratios, the most successful of which gave a block co-polymer of experimental molecular weight  $58,000 \text{ g mol}^{-1}$  (target  $58,600 \text{ g mol}^{-1}$ ) with a composition of 54% by mass of MMA (target 54%) in 99% yield and polydispersity of 1.07 (target  $\leq 1.05$ ).

Monobromination of the *para* position of the styrene rings in examples of polystyrene, poly(styrene-*b*-MMA) and poly(styrene-*b*-PFHMA) co-polymers was achieved quantitatively by a simple, direct bromination method. There was no



concomitant cleavage of the backbone of either co-polymer, or of the ester linkage of either the MMA or the PFHMA.

Thus, three types of high-contrast refractive index block co-polymers were prepared, namely, poly(styrene-*b*-fluoromethacrylate), poly(*p*-bromostyrene-*b*-MMA) and poly(*p*-bromostyrene-*b*-fluoromethacrylate), of differing block molar ratios and differing molecular weights.

Preparation and analysis of well-defined polystyrene and poly(methyl methacrylate) were also achieved. Preparation and analysis of fluoromethacrylate homopolymers of comparable molecular weights to the co-polymers were less easily achieved, possibly due to the poor solubility of these polymers in common solvents.

Evidence for the self-assembly of the block co-polymer poly(styrene-*b*-PFHMA), of molar ratio 3.23:1 respectively, of polydispersity 1.02 and of molecular weight  $61,000\text{gmol}^{-1}$  (expt. 18, Table 2.6) into the lamellar morphology was achieved using Small Angle X-ray Scattering.

## 4.2 Future Work.

Living anionic polymerisation by the technique detailed in this thesis proved to be of limited use in the preparation of novel block co-polymers as potential photonic materials, in that only polymers of relatively low molecular weights were achieved before loss of “control” was encountered. Therefore other methods of controlled polymerisation such as those reviewed by Davis<sup>30</sup> and the RAFT technique described by Chiefari<sup>87</sup> are worthy of investigation.

## **References.**



1. Yablonovitch E; *Phys. Rev. Lett.* 1987 58 2059-2062
2. John S; *Phys. Rev. Lett.* **1987** 58 2486-2489
3. Pollock CR and Lipson M; *Integrated Photonics*, Kluwer Academic Press, Boston, 2003
4. Boyle R; *Experiments & Considerations Touching Colours*, **1664**, Part the Third, Experiment XIX
5. Young T; *Philos. Trans. R. Soc. London*, **1802** 92 12-48
6. Bragg WL; *X-Rays and Crystal Structure* **1915**
7. Tayeb G *et al.*; *Optics & Photonics News* 40-49 Feb **2003**
8. Vukusic P and Sambles JR; *Nature* **2003** 424 852-855
9. Romanov S *et al.*; *J. Phys.: Condens. Matter* **1999** 11 3593-3600
10. Vukusic P *et al.*; *Proc. R. Soc. London, Ser. B* **1999** 266 1403-1411
11. Yoshioka S and Kinoshita S; *Forma*, **2002** 17 169-181,
12. Parker AR *et al.*; *Nature* **2001** 409 36,37
13. McPhedran RC *et al.*; *Aust. J. Chem.* **2001** 54 241-244
14. Lee DW; *American Scientist* **1997** 85 56-63
15. Lee DW; *Nature* **1991** 349 260-262
16. Haes AJ and Van Dyne RP; *Anal. Bioanal. Chem.* **2004** 379 920-930
17. Isaacs A (Ed.); *A Dictionary of Physics* 4th Edn., **2000** OUP, Oxford
18. Strutt J; *Philosophical Magazine* **1899** 47, 375-384.
19. Vogelmann TC; *Annu. Rev. Plant Physiol. Plant Mol. Biol.* **1993** 44 231-251
20. Bjarklev A *et al.*; *Photonic Crystal Fibres*, Kluwer Academic Press, Boston & London, 2003
21. Saleh BEA and Teich MC; *Fundamentals of Photonics*, Wiley, New York, 1991
22. Gaynor J *et al.*; *J. Appl. Polym. Sci.* **1993** 50 1645-1653
23. Nguyen T and Wakselman C; *J. Fluorine Chem.* **1996** 80 95-99

24. Hougham G *et al.*; *Macromolecules* **1996** 29 3453-3456
25. Sheppard WA and Sharts CM; *Organic Fluorine Chemistry*, WA Benjamin, New York, **1969**
26. Jariwala CP and Mathias LJ; *Macromolecules* **1993** 26 5129-5136
27. Scheirs J (Ed.); *Modern Fluoropolymers: High Performance Polymers for Diverse Applications*, Wiley, Chichester, **1997**
28. Aldrich Catalogue 2005/2006
29. Jenekhe SA and Wynne KJ (Eds.); *Photonic and Optoelectronic Polymers*, ACS, Washington DC, **1997**
30. Van Krevelen DW; *Properties of Polymers: Their Estimation and Correlation with Chemical Structure*, 3rd Edn., Elsevier, Amsterdam & London, **1990**
31. Brandrup J *et al.*; *Polymer Handbook*, 4th Edn., Wiley-Interscience, New York, **1999**
32. Ozin G; *Chem. Commun.* **2003** 2639-2643
33. Inoue K and Ohtaka K (Eds); *Photonic Crystals: Physics, Fabrication and Application*, Springer, Berlin **2004**
34. Mijatovic D *et al.*; *Lab. Chip* **2005** 5 492-500
35. Hawker CJ and Russell TP; *MRS Bulletin* **2005** 30 (12): 952-966
36. Wang D and Möhwald H; *J Mater Chem* **2004** 14 459-468
37. Baumberg JJ; *Nature Materials* **2006** 5 2-5
38. Huck WTS; *Int J of Nanotechnology* **2004** 1 1/2 119-129
39. Edrington AC *et al.*; *Adv. Mater.* **2001** 13 6 421-425
40. Iyengar DR *et al.*; *Macromolecules* **1996** 29 1229-1234
41. Muthukumar M *et al.*; *Science* **1997** 277 1225-1232
42. Urbas A *et al.*; *Macromolecules* **1999** 32 4748-4750
43. Mark HF *et al.*; *Encyclopaedia of Polymer Science and Engineering*, 2nd Edn., vol 2 Wiley-InterScience, New York, **1989**
44. Hadjichristidis N *et al.*; *Block Copolymers: Synthetic Strategies, Physical Properties and Applications*, Wiley-Interscience, **2003**

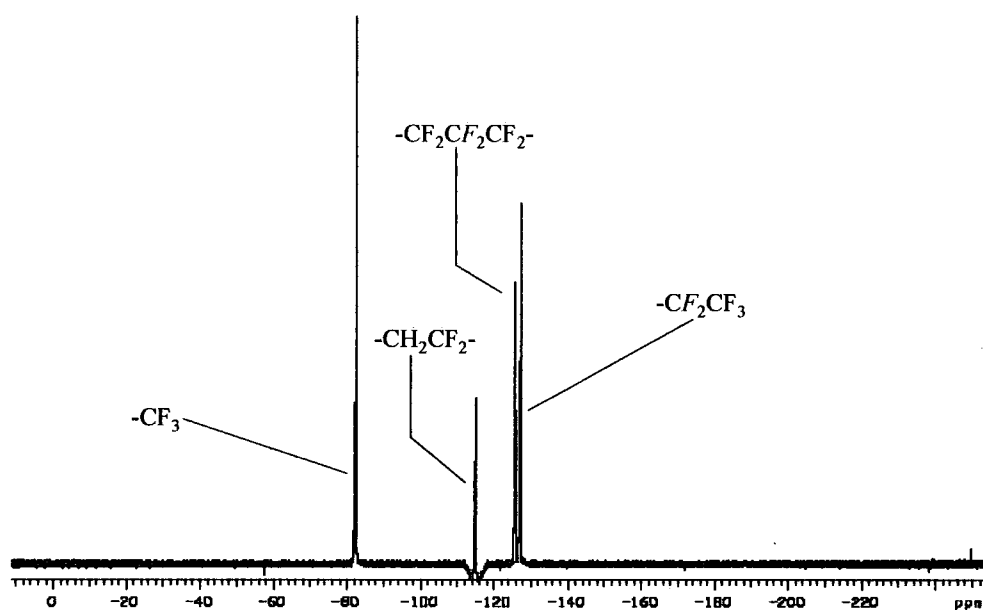
45. Quirk RP (Ed.); *Applications of Anionic Polymerisation Research*; ACS Symp. Ser. 696
46. Hsieh HL and Quirk RP; *Anionic Polymerisation: Principles and Practical Applications*, Marcel Dekker, New York 1996
47. Szwarc M; *J. Polym. Sci., Part A: Polym. Chem.* **1998** 36 ix-xv
48. Mays JW and Uhrig D; *J. Polym. Sci., Part A: Polym. Chem.* **2005** 43 (24)
49. Mark HF *et al.*; *Encyclopaedia of Polymer Science and Engineering*, 2nd Edn., vol 8 Wiley-InterScience, New York, 1989
50. Mark HF *et al.*; *Encyclopaedia of Polymer Science and Engineering*, 2nd Edn., Supplement vol Wiley-InterScience, New York, 1989
51. Reichardt C; *Solvents and Solvent Effects in Organic Chemistry*, VCH Publishers, 2nd ed., 1988
52. Kneen N *et al.*; *Chemistry: Facts Patterns and Principles*, Addison-Wesley, London, 1972
53. Margerison D and East GC; *An Introduction to Polymer Chemistry*, Pergamon Press, Oxford, 1967
54. Davis TP *et al.*; *J. Macromol. Sci., Rev. Macromol. Chem. Phys.* **1994** C34 (2)
55. Wieland PC *et al.*; *Macromol. Rapid Commun.* **2001** 22 700-703
56. Varshney SK *et al.*; *Macromolecules* **1990** 23 2618-2622
57. Kunkel D and Muller AH; *Makromol. Chem. Macromol. Symp.* **1992** 60 315-326
58. Wang JS *et al.*; *Macromolecules* **1993** 26 5984-5990
59. Wang JS *et al.*; *Macromolecules* **1993** 26 6776-6781
60. Ishizone T *et al.*; *Macromolecules* **2003** 36 42-49
61. Quirk RP and Lee Y; *J. Polym. Sci., Part A: Polym. Chem.* **2000** 38 145-151
62. Ballard DGH *et al.*; *Macromolecules* **1992** 25 5907-5913
63. Haddleton DM *et al.*; *Macromol. Symp.* **1995** 91 93-105
64. Krupers MJ *et al.*; *Macromol. Symp.* **1996** 102, 99-106
65. Krupers MJ and Moller M; *Macromol. Chem. Phys.* **1997** 198, 2163-2179

66. Yong TM *et al.*; *Chem. Commun.* **1997** 18 1811-1812
67. Hems WP *et al.*; *J. Mater. Chem.* **1999** 9 1403-1407
68. Ishizone T *et al.*; *Polym. J.* **1999** 31 11-2 983-988
69. Sugiyama K *et al.*; *Macromol. Symp.* **2002** 181 135-153
70. Yoshida E *et al.*; *Polym. Prepr. (Am. Chem. Soc., Div. Polym. Chem.)* **2000** 41 (1) 185
71. Stevens MP; *Polymer Chemistry: An Introduction*, 3rd Edn., OUP, New York, 1999
72. Gunther H; *NMR Spectroscopy: An Introduction*, Wiley, Chichester, 1980
73. Bovey FA; *Nuclear Magnetic Resonance Spectroscopy*, 2nd Edn. Academic Press, San Diego, 1988
74. Mooney EF; *An Introduction to <sup>19</sup>F NMR Spectroscopy*, Heyden (Sadtler Research Laboratories, Philadelphia), London, 1970
75. Booth C and Price C (Eds.); *Comprehensive Polymer Science*, 1st Edn., 1 348, Pergamon, Oxford, 1989
76. Akitt JW; *NMR and Chemistry: An Introduction to Modern NMR Spectroscopy*, 3rd Edn., Chapman and Hall, London, 1992
77. Hamley IW; *The Physics of Block Copolymers*, OUP, Oxford, 1998
78. Eggleston S; University of Durham Report, December **2004**
79. Cooper AI *et al.*; *Macromol. Rapid Commun.* **1998** 19 353-357
80. Krupers MJ *et al.*; *Polym. Bull.* **1998** 40 211-217
81. Tsibouklis J *et al.*; *Macromolecules* **2000** 33 8460-8465
82. Kambour RP and Bendler JT; *Macromolecules* **1986** 19 2679-2682
83. Kalinowski HO; *<sup>13</sup>Carbon NMR Spectroscopy*, Wiley, Chichester, 1988
84. Eggleston S; University of Durham Report, October **2004**
85. Schadler V and Wiesner U; *Macromolecules* **1997** 30 6698-6701
86. Eggleston S; University of Durham Report, June **2005**
87. Chiefar J *et al.*; *Macromolecules* **1998** 31 5559-5562

## **Appendices.**

## Appendix 1.

$^{19}\text{F}$ -NMR of poly(styrene-b-PFHMA) co-polymer (Table 2.8, expt. 18).



## Appendix 2.

$^{19}\text{F}$ -NMR of poly(styrene-b-PFMHMA) co-polymer. (Table 2.8, expt. 19).

